

Calibration Procedures for Seismic and Deflection-Based Devices

by

Vivek Tandon, Ph.D.

and

Soheil Nazarian, Ph.D., P.E.

Research Project 7-2984

**Development of Instrumentation Testing and
Calibration Procedures and Facilities**

Conducted for

Texas Department of Transportation

Research Report 2984 - S1

April 2000

**The Center for Highway Materials Research
The University of Texas at El Paso
El Paso, TX 79968-0516**

This page replaces an intentionally blank page in the original.

-- CTR Library Digitization Team

TECHNICAL REPORT STANDARD TITLE PAGE

1. Report No. TX - 99 2984 - S1	2. Government Accession No.	3. Recipient's Catalog No.	
4. Title and Subtitle CALIBRATION PROCEDURES FOR SEISMIC AND DEFLECTION-BASED DEVICES		5. Report Date April 2000	
		6. Performing Organization Code	
7. Authors V. Tandon and S. Nazarian		8. Performing Organization Report No. Project Summary Report 2984-S1	
9. Performing Organization Name and Address Center for Highway Materials Research The University of Texas at El Paso El Paso, Texas 79968-0516		10. Work Unit No.	
		11. Contract or Grant No. Project No. 7-2984	
12. Sponsoring Agency Name and Address Texas Department of Transportation Construction Division/Research and Technology Transfer Section P.O. Box 5080 Austin, Texas 78763-5080		13. Type of Report and Period Covered Summary Report 9/96 - 8/98	
		14. Sponsoring Agency Code	
15. Supplementary Notes Research Performed in Cooperation with TxDOT Research Project Title: Development of Instrumentation Testing and Calibration Procedures and Facilities			
16. Abstract <p>TxDOT has acquired fifteen Falling Weight Deflectometers (FWD), one Seismic Pavement Analyzer (SPA), and five Portable Seismic Pavement Analyzers (PSPA) for evaluating the structural integrity of pavements. These nondestructive testing devices use different types of sensors for measuring deflection, travel time and load intensity. The accuracy and precision levels of these devices diminish over the years due to wear and tear of the testing devices. Thus, it is essential to develop calibration procedures for these sensors.</p> <p>The primary function of the FWD device is to measure a deflection basin due to a load imparted to the pavement. Velocity transducers (a.k.a. geophones) are used to determine the deflection, and load cells are utilized to measure the applied load. The SPA uses several accelerometers and geophones to measure the propagation of waves and the deformation of pavements due to imparted loads. Load cells are used to measure the loads applied to the pavement. The PSPA only uses accelerometers to measure wave propagation patterns.</p> <p>Calibration procedures for three different sensors: a) accelerometers, b) geophones, and c) load cells, which are essential for accurate and precise structural evaluation of pavements, have been developed as part of this study. The unique features of the proposed procedures are that: 1) each sensor is calibrated in place as a system, 2) none of the devices has to be disassembled for calibration, and 3) any desired frequency range and amplitude can be conveniently reproduced.</p>			
17. Key Words FWD, PSPA, SPA, Geophone, Accelerometer, Calibration, Load Cell.		18. Distribution Statement No restrictions. This document is available to the public through the National Technical Information Service, 5285 Port Royal Road, Springfield, Virginia 22161	
19. Security Classified (of this report) Unclassified	20. Security Classified (of this page) Unclassified	21. No. of Pages 110	22. Price

This page replaces an intentionally blank page in the original.

-- CTR Library Digitization Team

The contents of this report reflect the view of the authors, who are responsible for the facts and the accuracy of the data presented herein. The contents do not necessarily reflect the official views or policies of the Texas Department of Transportation. This report does not constitute a standard, specification, or regulation.

The material contained in this report is experimental in nature and is published for informational purposes only. Any discrepancies with official views or policies of the Texas Department of Transportation should be discussed with the appropriate Austin Division prior to implementation of the procedures or results.

**NOT INTENDED FOR CONSTRUCTION, BIDDING, OR
PERMIT PURPOSES**

Vivek Tandon, Ph.D.
Soheil Nazarian, Ph.D., P.E. (69263)

This page replaces an intentionally blank page in the original.

-- CTR Library Digitization Team

Acknowledgments

The authors would like to express their sincere appreciation to Mr. Carl Bertrand of the Design Division of the Texas Department of Transportation for his ever-present support. Thanks are also due to Mr. Randy Beck of the Design Division of the Texas Department of Transportation for providing expertise in debugging the FWD system. The authors would like to thank El Paso and Odessa District personnel for providing us with the FWD system.

The authors would also like to thank the undergraduates who worked on this project. Specifically, recognition is extended to Cijifredo Zuniga and Javier Dominguez for their enthusiasm in performing all the necessary tests for this project and their help in the preparation of this report.

This was a joint project between UTEP and The University of Texas at Arlington, and the constant interaction with Dr. Roger Walker was very beneficial and constructive.

This page replaces an intentionally blank page in the original.

-- CTR Library Digitization Team

Abstract

TxDOT has acquired fifteen Falling Weight Deflectometers (FWD), one Seismic Pavement Analyzer (SPA), and five Portable Seismic Pavement Analyzers (PSPA) for evaluating the structural integrity of pavements. These nondestructive testing devices use different types of sensors for measuring deflection, travel time and load intensity. The accuracy and precision levels of these devices diminish over the years due to wear and tear of the testing devices. Thus, it is essential to develop calibration procedures for these sensors.

The primary function of the FWD device is to measure a deflection basin due to a load imparted to the pavement. Velocity transducers (a.k.a. geophones) are used to determine the deflection, and load cells are utilized to measure the applied load. The SPA uses several accelerometers and geophones to measure the propagation of waves and the deformation of pavements due to imparted loads. Load cells are used to measure the loads applied to the pavement. The PSPA only uses accelerometers to measure wave propagation patterns.

Calibration procedures for three different sensors: a) accelerometers, b) geophones, and c) load cells, which are essential for accurate and precise structural evaluation of pavements, have been developed as part of this study. The unique features of the proposed procedures are that: 1) each sensor is calibrated in place as a system, 2) none of the devices has to be disassembled for calibration, and 3) any desired frequency range and amplitude can be conveniently reproduced.

This page replaces an intentionally blank page in the original.

-- CTR Library Digitization Team

Implementation Statement

The calibration methods proposed in this study can be immediately implemented by TxDOT. The calibration of the sensors used in the nondestructive testing devices is essential in obtaining high-quality data and in ensuring that similar devices provide comparable answers throughout the state.

A prototype slab that can accommodate the necessary instrumentation for most calibration setups has been developed at UTEP during the course of this study. It is proposed that such a facility be replicated for use by TxDOT.

This page replaces an intentionally blank page in the original.

-- CTR Library Digitization Team

Table of Contents

Acknowledgments	vii
Abstract	ix
Implementation Statement	xi
List of Tables	xvii
List of Figures	xix
Chapter 1	
Introduction	1
Problem Statement	1
Research Objective and Approach	1
Chapter 2	
Falling Weight Deflectometer	3
SHRP Calibration Method	3
Relative Calibration Procedure	4
Reference Calibration Procedure for Geophone and Load Cells	4
Texas Calibration Method	5
Proposed Calibration System for Geophones	6
Calibration of Reference Geophone	6
Calibration of FWD Geophone	11
Proposed Calibration Setup for the Load Cell	14
Calibration of Reference Load Cells	14
Calibration of the FWD Load Cells	17
Comparison of FWD Calibration Results	17
Characteristics of Geophones	17
Calibration with Texas System	21

Calibration with Proposed System	21
FWD Calibration Strategy	24
FWD Geophone Calibration Strategy	24
Reference Geophone Calibration Strategy	24
Geophone Holder Calibration Strategy	27
FWD Load Cell Calibration Strategy	29
Chapter 3	
Portable Seismic Pavement Analyzer	30
Proposed Calibration of Accelerometers	31
Phase Shift Calibration	31
Amplitude Calibration	40
PSPA Calibration Strategy	48
Relative PSPA Calibration	51
Reference PSPA Calibration	51
Accelerometer Assembly Diagnosis	54
Chapter 4	
Seismic Pavement Analyzer	55
Proposed Calibration of Accelerometers	57
Phase Shift Calibration	57
Amplitude Calibration	59
Phase Shift Calibration	65
Amplitude Calibration	65
Proposed Calibration of Load Cells	71
SPA Calibration Strategy	75
Relative Calibration	75
Reference Calibration	75
Accelerometer or Geophone Assembly Diagnosis	79
Accelerometers	79
Geophones	80
Load Cell Calibration	81
Chapter 5	
Closure	82
References	84
Appendix A	
Specifications of Equipment Used	86

List of Tables

Table 2.1 - Geophone Characteristics	20
Table 3.1 - Poles and Zeros Obtained from Curve Fitting of the Data of Figure 3.7	39
Table 3.2 - Poles and Zeros Obtained from Curve Fitting of Spectra Shown in Figure 3.12 ...	46
Table 4.2 - Poles and Zeros Obtained from Fitting a Curve to Data Shown in Figure 4.7	63
Table 4.3 - Poles and Zeros Obtained from Fitting Curve to Data Shown in Figure 4.9	68
Table 4.4 - Optimal Frequency Ranges to be Considered in Reference Calibration of SPA Accelerometers for Phase Shift	80

This page replaces an intentionally blank page in the original.

-- CTR Library Digitization Team

List of Figures

Figure 2.1 - Proximitor Calibration Test Setup	7
Figure 2.2 - A Typical Calibration Curve of a Proximitor Probe	8
Figure 2.3 - Test Setup for Geophone Calibration	9
Figure 2.4 - A Typical Frequency and Coherence Response of Geophone	10
Figure 2.5 - Calibration Curves of Geophones	12
Figure 2.6 - A Schematic of Field Calibration of FWD Geophone	13
Figure 2.7 - In-Place Calibration of FWD Geophone	15
Figure 2.8 - A Calibration Curve of a Typical FWD Geophone	15
Figure 2.9 - A Schematic of Load Cell Calibration in the Laboratory	16
Figure 2.10 - A Typical Calibration Curve for a Reference Load Cell	18
Figure 2.11 - A Schematic of FWD Load Cell Calibration	18
Figure 2.12 - Components and Mechanical Model of Geophone	19
Figure 2.13 - Comparison of Calibration Factors from SHRP and Texas Protocols	22
Figure 2.14 - Comparison of Raw Geophone Outputs Under a 30 msec Impulse	23
Figure 2.15 - Comparison of Deflections Obtained from Geophones Under 30 msec Impulse	23
Figure 2.16 - Flow Chart Summarizing FWD Calibration Steps	25
Figure 2.17 - FWD Geophone Calibration Strategy	26
Figure 2.18 - Steps for the Calibration of Geophone Holders	28
Figure 3.1 - Schematic of Portable Seismic Pavement Analyzer	30
Figure 3.2 - A Schematic Diagram of PSPA Calibration System	32
Figure 3.3 - PSPA Calibration Test Setup	33
Figure 3.4 - Response of Accelerometer Outside PSPA Holder	35
Figure 3.5 - Responses of a Typical PSPA Accelerometer Before and After Placed Inside the Sensor Holder	36
Figure 3.6 - Comparison of Response of Accelerometers 1 and 2 of PSPA	37
Figure 3.7 - Ratio of Frequency Response Curves of Accelerometer 1 and 2	38
Figure 3.8 - A Schematic of Test Setup for Amplitude Calibration	40
Figure 3.9 - Calibration Device Test Setup for Amplitude Calibration	40
Figure 3.10 - A Typical Frequency Response of Built-in Accelerometer of Piezo-electric Shaker	42
Figure 3.11 - A Typical Frequency Response of PSPA Accelerometer	44
Figure 3.12 - Calibration Curves for PSPA Accelerometer	45

Figure 3.13 - Raw and Calibrated Response of PSPA During IE Tests	46
Figure 3.14 - PSPA Source Calibration Test Setup	47
Figure 3.15 - A Typical Time-History of PSPA Source Signal	48
Figure 3.16 - Summary of Proposed PSPA Calibration	49
Figure 3.17 - Proposed PSPA Calibration Strategy	50
Figure 3.18 - Proposed Reference PSPA Calibration Strategy	52
Figure 4.1 - A Schematic of Seismic Pavement Analyzer	56
Figure 4.2 - A Schematic of Field Calibration of SPA Accelerometer or Geophone	57
Figure 4.3 - SPA Accelerometer and Geophone Calibration Test Setup	58
Figure 4.4 - Comparison of Response of Accelerometers 2 and 3 of SPA	60
Figure 4.5 - Phase Calibration Spectrum for Accelerometers 2 and 3 Pair	61
Figure 4.6 - Amplitude Ratio Spectrum of Accelerometer 1 of SPA	62
Figure 4.7 - Amplitude Calibration of SPA Accelerometer 1	64
Figure 4.8 - Comparison of Response of Geophones 2 and 3 of SPA	66
Figure 4.9 - Ratio of Frequency Response Curves of Geophone 2 and 3	67
Figure 4.10 - Field Calibration of SPA Geophone 1	69
Figure 4.11 - Calibration Amplitude Spectra for Geophone 1 of SPA	70
Figure 4.13 - SPA Pressure Level Setup	72
Figure 4.12 - SPA Load Cell Calibration Test Setup	72
Figure 4.14 - A Typical Load Time-History from the Calibration and Low-Frequency SPA Load Cells	73
Figure 4.15 - A Typical Calibration Curve of SPA Low-Frequency Load Cell	73
Figure 4.16 - A Typical Frequency Response of Low-Frequency Load Cell	74
Figure 4.18 - A Typical Calibration Curve of SPA High-Frequency Load Cell	75
Figure 4.17 - A Typical Load Time-History from the Calibration and High-Frequency SPA Load Cells	76
Figure 4.19 - Summary of Proposed SPA Calibration	77
Figure 4.20 - Proposed Reference SPA Calibration Strategy	78

Chapter 1

Introduction

Problem Statement

Nondestructive testing (NDT) devices are routinely used by TxDOT for evaluating the structural integrity of pavements. For this reason, TxDOT has acquired a number of Falling Weight Deflectometers (FWD), a Seismic Pavement Analyzer (SPA), and several Portable Seismic Pavement Analyzers (PSPA). These nondestructive testing devices use different types of sensors for measuring deflections (or deformation), wave propagation patterns and applied loads. The accuracy and precision levels of these devices diminish over the years due to wear and tear. Thus, it is essential to develop appropriate calibration procedures for these sensors.

The primary function of the FWD device is to measure a deflection basin due to a load imparted to the pavement. Velocity transducers (a.k.a. geophones) are used to determine the deflection, and load cells are utilized to measure the applied load. The SPA uses several accelerometers and geophones to measure the propagation of waves and the deformation of pavements. In this device, the magnitude and duration of load imparted to the pavement are measured by load cells. The PSPA uses only accelerometers to measure wave propagation patterns.

The calibration procedures for accelerometers, geophones, and load cells, which are essential for accurate and precise structural evaluation of pavements, have been developed as part of this study. Also, to provide practical guidelines for the end user, a calibration strategy has been proposed for each of the nondestructive testing devices.

Research Objective and Approach

The main objective of this study was to develop calibration procedures for the three types of sensors used in FWD, SPA, and PSPA. Although similar sensors are used in different devices, the amplitude levels and the frequency ranges utilized in the analysis differ from one testing device to another. Hence, it is essential to develop calibration procedures for each sensor for each testing device.

The main objectives for this research study have been accomplished by identifying the role of each sensor in evaluating the structural integrity of pavements and devising methods to ensure that the information obtained from the sensor is accurate and precise.

In view of the above discussion, this study was divided into three phases. In the first phase, calibration procedures for the sensors used in the FWD devices were developed. In the second and third phases, calibration procedures for the sensors used in the SPA and PSPA were developed.

For each phase, current calibration test methods for each sensor were identified, evaluated, and modified. New calibration procedures were developed when necessary. The calibration procedures were developed by keeping in view three objectives. First, each calibration procedure should be able to identify the accuracy and precision of the sensor being calibrated. Second, the calibration procedures should be practical and easy so that they can be routinely performed by TxDOT personnel. Third, the acquisition and maintenance of the calibration system should be reasonable and not prohibitively expensive. In that regard, some compromises were made in regards to the accuracy of the calibration device with respect to the cost. The rationale for such a decision is included in an appropriate location in the text.

This report is divided into five chapters. In the first chapter, the problem statement and research objectives are reported. The second chapter consists of a review of the existing calibration procedures for sensors used in FWD, along with several modifications to the existing procedures to make them more robust and convenient. The third and fourth chapters include the newly devised calibration procedures for sensors used in PSPA and SPA, respectively. The fifth chapter summarizes the findings of the report and provides suggestions for future activities to smoothly implement the procedures in TxDOT activities.

Chapter 2

Falling Weight Deflectometer

Most highway agencies use FWD to evaluate the structural integrity of pavements. TxDOT has acquired a fleet of fifteen FWDs over a decade or so and has successfully used them in its pavement evaluation activities. The primary function of the FWD is to measure a deflection basin due to a load imparted to the pavement. The deflection basin, measured in the field, is input into a backcalculation routine to determine the modulus of each pavement layer. Various computer programs are available for backcalculation of pavement layer properties.

An accurate determination of the deflection basins and imparted loads is critical. Nazarian and Stokoe (1986) indicate that a small error in deflections measured in the field may yield significantly erroneous modulus values. Hence, a reliable method for evaluating the accuracy of the FWD sensors is needed.

Two different calibration systems for evaluating the accuracy and precision of FWDs have been used by TxDOT. The system developed by the Strategic Highway Research Program (SHRP) can be used to perform a relative as well as a reference calibration of the geophones. The second method is the so-called Texas Calibration Method developed at The University of Texas at El Paso (UTEP) for TxDOT. Both of these methods have been recently included in the ASTM standards for the FWD testing.

In this chapter, the available test methods are discussed, and a new calibration test method is proposed. Based on the newly developed calibration procedure, a calibration strategy is also proposed. The calibration strategy contains various steps that are necessary for the evaluation of the sensors, the sensor holders and the electronic components used in the system.

SHRP Calibration Method

In the SHRP calibration method, two types of calibrations are recommended: 1) a relative calibration and 2) a reference calibration. The reference calibration compares an FWD reading against independent references that meet benchmarks traceable to the National Institute of Standards and Technology. The relative calibration ensures that the FWD sensors are providing consistent results and are functioning correctly. A brief description of these procedures is included in this section. A detailed description can be found in ASTM D4694.

Relative Calibration Procedure

The goal of the relative calibration procedure is to ensure that all sensors reproduce the same deflection under a given impact. The relative deflection calibration requires a sensor holding tower. The tower is positioned at a distance of less than 2 feet from the FWD load plate. The tower must have sufficient positions to accommodate all sensors used in the FWD. The sensors are positioned one above the other along a vertical axis. During the calibration, the sensors are rotated so that each sensor occupies every level in the tower. At each tower position, seven deflections are recorded for each sensor. Deflection magnitudes of between 16 and 20 mils (406 μm and 508 μm) are desired. Deflection ratios are determined for each sensor by dividing the average for all the sensors by the average of that sensor. If any of the resulting ratios are not within 1.003 or 0.997, all of the calibration factors should be adjusted. If the average difference between any two sensor readings is 0.08 mils (2 μm) or less, the calibration factors should not be altered. On the other hand, if the differences in the average deflections are greater than 0.08 mils (2 μm), the device should be repaired and re-calibrated according to the manufacturer's recommendations.

Reference Calibration Procedure for Geophone and Load Cells

The relative calibration ensures that all geophone readings are consistent, but it does not ensure that the deflections are accurate. The reference calibration is conducted to determine the accuracy of the sensors. The SHRP reference calibration system uses a linear variable differential transformer (LVDT) as the reference deflection measurement device because it can be accurately and independently calibrated with a micrometer. The LVDT and the geophones are mounted in special holders so that the magnetized tip of the LVDT core is always in contact with the top of the geophone holder. Hence, the LVDT is always subjected to the same movement as the geophone. The LVDT is mounted to the end of a section of a wide-flange beam, and the geophone holder is designed to rest on the pavement. During the calibration, each geophone is taken out of the holder and placed inside the reference calibration beam. The geophone calibration data are collected at four deflection levels similar to those of relative calibration procedure. Five sets of deflection data are collected for each deflection level. The calibration factors are then calculated for each geophone. The new calibration factors are keyed into the field program prior to the relative calibration procedure being performed.

The load cell calibration is performed by using a reference load cell system. The system consists of an aluminum case, 11.8 in. (300 mm) in diameter and 3.25 in. (83 mm) high, with four measuring links equally spaced in a 7.5-in. (190 mm) circle. A ribbed rubber sheet, identical to the one on the bottom of the FWD loading plate, is glued to the bottom of the reference load cell system to ensure uniform pressure on the pavement surface. For each FWD, a load cell calibration is performed by dropping weights from four drop heights, with five drops at each drop height. A linear relationship is developed between the FWD load cell and the reference load cell. The developed relationship can then be used for adjusting the FWD load cell readings.

This method of calibration has two disadvantages. First, the geophone is taken out of the holder and placed on a rigid frame. Consequently, this method does not calibrate the geophone system but rather the geophone. In other words, it is possible that the geophone is working properly, but the spring holding mechanism is worn out. In that case, the geophone will calibrate

satisfactorily; however, the results obtained from the FWD system may not be accurate. Second, the accuracy of the system at higher deflections is uncertain. The geophone calibration is performed at deflection levels of 26 mil and 8 mil (660 μm and 203 μm). Even though these levels are reasonable for outer sensors, the deflections measured in the field by the central geophone can be as high as 100 mil (2.5 mm).

In recent years, several highway agencies have started focusing on the issue of using the whole time history record of the geophone rather than using peak deflections. For accurate and precise measurement of the deflection time history, it is essential to evaluate the performance for a frequency range and for multiple deflection levels. This procedure is not capable of providing the calibration parameters for a range of frequencies and deflections.

Texas Calibration Method

A reference calibration system has also been developed at UTEP. This calibration system consists of two or three well-calibrated geophones, three load cells, a load-bearing plate, and a data acquisition system (Nazarian et al., 1991). This device allows the calibration of two or three geophones at a time. The well-calibrated geophones are placed next to the FWD geophones with the help of modeling clay or vacuum grease. After placement of the geophones, the load is dropped ten times at each drop height. The deflection measured from the FWD geophones and the calibration system geophones are compared to identify the accuracy of the individual geophone similar to the SHRP procedure.

This calibration system is portable and can be used in the field. One advantage of the system is that the FWD geophone is not removed from the FWD holders and, therefore, provides the geophone system calibration (not the geophone alone). This method has two disadvantages. First, the geophone on top of the FWD loading plate cannot be calibrated because a well-calibrated geophone cannot be placed next to it. In addition, only peak deflections measured from the system and the FWD can be compared, not the whole time history.

The load cell calibration procedure is similar to the SHRP procedure except that the three dynamic load cells, sandwiched between two steel plates, have been used in the Texas Calibration method. The load cells are affixed to the bottom plate, and the load is transferred to them through the top plate. The summation of peak loads obtained from the three load cells is equivalent to the load measured by the FWD load cell.

Based on the shortcomings of the two systems, a more comprehensive calibration system is needed. The system should be capable of calibrating geophones over the ranges of frequency and deflection observed in the field such that the whole time history of a deflection basin can be measured accurately and precisely. The developed calibration method should also be capable of identifying the problems associated with the geophone holding system or the geophone. Thus, the agency can determine when to replace the geophone holders or the geophones.

Proposed Calibration System for Geophones

The proposed calibration setup uses the technology developed during the Texas Calibration Protocol (TCP) development. In the TCP, a reference geophone is calibrated in the laboratory, and the

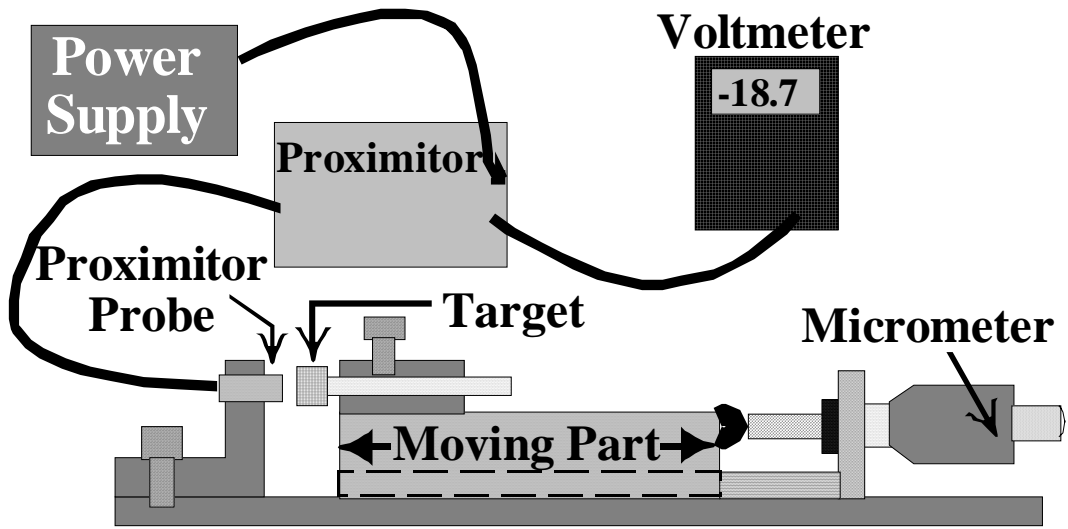
calibrated geophone is used in the field to verify the FWD geophones accuracy and precision. In the proposed process, the laboratory setup is placed in a calibration slab. The calibration is carried out in two steps: calibration of a reference geophone and calibration of the FWD geophone.

Calibration of Reference Geophone

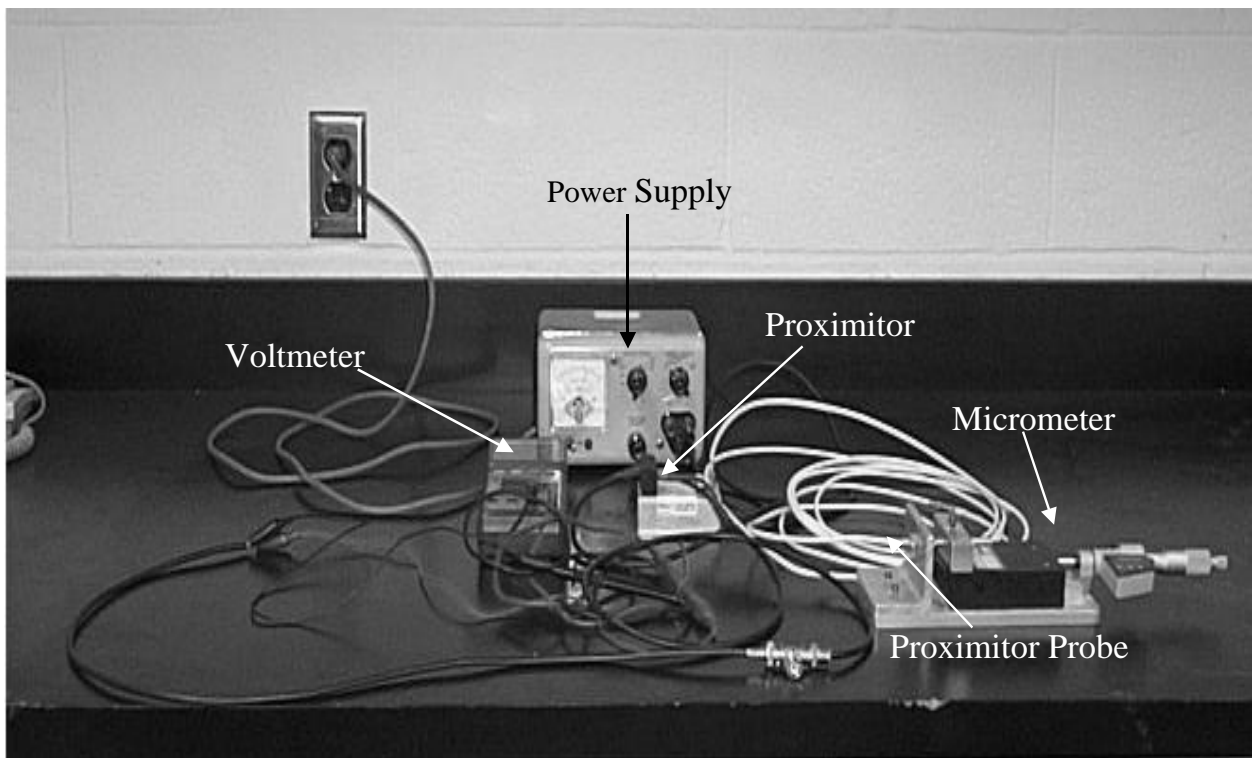
A reference geophone is calibrated in the laboratory using a proximator. A proximator is a non-contact transducer which monitors the movement of a target by converting the change in the eddy current field to a change in voltage (Tandon, 1990). As shown in Figure 2.1, a proximator transducer system consists of a probe, an extension cable and a proximator. The proximator can be accurately and independently calibrated with an accurate micrometer. The proximators have several distinct advantages over other displacement measuring devices. They are reasonably priced, non-contact, accurate, and sensitive, and they maintain their accuracy over a wide range of frequencies. The accuracy and precision of proximators was experimentally verified in Project 7-913. The specifications of the proximator used in this study are given in Appendix A. The calibration values of the proximators are sensitive to the properties of the target used and, to some extent, to the input voltage. They should be re-calibrated whenever a new target material is used or the input power range is changed.

The laboratory test setup, for the calibration of proximator, is shown in Figure 2.1. A voltmeter, a micrometer, and a moving target were used. The micrometer selected for this study had a least count of 0.05 mil (10 μ mm). Although a higher resolution micrometer may be desirable, the cost of acquiring such a device may not be justifiable. The voltmeter used in the calibration was an ordinary voltmeter and can be obtained from any electronic shop. The target used in this study was made of ANSI 4140 steel material, as recommended by the manufacturer.

The calibration of the proximator is performed by moving the target until it almost touches the probe. The micrometer reading is zeroed for the sake of convenience and is moved away from the target at 0.05 mil (10 μ mm) intervals until the target goes out of range. At each interval, the voltmeter reading is recorded. The results obtained from this procedure are plotted as shown in Figure 2.2. The movement of the micrometer is plotted on the X-axis, and the voltage output is plotted on the Y-Axis. A linear fit to the data provides the calibration factor. In this case, the calibration factor is 217 V/in. (8.568 V/mm). The nominal calibration factor provided by the manufacturer is 200 V/in. (8 V/mm). The figure shows that the calibration is linear throughout the displacement range of the proximator ($R^2 = 0.99$), and the standard error of estimate is 0.1945. The calibrated proximator can then be used for the calibration of the reference geophone.



a) Schematic



b) Test Setup

Figure 2.1 - Proximitors Calibration Test Setup

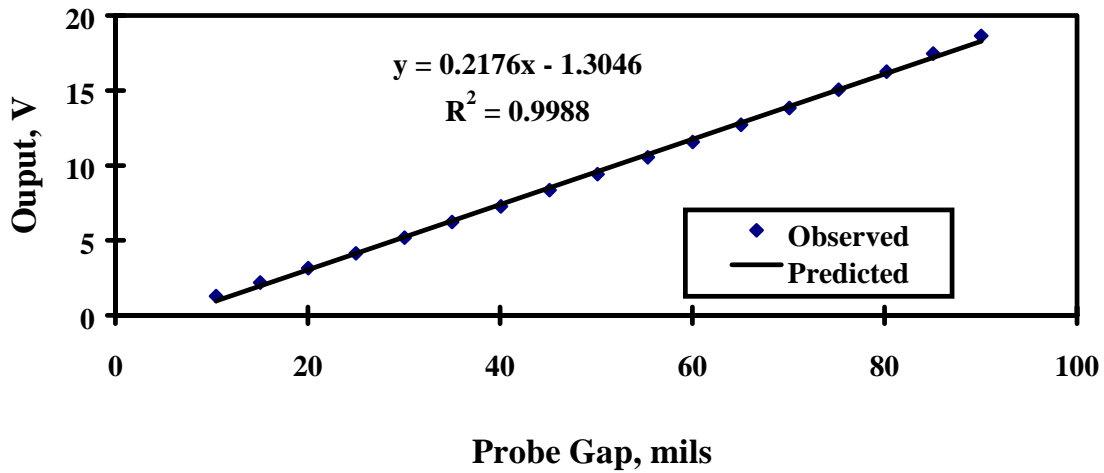


Figure 2.2 - A Typical Calibration Curve of a Proximator Probe

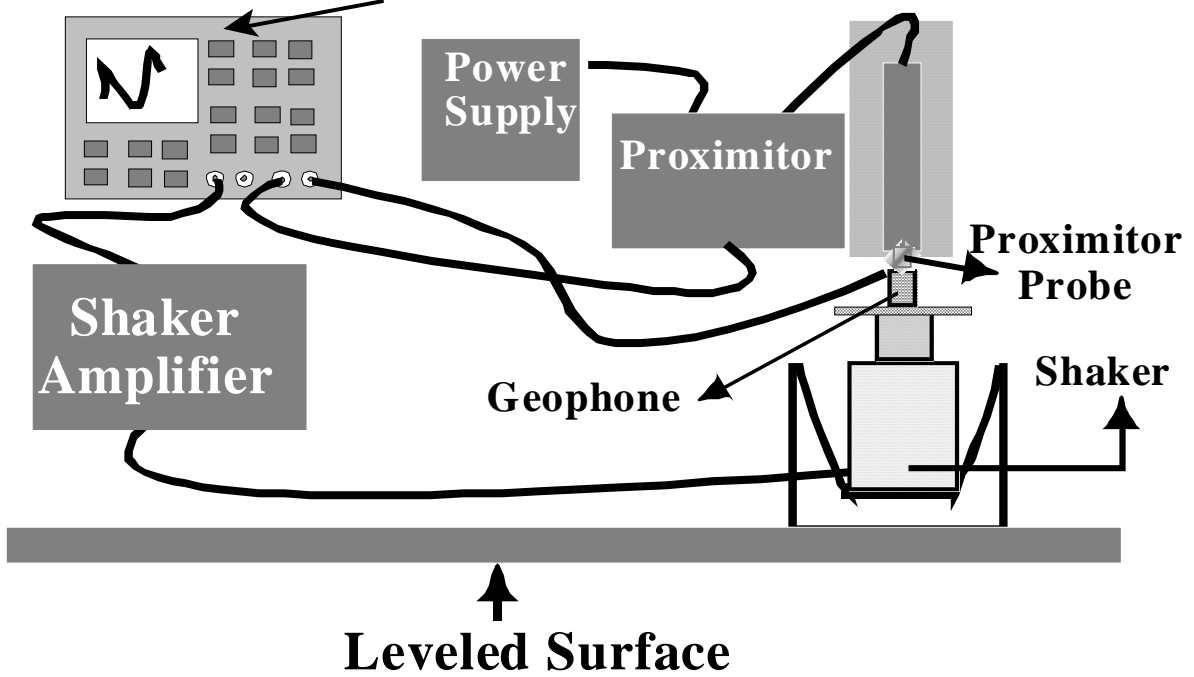
The range of movement within which the calibration factor is linear is specified by the manufacturer. The calibration should be carried out in that range. In addition, the calibration of the reference geophone should be performed by maintaining the gap between probe and target within the linear range. In general, the calibration factor of the proximator does not change with time. However, the proximator should be calibrated every year and whenever the target or the voltage supply is changed.

A test setup for the reference geophone calibration is shown in the Figure 2.3. The test setup requires a dynamic signal analyzer equipped with a random function generator, a shaker with an amplifier, a proximator transducer system and a geophone. The specifications for the devices used are included in Appendix A. The geophone is securely placed on top of the shaker, as shown in the figure. A target is placed on top of the geophone assembly such that the movement induced in the geophone and the target (for the proximator probe) is the same. This assembly is placed below a proximator probe such that the gap between probe and geophone is not outside the linear range of the proximator.

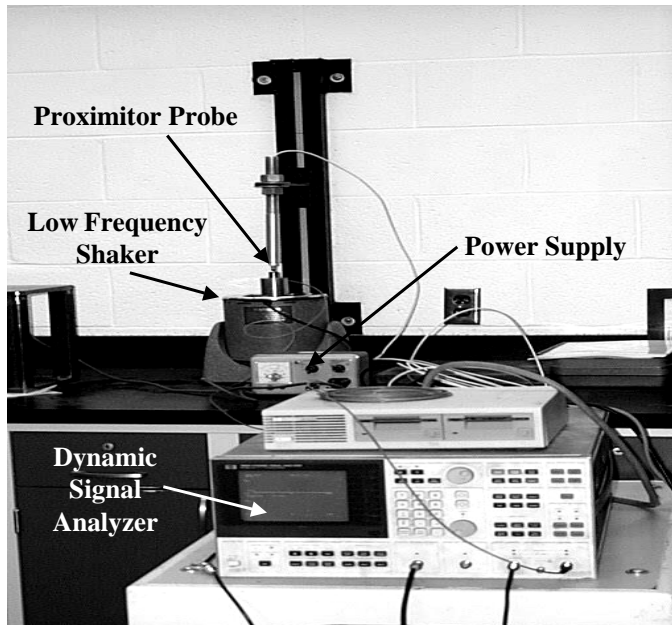
A random signal or a swept-sine signal in the frequency range of 0 to 50 Hz is sent to the shaker via the shaker amplifier. The random signal is recommended because the testing time is substantially shorter. Tandon and Nazarian (1991) have shown that the geophone response is very similar under both the random and swept sine signals. The response beyond 50 Hz is not considered since it is not of much significance to the performance of the geophone and since the response does not significantly change beyond that frequency.

The voltage outputs from the geophone and proximator are transmitted to the dynamic signal analyzer so that the frequency response and the coherence function from the outputs of the two signals are determined. A typical frequency response and coherence function are shown in Figure 2.4. As expected, the response is rather flat up to a frequency of about 5 Hz and rapidly increases above that frequency. The coherence function is practically equal to 1, corresponding to an

Dynamic Signal Analyzer with Random Function Generator



a) Schematic



b) Test Setup

Figure 2.3 - Test Setup for Geophone Calibration

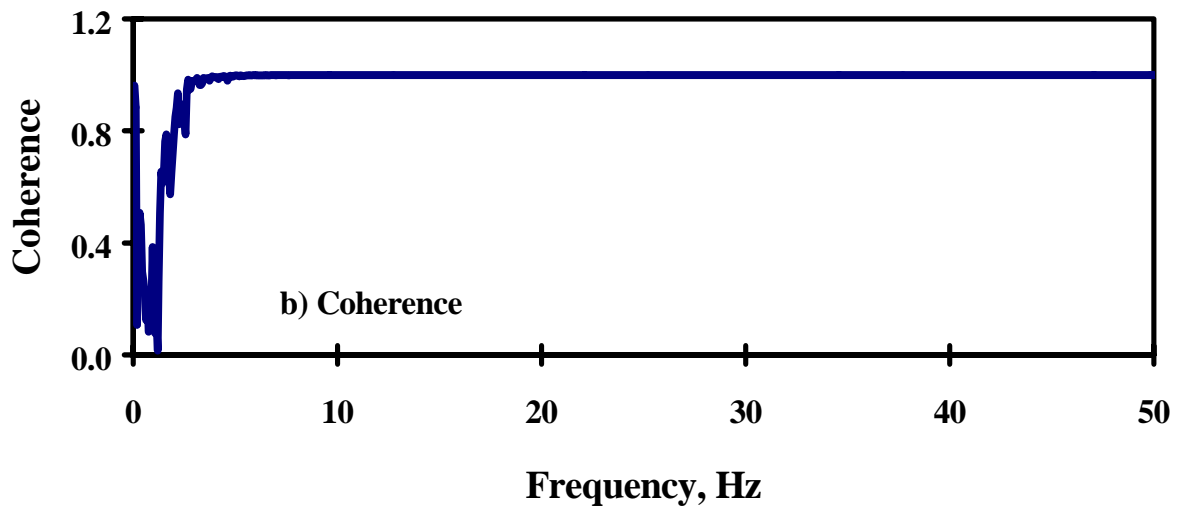
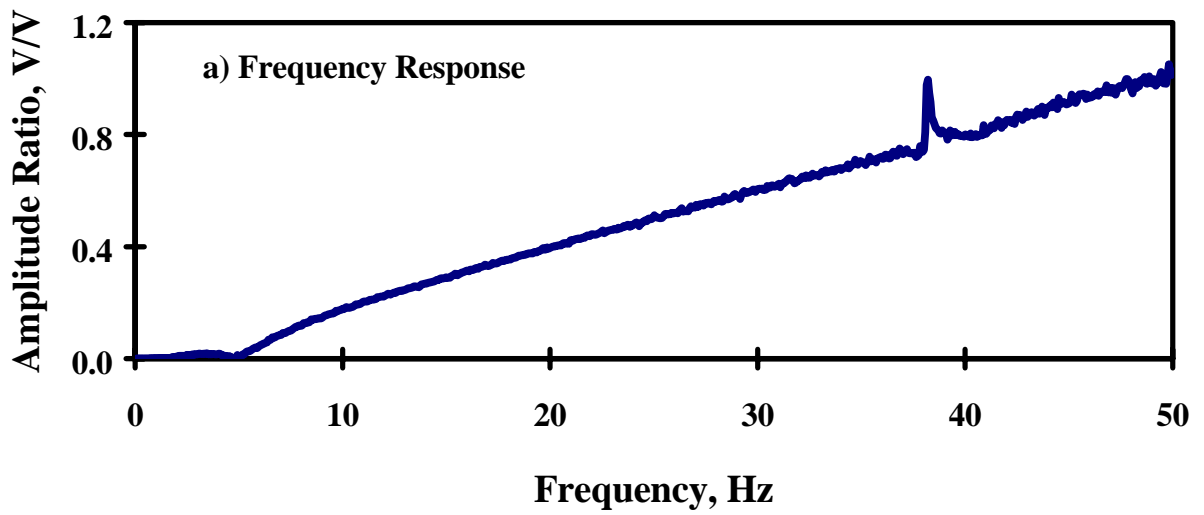


Figure 2.4 - A Typical Frequency and Coherence Response of Geophone

extremely high signal-to-noise ratio. Below a frequency of about 2 Hz, the coherence values are lower than 1, indicating lower quality data, which can be attributed to the performance of the shaker in that range. This problem can be readily eliminated by sending a swept sine signal rather than a random signal during the calibration process. However, the modified setup will increase the calibration period by a factor of 10. Many years of experience have shown that the difference in the extracted calibration parameters from the random signal and swept sine inputs is negligible. The localized peak at about 38 Hz in Figure 2.4a may be related to the setup. Since it is very localized, it would not impact the calibration parameters.

The output of a geophone is velocity and of a proximator is displacement. To determine the calibration parameters of the geophone, the frequency response is integrated. The integrated signal is divided by the calibration factor of the proximator to obtain the calibration curve of the reference geophone.

The calibration curves, after data reduction, are shown in Figure 2.5. In Figure 2.5a, the variation in amplitude with frequency is shown. The amplitude above a frequency of 15 Hz is constant. However, below that frequency, the amplitude gradually decreases. The variation in phase with frequency is shown in Figure 2.5b. A phase shift of 180 degrees is observed in the first 15 Hz of the phase spectrum. Both graphs exhibit the classical behaviors of a single-degree-of-freedom system. By fitting a curve to the data, the natural frequency, the damping ratio and the gain factor are determined.

A FWD geophone was disconnected from the trailer and was calibrated in the laboratory. The results are included in Figure 2.5 as well. The calibration curve is similar to the reference geophone. The constant amplitudes (of FWD geophone) at higher frequencies are smaller than the reference geophone. This observation indicates that the FWD sensor is less sensitive than the reference geophone. The phase characteristics from the two geophones are fairly similar, indicating that the natural frequencies and damping ratios are fairly similar.

Calibration of FWD Geophone

The calibration setup developed in the laboratory can be transported to the field. The difference is that the proximator is replaced by the reference geophone and the data analysis steps are modified.

A 16 in. (0.4 m) by 12 in. (0.3 m) utility box was incorporated in a 5.5 in. (140 mm) thick PCC slab, as shown in Figure 2.6. The shaker can be placed in the utility box below ground level. The depth of the box was selected to ensure that the top of the shaker table is flush with the surface of the slab. Thus, the FWD geophone holder can be easily placed on top of the shaker without any disassembly. The utility box surface, on which the shaker is placed, was leveled to minimize any eccentric movement of the reference, or the FWD, geophone.

A well-calibrated geophone (reference geophone) is securely placed on the shaker. The FWD geophone, in its holder, is then lowered onto the shaker using the FWD raise-lower mechanism. A random signal is sent to the shaker via an amplifier. The data is recorded using a setup similar to that of the laboratory calibration. In addition, a DC offset voltage is applied to the shaker to counterbalance the weight of the FWD holder on top of the shaker.

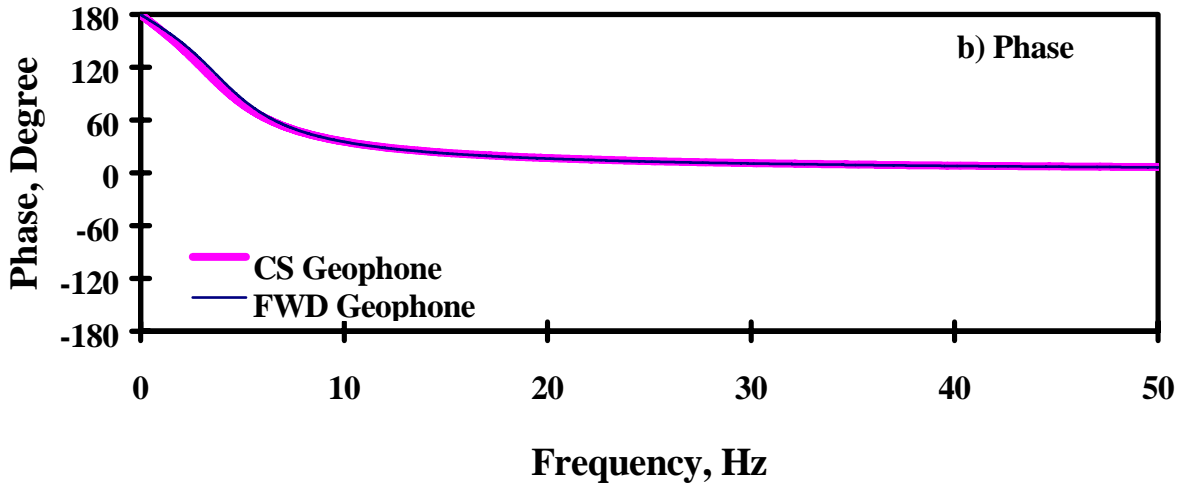
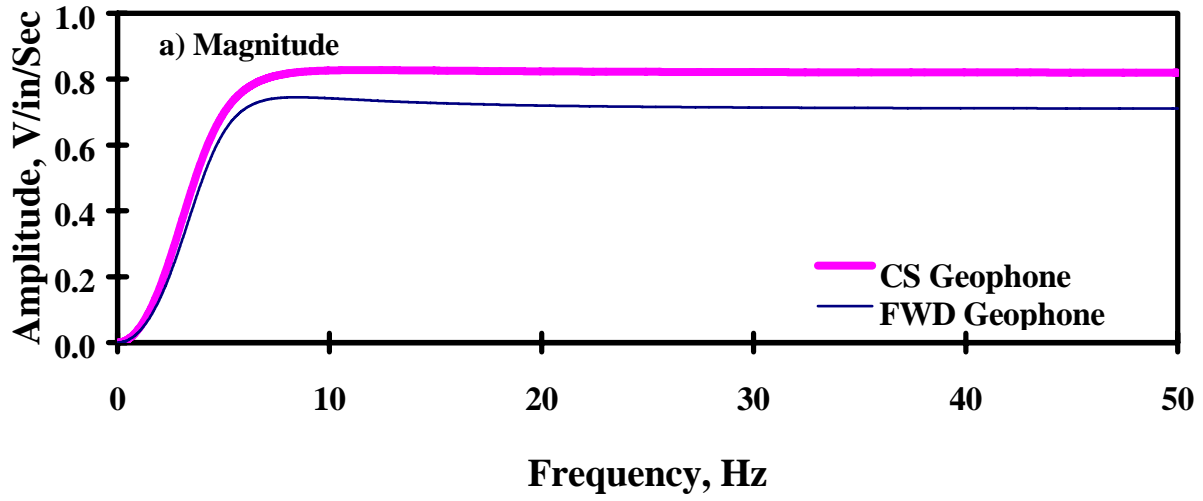


Figure 2.5 - Calibration Curves of Geophones

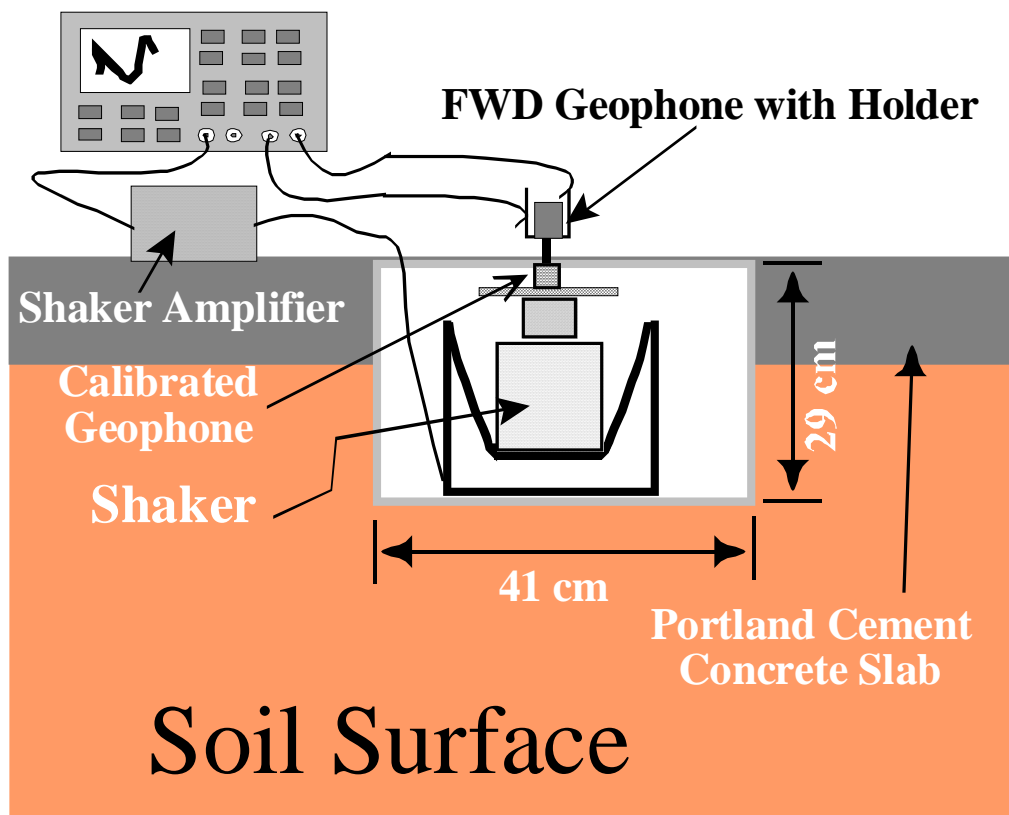


Figure 2.6 - A Schematic of Field Calibration of FWD Geophone

The results from one test are shown in Figure 2.7. The amplitude spectrum of the ratio of the outputs of the FWD geophone and the reference geophone is shown in this figure. If the calibration curve of the FWD geophone was identical to the reference geophone, the amplitude ratio would have been independent of frequency and equal to unity (Figure 2.7). The drop in the amplitude ratios, below a frequency of 5 Hz, indicates that the natural frequency of the FWD geophone is somewhat lower than that of the reference geophone. A peak at 5 Hz indicates that the FWD geophone is less damped than the reference geophone. The constant amplitude ratio of 0.9 in the range of frequencies of 10 to 30 Hz indicates that the FWD geophone has a gain which is about 10% less than that of the calibration geophone.

The results from the same experiment, when the FWD geophone was removed from its holder and securely placed on top of the shaker, are also shown in Figure 2.7. The difference between the two curves can be attributed to the interaction between the holder and the shaker. The two curves follow each other quite well up to a frequency of 30 HZ. At higher frequencies, the differences, on the order of 3 to 5 percent, can be observed. Such differences may adversely affect the deflections measured with the FWD, especially when full-waveform analysis has to be carried out.

If the frequency response curve shown in Figure 2.7 is multiplied by the calibration curve of the reference geophone obtained in the laboratory, the calibration curve of the FWD geophone can be obtained (Figure 2.8). The calibration curve of the FWD geophone is similar to that shown in Figure 2.5. The results of the calibration test setup indicate that the FWD geophone can be calibrated in its holder using the test setup of Figure 2.6.

Proposed Calibration Setup for the Load Cell

The SHRP and the Texas Calibration methods for the load cell are included in the ASTM standard D4694. The proposed calibration setup uses the same concept. Again, the reference load cells to be used are calibrated in the laboratory first. The calibrated load cells are then used in the field to calibrate the FWD load cells.

Calibration of Reference Load Cells

The calibration of the reference dynamic load cells is necessary to ensure that the behavior of the load cells does not change when they are mounted on the load cell plate. The laboratory calibration of the dynamic load cells, as shown in Figure 2.9, is done with the assistance of an MTS system. The load cell of the MTS system is well-calibrated, and the calibration is traceable to the National Institute of Standards and Technology (formerly known as NBS). The encased load cell is placed between the upper and lower platens of the MTS system. A seating load of about 100 lb (450 N) is applied to ensure proper contact between the load cell and the platens. A haversine wave dynamic loading with a duration of 0.1 sec is used. The dynamic load magnitude is changed to cover the range of loads observed in the field. The peak load obtained from the MTS load cell and the peak voltage obtained from the dynamic load cells are recorded for five cycles at each dynamic load magnitude.

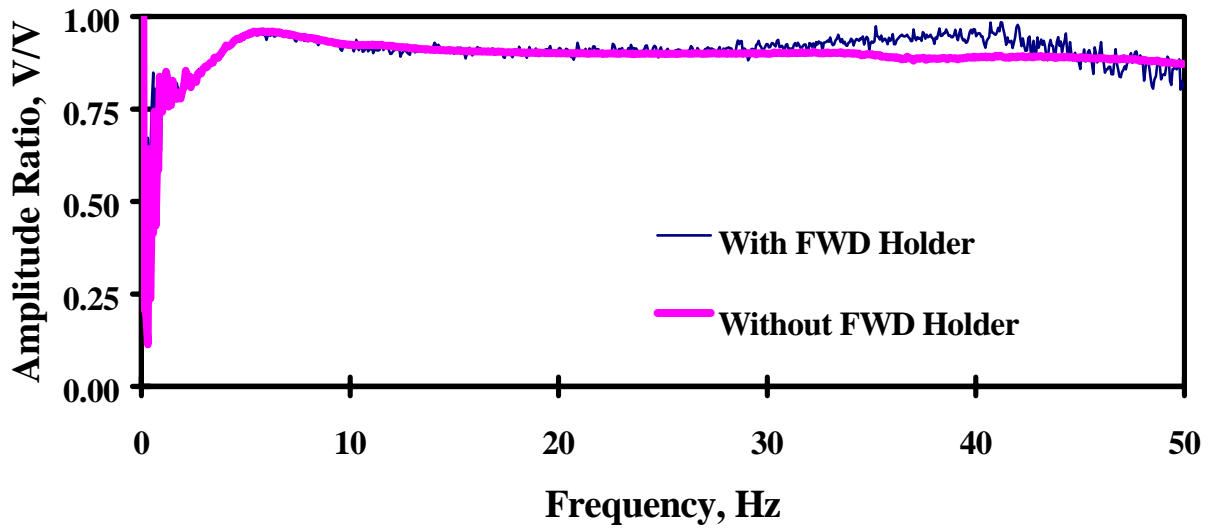


Figure 2.7 - In-Place Calibration of FWD Geophone

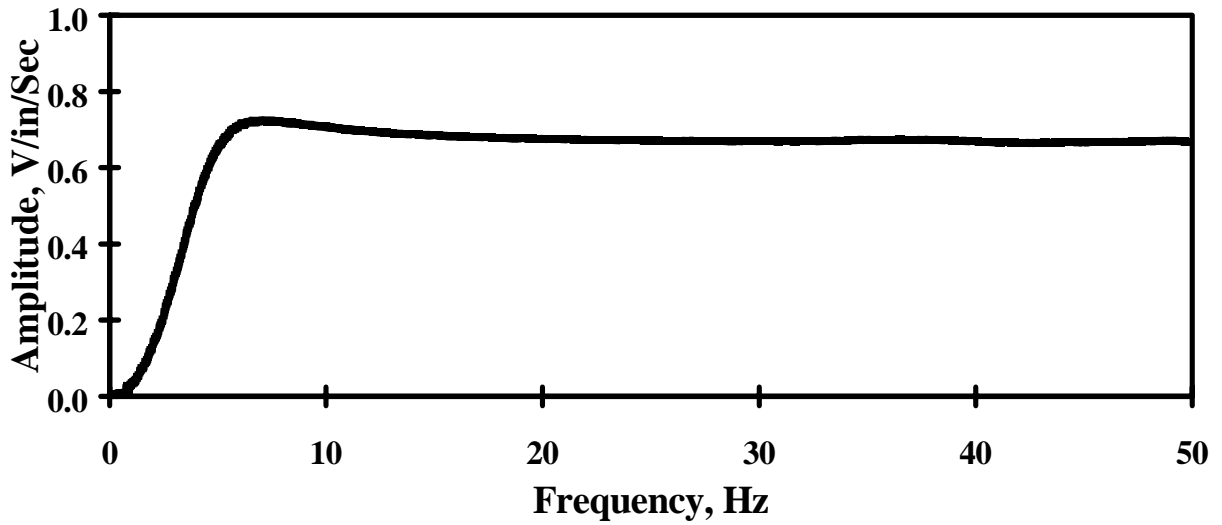


Figure 2.8 - A Calibration Curve of a Typical FWD Geophone

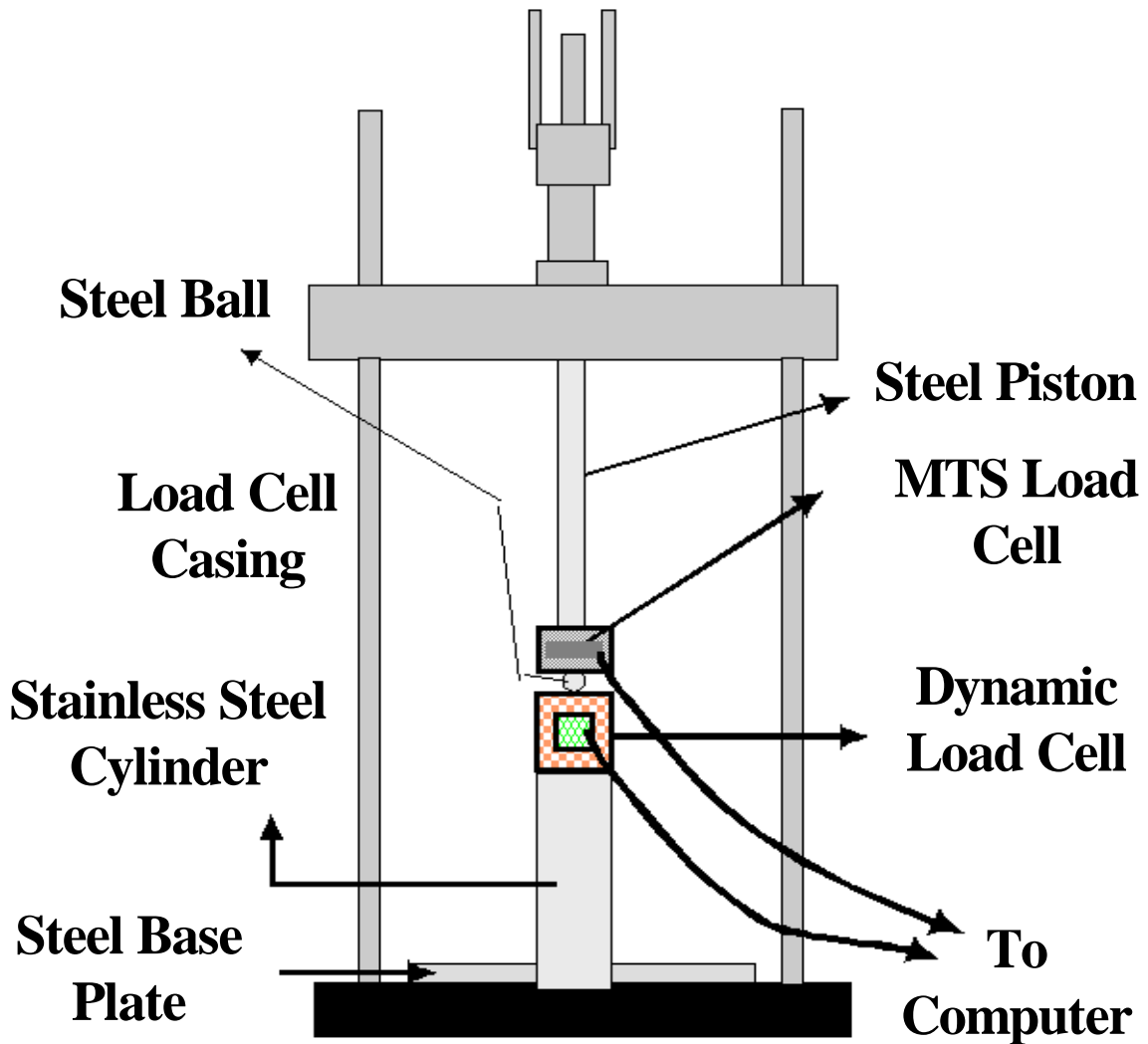


Figure 2.9 - A Schematic of Load Cell Calibration in the Laboratory

The results from all cycles and load levels are correlated to determine the calibration constant of the load cell.

The results from one test are shown in Figure 2.10. The X-axis is the applied load as measured by the MTS load cell, and the Y-axis is the voltage measured from the dynamic load cell. A least-squares best fit line through the data points yielded a calibration factor of 0.8 V/kip. The coefficient of determination (R^2) is 0.99, and the standard error of estimate is 0.025. Similarly, the other two reference load cells can be calibrated in the laboratory.

Calibration of the FWD Load Cells

The calibration of the FWD load cell can be performed using the Texas Calibration method with slight modifications, as shown in Figure 2.11. A recess is made in the PCC slab to accommodate the calibration plates. The depth of the recess is such that the top plate is flush with the slab surface. The advantage of this method, aside from convenience, is that lateral movement of the bottom and top plates is minimized. This procedure for calibration is similar to the Texas Calibration method and can be found in Research Report 913-1.

Comparison of FWD Calibration Results

A TxDOT FWD was loaned to UTEP for a comparison of calibration methods and for an evaluation of the proposed calibration test setup. The results from this activity are reported in the following sections. The characteristics of the geophones are reported first. The results obtained from the SHRP, the Texas Calibration, and the newly proposed test setups are then compared.

Characteristics of Geophones

The characteristics of the reference and the FWD geophones were obtained using the calibration curves of the geophones measured as per the proposed test setup. As the calibration curves of the two geophones indicate in Figure 2.5, the responses of the two geophones are similar. A detailed explanation of the characteristics of a geophone and the mechanical and electric model that describes it can be found in Nazarian and Bush (1988). A brief description is provided here. The components of a typical geophone and its mechanical equivalent are shown in Figure 2.12. The mechanical model resembles a single-degree-of-freedom (SDOF) system with a mass suspended over a spring and a dashpot. To obtain the characteristics of the geophone, the natural frequency of the system, the damping ratio of the dashpot, and the stiffness of the spring have to be determined.

The natural frequency of the geophone defines the initial slope of the calibration curve (Figure 2.8). Nazarian and Bush (1988) suggested that the natural frequency should be much lower than the impulse frequency (or the natural period should be much greater than the impulse period) of the system; thus, the shape of the load impulse does not affect the response of the geophone. Therefore, the natural frequency of the geophones is of importance both in terms of defining the calibration curve as well as a response due to the FWD load impulse.

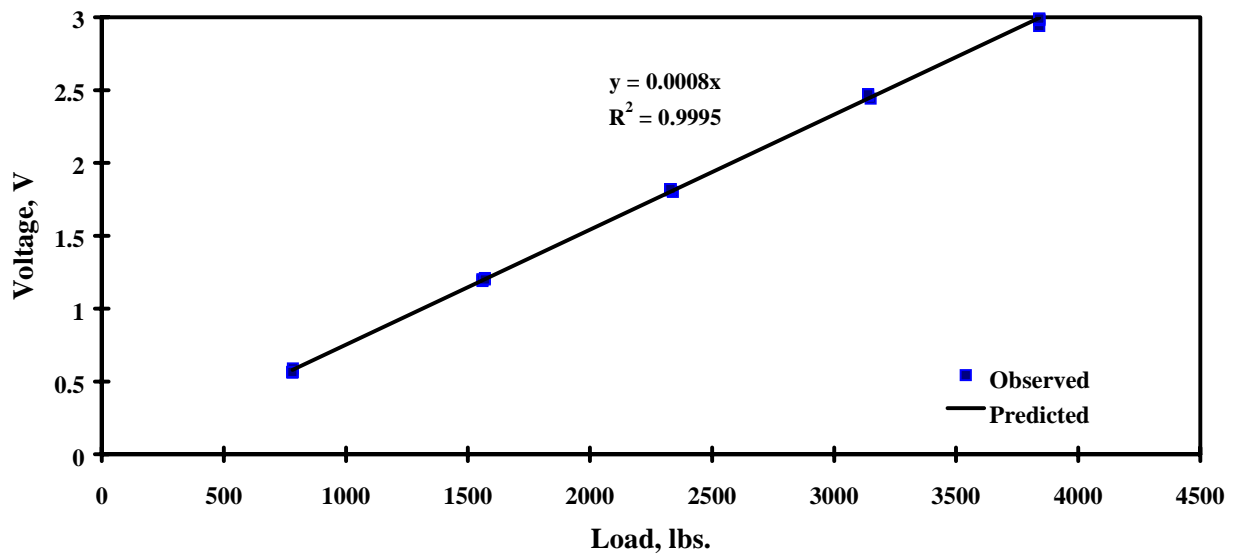


Figure 2.10 - A Typical Calibration Curve for a Reference Load Cell

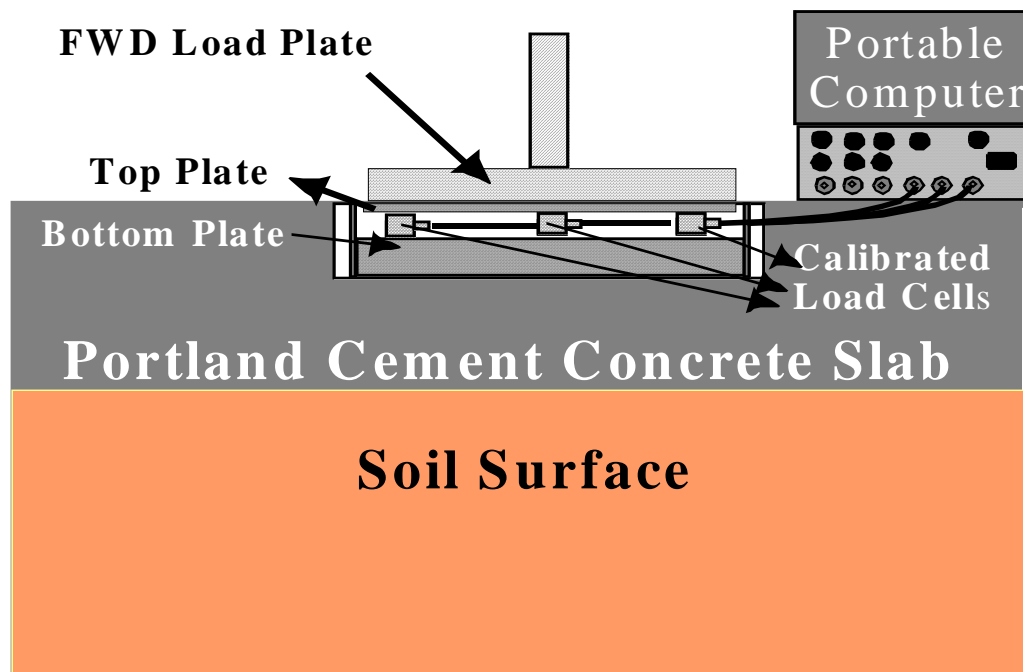
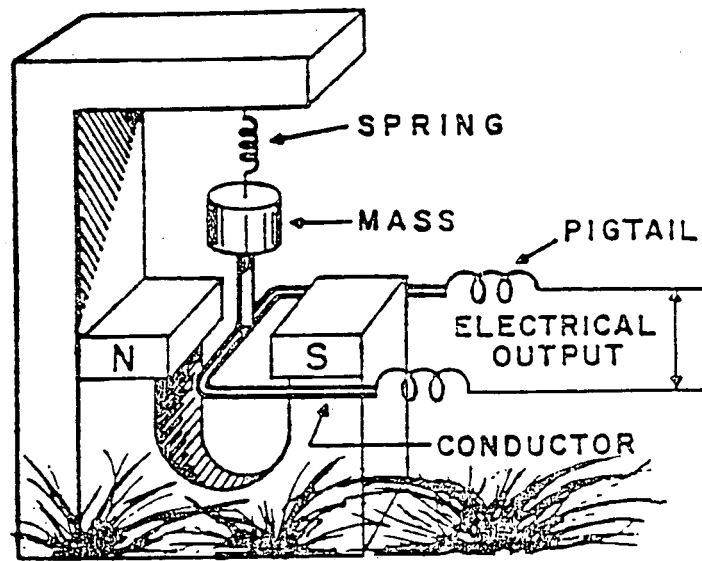


Figure 2.11 - A Schematic of FWD Load Cell Calibration



a) Elements of Geophone (from Mark Products, 1985)

b) Idealized Model

Figure 2.12 - Components and Mechanical Model of Geophone

The damping ratio dictates the attenuation of the motion with time. The damping ratio of a geophone indicates how quickly a geophone coil magnet system stops moving after an impact. Ideally, the movement should attenuate shortly after the impulse is applied.

The stiffness of the spring dictates the voltage output of the geophone, which is called the gain factor. The factor of proportionality between the velocity and the output voltage is defined as the gain factor. The gain factor of the geophone is represented in units of volts/velocity. A geophone with a high gain factor is considered to have high sensitivity. A geophone with high sensitivity can measure small motions more accurately.

To extract the three parameters that define the response of the geophone, a particular master curve has to be fitted to the frequency response measured during the calibration. The master curve that best describes the response of the geophone, $R(f)$, is in the form of the following polynomial

$$(2.1)$$

where: f = frequency, $s = j(2\pi)f$, $j = \sqrt{-1}$, and G = gain factor. In this equation, parameters z_1 and z_2 are called the zeros and p_1 and p_2 the poles. Once the poles and zeros are obtained, the natural frequency, damping ratio, and gain for each geophone can be readily obtained as described in Nazarian and Bush (1988).

The characteristics of the two geophones are summarized in Table 2.1. The geophone used in the calibration system is slightly more sensitive and slightly more damped than the FWD one. This exercise shows that the FWD sensors can be readily calibrated.

Table 2.1 - Geophone Characteristics

Geophone	Natural Frequency, Hz	Damping Ratio, percent	Gain, v/in/sec
FWD	4.38	57.7	0.71
Calibration System	4.42	65.4	0.82

The results from a typical calibration of a FWD using the Texas System are summarized in Figure 2.13. Two calibration methods were used. In the first method, the geophone of the calibration system was placed next to the FWD sensor while it was in its holder. In the second experiment, a holder, similar to the one used in the SHRP calibration protocol, was secured to a slab. The FWD geophone and the geophone of the calibration system were rigidly attached to the holder. As reflected in Figure 2.13, the calibration factor for the FWD geophone changed from 0.92 to 0.97 when the placement system changed. The difference can be attributed to the interaction between the FWD sensor and the sensor holder. Also, the levels of the deflections obtained from tests were not similar. The reason for this is that in the SHRP protocol the loading plate is moved until the sensor experiences a deflection of 15 mils. However, in the Texas system, the sensors are calibrated in their respective holders. This experiment demonstrates the importance of calibrating the FWD sensors in their original holders along the range of deflections they usually experience.

Calibration with Proposed System

Following the SHRP recommendation, the calibration has to be performed on a thin concrete slab with a very weak subgrade. The researcher's interview with the operators of the four SHRP regional centers (under Project 7-2935) indicated that all four centers had carefully designed their slabs to obtain desired deflections. Vibration isolation between the block holding the LVDT and the slab was of concern. To minimize the cost of construction and to improve the stability of the calibration facility, it may be desirable to use a shaker to apply a half sine-wave impulse instead of a FWD impulse. To test this concept, one of the sensors of the FWD was placed on the shaker located in the utility box under the slab (Figure 2.6). A 30-msec pulse was applied to the shaker using a signal generator. The raw voltage from the FWD and the reference geophones are shown in Figure 2.14. The two curves follow each other quite well, except that the voltage measured by the reference geophone is slightly higher. This difference in the amplitude is due to the fact that the reference geophone has higher sensitivity. The abrupt change in the slope of the curves coincides with the completion of the 30 msec impulse. The actual displacements obtained from the two geophones, as shown in Figure 2.15, indicate that the two geophones experience similar deflections.

This calibration method can be used for all the geophones of the FWD and for a wide deflection range. The only change to the setup is the amplitude of the impulse. The advantage of this method is that calibration and verification are easier as compared to SHRP or the Texas method. Another added advantage is that the whole deflection time history can be obtained to estimate the dynamic modulus.

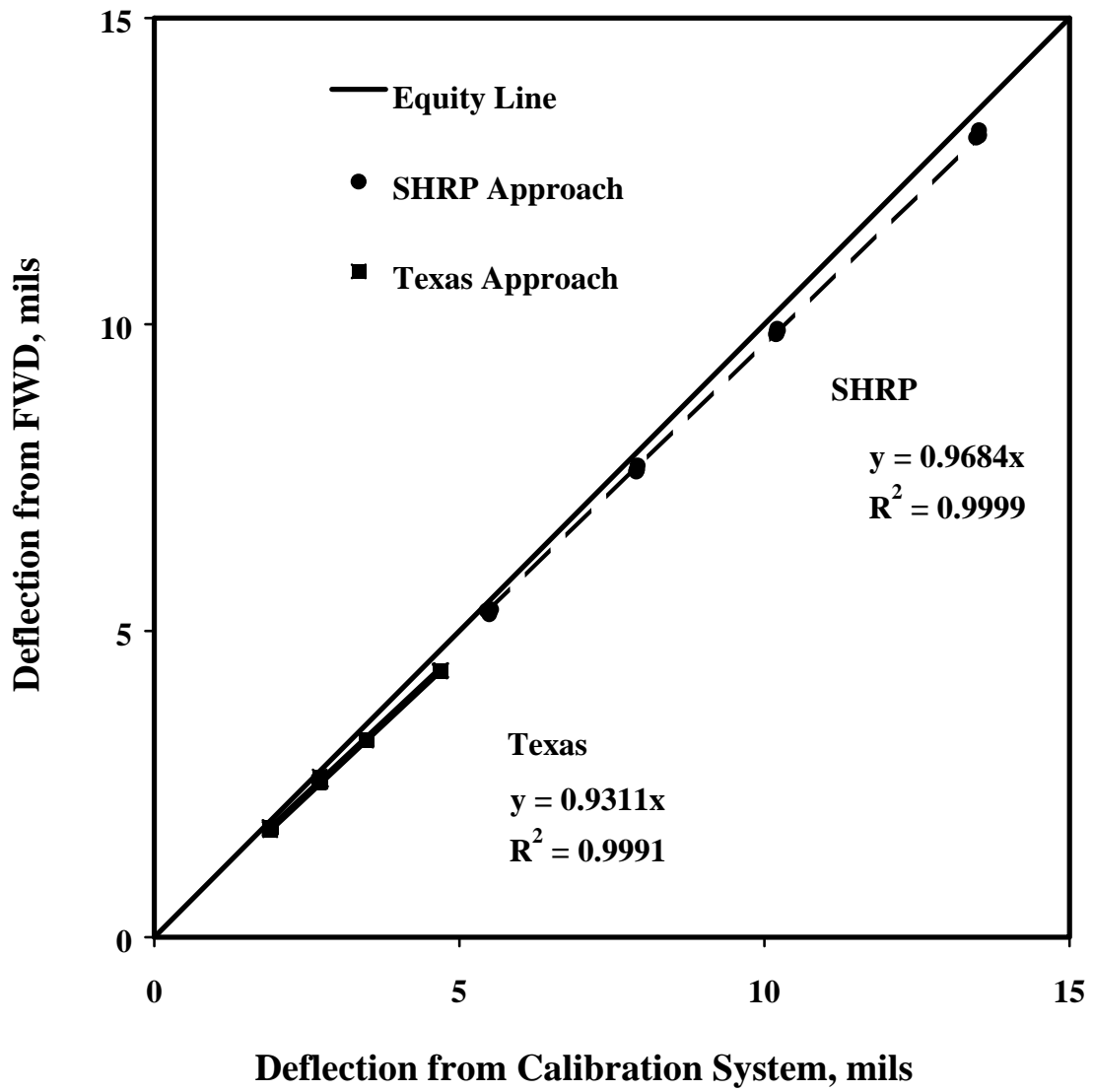


Figure 2.13 - Comparison of Calibration Factors from SHRP and Texas Protocols

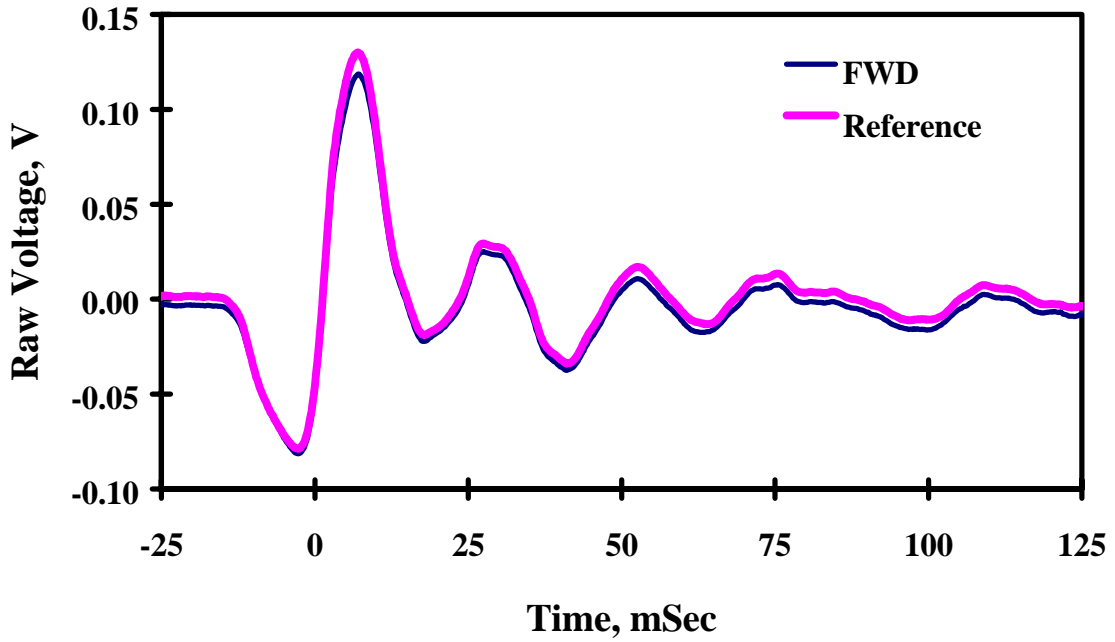


Figure 2.14 - Comparison of Raw Geophone Outputs Under a 30 msec Impulse

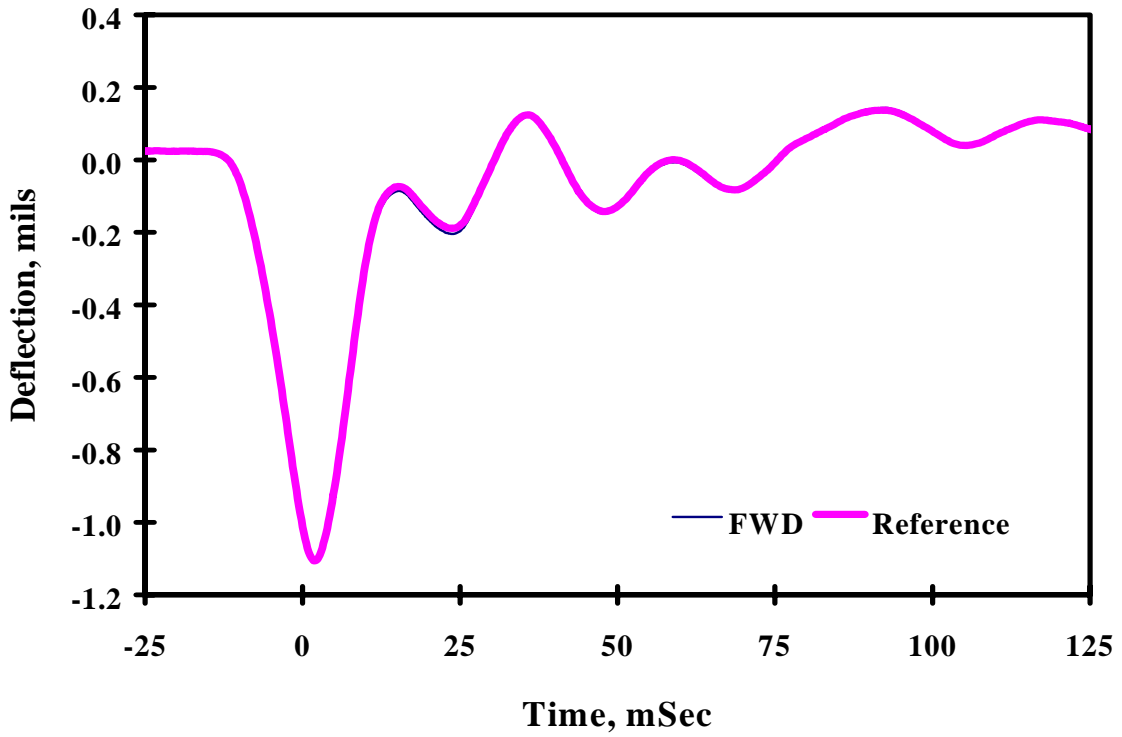


Figure 2.15 - Comparison of Deflections Obtained from Geophones Under 30 msec Impulse

FWD Calibration Strategy

Various procedures available for the calibration of FWDs are discussed in the previous sections. In this section, a preliminary strategy for determining the suitability of new parts, the adequacy of existing components, and an overall calibration procedure are described.

A flow chart summarizing the three calibration procedures is included in Figure 2.16. The SHRP calibration process can be divided into two phases: the relative and the reference calibration procedures. The SHRP procedure is well defined and is not discussed any further. The Texas and proposed procedures also consist of two phases: tests at the laboratory of the calibration facility and tests at the calibration slab. Each step was described in the previous sections.

FWD Geophone Calibration Strategy

A flow chart describing the steps which should be taken for the calibration of geophones is included in Figure 2.17. To successfully calibrate the geophone, the following steps should be followed:

1. Perform a calibration of the FWD using the Texas method proposed in Project 913 since this method considers the combined impact of the electronics, geophone and holder. If the geophone response is acceptable and the FWD is not used for full-waveform analysis, the calibration can be considered complete.
2. If the FWD geophone does not reproduce the results obtained from the Texas calibration system, perform additional tests using the calibration slab. Calibrate the geophone in the holder and geophone directly (as described previously and as summarized below) to identify whether the geophone or the geophone holder is contributing to the change in the performance of the FWD or if the electronic components require adjustment or replacement. Replace the appropriate component as described below. If the geophone seems to be the problem, conduct a laboratory calibration for troubleshooting.
3. If the device has to be used for full-waveform analysis, calibrate the geophone in the holder. The calibration curve should be incorporated in the analysis software since the FWD software is proprietary.

Reference Geophone Calibration Strategy

The deflection measurements obtained from a geophone may become inaccurate either because the geophone unit is performing poorly, the holder is worn out, or the processor is faulty. To perform the calibration of geophones, it is essential to ensure that the reference geophones and the proximator are functioning properly and are calibrated. The make and specifications of the proximator and geophone used in this study are included in Appendix A.

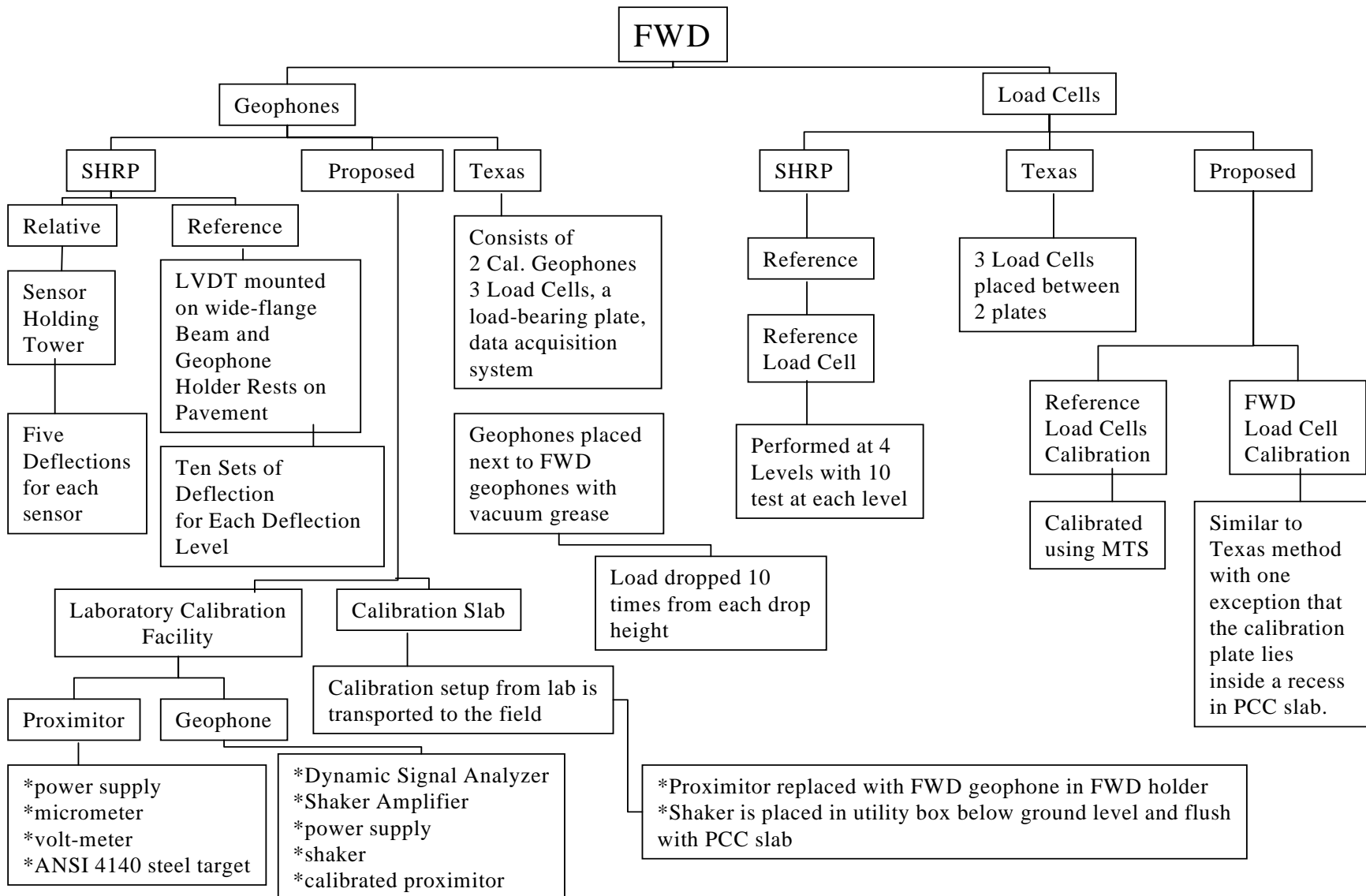


Figure 2.16 - Flow Chart Summarizing FWD Calibration Steps

FWD Geophone Calibration Strategy

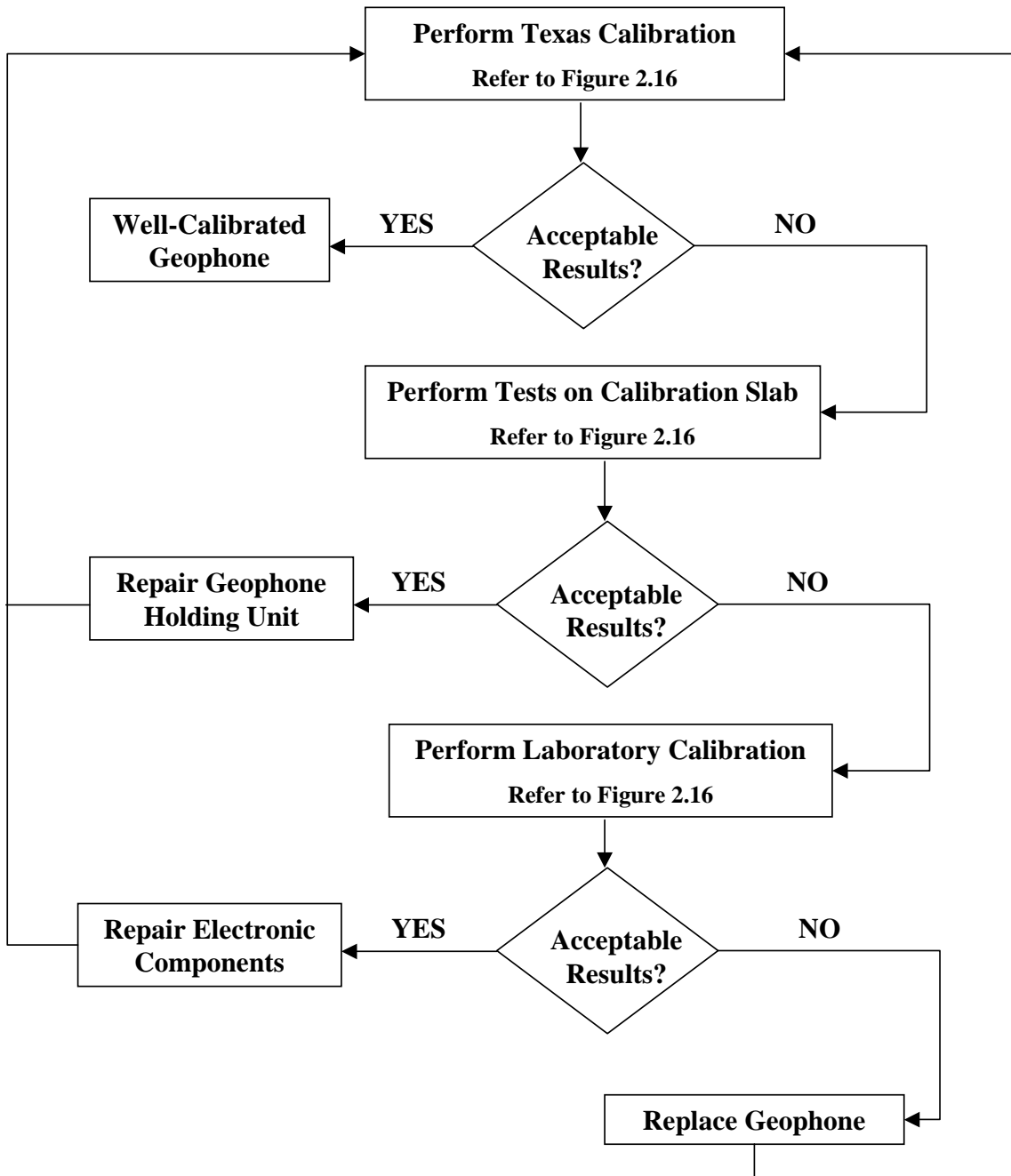


Figure 2.17 - FWD Geophone Calibration Strategy

The proximator has a nominal calibration factor of about 200 mv/mils (7.8 mv/ μ m) and a range of about 80 mils (2 mm). A calibration of the proximator is necessary whenever the target or the power source is changed. In the researchers' 10 years of experience, the calibration factors observed in the laboratory are typically within $\pm 10\%$ of nominal value proposed by the manufacturer. The distance range, along which the proximator's calibration is linear, is almost always wider than those suggested by the manufacturer. Therefore, in the researchers' opinion, that range can be used with confidence.

The geophones have a nominal natural frequency of about 4.5 Hz, a damping ratio of about 70 percent, and a gain (referred to as transductivity by the manufacturer) of about 800 mv/in./sec (30 mv/mm/sec). The manufacturer specifies a variation of about 10% from the nominal values. Our fifteen years of experience with a large number of geophones concur with that value.

After the laboratory calibration of 15 FWD geophones, a typical TxDOT FWD geophone has a natural frequency of about 4.5 Hz, a damping ratio of about 60% and a gain factor of about 700 mv/in./sec (28 mv/mm/sec). A coefficient of variation of about 10% has been observed for all parameters. Based on experience, the geophones obtained from TxDOT for their FWD fleet should be calibrated in the laboratory as soon as they are acquired to ensure that the calibration parameters are within 10% of the nominal values suggested by the manufacturer or distributor. If the laboratory calibration of the FWD or the reference geophone does not meet the above specifications, it should be replaced. Calibration records should be maintained for future reference. After a satisfactory laboratory calibration, the geophone can be transferred to the FWD.

To optimize the calibration process, the researchers propose that the Texas calibration procedure developed under Project 7-913 be used first to calibrate the FWD geophone in the holder. With the new breakthrough in the triggering mechanism and a new LABVIEW-based software, this system should be rather rapid and easy to use. In addition, since this system is portable, it may be possible to perform the preliminary calibration in the districts. Whenever a FWD does not calibrate properly or if an FWD has to be used for full-waveform analysis, it can then be calibrated using the proposed calibration method as described next.

Geophone Holder Calibration Strategy

To determine whether the holder is impacting the response of the system, the voltage output of the geophone is monitored at the junction box located on the trailer. The setup shown in Figure 2.6 should be used, where the FWD geophone can be placed on top of the well-calibrated geophone. The calibration should be performed two times for each geophone: once within the holder and once by directly placing the FWD geophone on top of the shaker. The calibration steps are shown in Figure 2.18. The results from the two calibrations should be plotted as shown in Figure 2.7. Both curves should follow each other for the tested frequency range. If the two curves significantly deviate from each other, one can conclude that the holder requires maintenance or replacement. At this point, the researchers do not have enough data to propose a definite guideline. However, it can be safely proposed that if, after obtaining the calibration curve of the geophone system (see Figure 2.8), the natural frequency, damping ratio, or gain factors differ by more than 10%, the holder should be maintained.

Calibration of FWD Geophones (With or Without Holders)

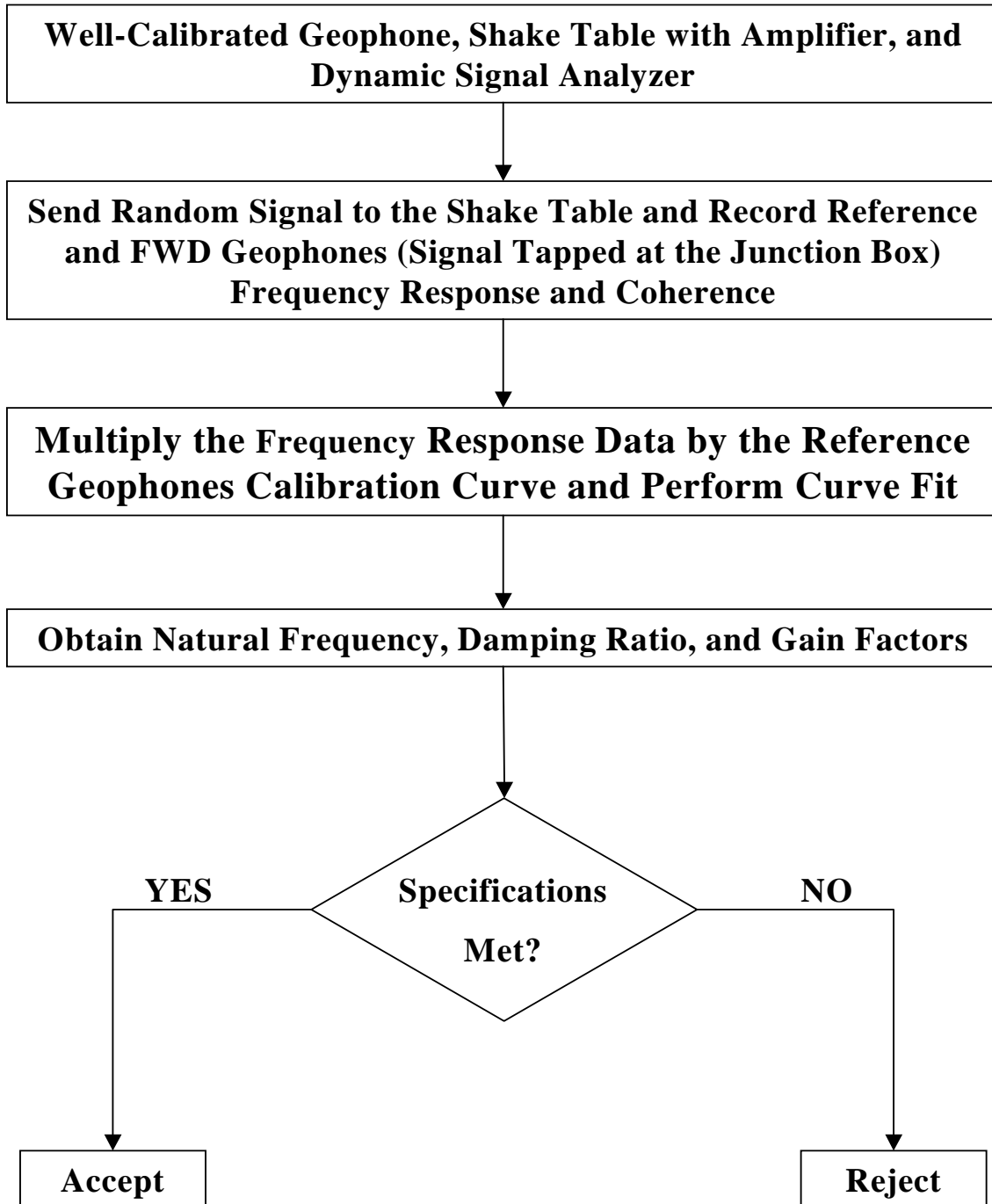


Figure 2.18 - Steps for the Calibration of Geophone Holders

If the calibration curves obtained with the geophone secured directly on the shaker and placed in the holder are similar, but the calibration parameters have significantly changed, the geophone unit by itself may be damaged. The preliminary criteria, suggested above, for the evaluation of the reference geophone are also applicable to this situation.

On the occasions when the geophone and the geophone holders seem to be performing satisfactorily, the electronic components and the processor should be evaluated. The FWD software normally conducts a set of electronic tests to ensure that the electronic components are functioning normally. Because of the proprietary nature of the hardware and software of the FWD, conducting further diagnostics should be done in consultation with the manufacturer.

FWD Load Cell Calibration Strategy

The specifications for the three reference load cells used in the calibration device are included in Appendix A. The nominal capacity of each load cell is about 5 kips (18 kN). The vendor provides a calibration sheet with each device, which is traceable to NIST. In our experience, the calibration provided is very accurate and can be readily used. The placement of the load cells on the calibration plate somewhat alters their calibration factors. A laboratory calibration of the reference load cell should be performed to fine-tune the calibration factor. The adjusted calibration factor is usually within 5% of the one provided by the manufacturer. The calibration factor measured in the laboratory should be used for the calibration of the FWD load cell. The test setup for the calibration should be similar to that shown in Figure 2.9. It is proposed that the reference load cells be calibrated annually. If the calibration factors vary by more than 5%, the load cells should be repaired or replaced by the vendor.

The information about the FWD load cell is difficult to obtain from the manufacturer. Hence, a strategy in terms of acceptance or rejection at the time of delivery could not be suggested. However, the development of a strategy can be further explored in future research.

The UTEP research team is developing a break-out box for collecting raw data from the FWD processor. The newly delivered FWD can be tested, and the FWD load cell data can be collected. The voltage obtained from the break-out box can be compared with the loads reported by the FWD software to obtain load cell calibration factors. These calibration factors can be used in the future calibrations. In other words, calibration factors measured at the time of delivery can be compared to the calibration factors measured after one or two years of usage. If the factor changes less than 3%, then the calibration factor should be adjusted. For larger differences, the connection of the FWD load cell to the system should be inspected and repaired. In addition, the FWD load cell seating along with seating screws should be inspected and repaired. A recalibration of the load cell should be performed. If the difference is still larger than 3%, then the load cell should be replaced.

Another alternative is that the FWD load cell can be calibrated using the proposed calibration procedure at the time of delivery and that the calibration factors can be obtained. An acceptance and rejection strategy similar to the one explained in the previous paragraph can be followed.

Chapter 3

Portable Seismic Pavement Analyzer

The Portable Seismic Pavement Analyzer (PSPA) has been developed at UTEP (Baker et al., 1995). The PSPA uses wave propagation techniques to estimate the modulus and layer thickness of PCC or AC pavement layers. A standard calibration procedure does not exist for the PSPA because it has been only recently developed. Since the usage of this device is increasing, a calibration procedure for the sensors used in the PSPA is needed.

A schematic of the PSPA is shown in Figure 3.1. The device consists of two accelerometers (receivers) and a source (hammer). A typical test with the PSPA consists of impacting the pavement with the source and monitoring the propagation of seismic energy sensed by the accelerometers. The recorded data are interpreted in two ways.

First, the Ultrasonic Surface Wave (USW) method or the Ultrasonic Body Wave (UBW) method are used for determining the modulus of the layer. In these methods, the interpretation of the results includes the direct or indirect determination of the velocity of waves propagating between the two accelerometers. In this case, the focus of the calibration procedure is to ensure that the travel time measured between the two PSPA accelerometers is not altered by the electronic components of the PSPA or affected by the method used to mount the sensors. In other words, if the two accelerometers are placed the same distance from the source, the difference in travel time between them should be equal to zero. Technically, this translates to ensuring a zero phase shift between the response of the two accelerometers over the range of frequencies of interest.

Second, the Impact-Echo (IE) method is used to determine the thickness. In this method, the resonant frequency associated with the wave energy trapped within the top layer is of interest (Nazarian et al., 1997). Therefore, one should ensure that the characteristics of the accelerometer or the mounting system are not interfering or contaminating the response from the pavement.

In this chapter, a calibration method is proposed for the calibration of accelerometers for both USW and IE methods. In addition, a calibration strategy is proposed for future calibrations by TxDOT.

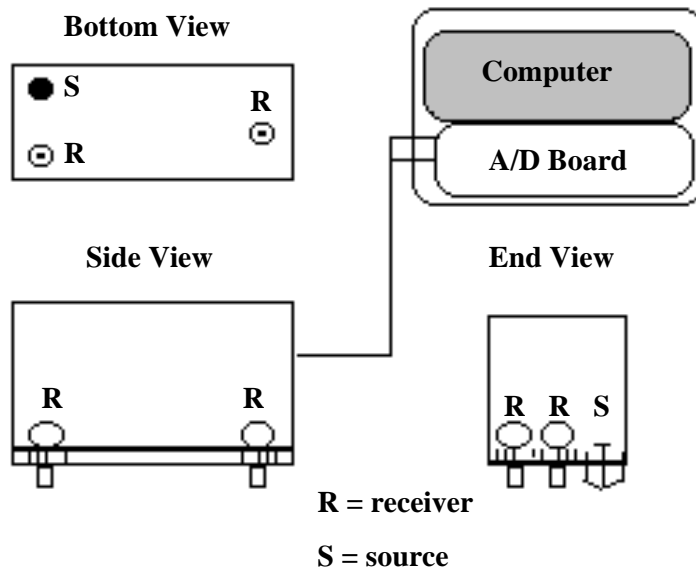


Figure 3.1 - Schematic of Portable Seismic Pavement Analyzer

Proposed Calibration of Accelerometers

The accelerometers used in PSPA need to be calibrated for a phase shift as well as for amplitude. The phase shift calibration factors are needed for USW and UBW tests, and the amplitude calibration factors are needed for the IE tests.

Phase Shift Calibration

The setup required for calibrating the PSPA is shown in Figure 3.2 and 3.3. This setup includes a rather heavy metal frame that can hold the PSPA in place and a high-frequency shaker. A combination of piezoelectric and electromagnetic shakers, which work in the range of frequencies of 10 Hz to 40 KHz, was found suitable for this task. The shaker is equipped with a built-in accelerometer with NIST-traceable calibration. The shaker assembly, which can be leveled as needed, is moved under each of the two accelerometers of the PSPA. The outputs of the built-in accelerometer and the PSPA accelerometers are connected to a dynamic signal analyzer for real-time analysis. A break-out box is needed to conveniently access the outputs of the PSPA accelerometers. The shaker is excited in a swept-sine mode in a range of frequencies of 100 Hz to 100 kHz using a built-in feature of the dynamic signal analyzer.

To eliminate the need to disassemble the PSPA for calibration, the behavior of each of the two accelerometers is compared with the shaker's built-in accelerometer first. Assuming that the characteristics of the calibration system do not change, by comparing the calibration of the two PSPA accelerometers relative to the built-in accelerometer, one can determine the phase shift calibration. The calibration curve is the ratio of the transfer functions of accelerometers 1 and 2

Dynamic Signal Analyzer with Random Function Generator

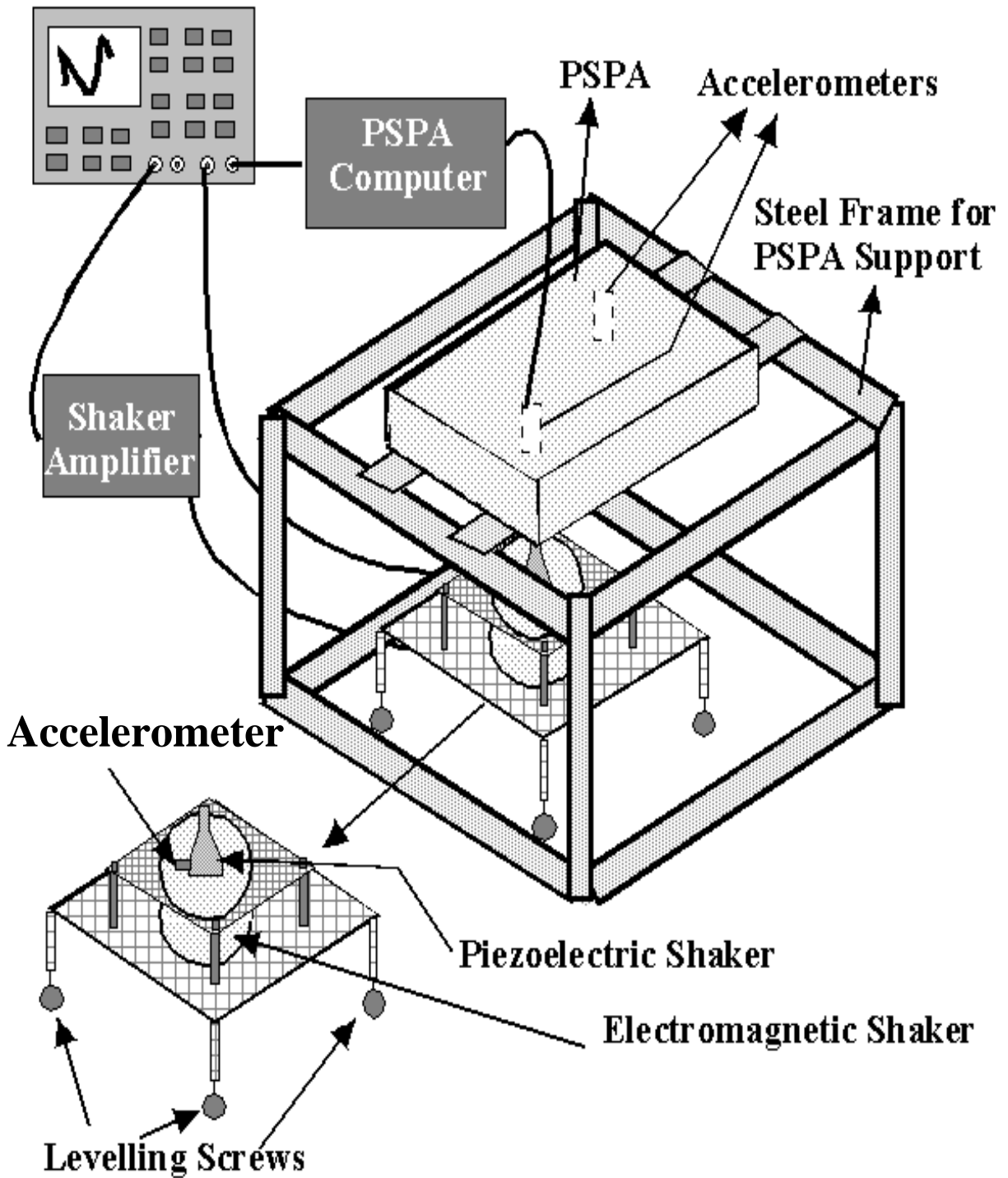


Figure 3.2 - A Schematic Diagram of PSPA Calibration System

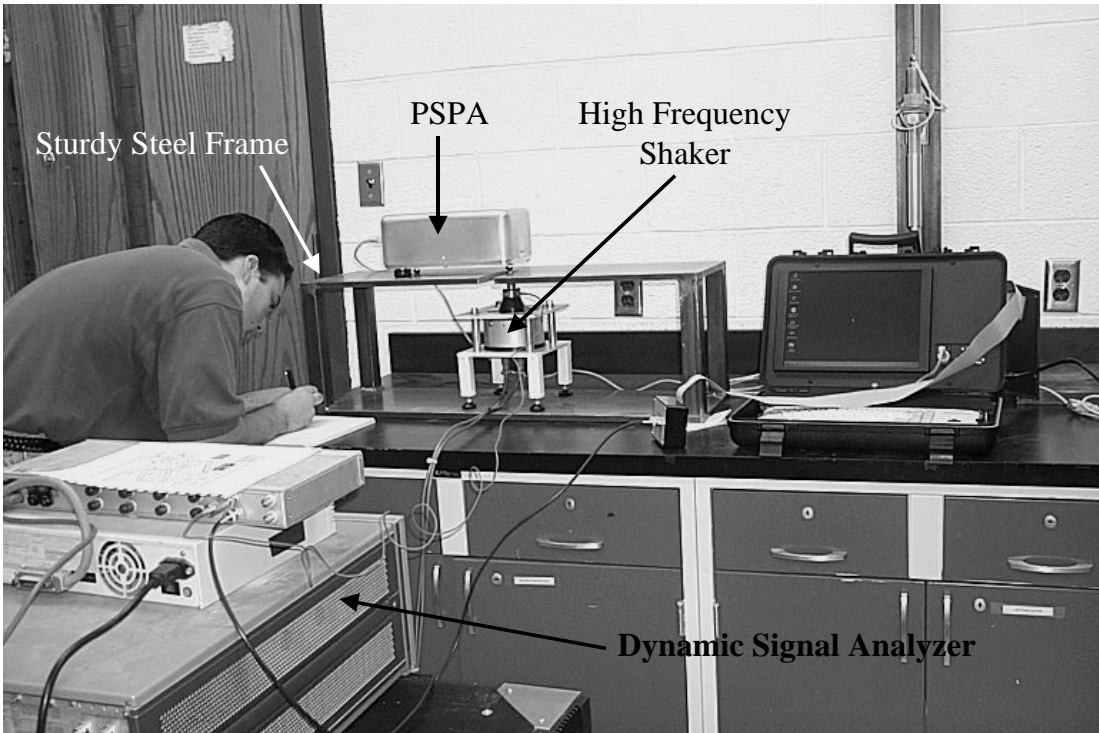
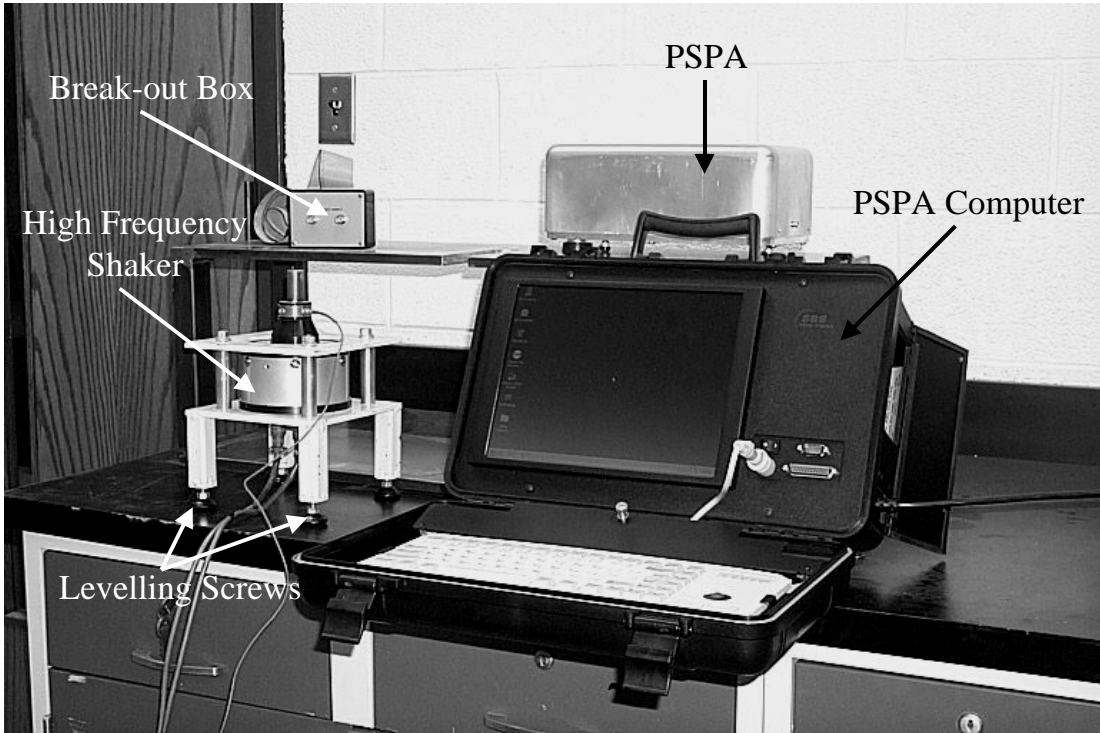


Figure 3.3 - PSPA Calibration Test Setup

obtained in that manner. The calibration results in the range of frequencies of 100 Hz to 40 kHz are of interest.

Typical characteristics of the PSPA accelerometer, before it is mounted in the device, are shown in Figure 3.4. The accelerometer was directly mounted on top of the high frequency shaker. The variation in the ratio of the response from the PSPA accelerometer and from the shaker's built-in accelerometer as a function of frequency is demonstrated. Up to a frequency of about 7 kHz, the response is flat and slightly larger than 10. This indicates that the two accelerometers have similar responses, with the PSPA sensor being approximately 10 times more sensitive. In the same range, the phase is about 180 degrees. This indicates that the two accelerometers have different polarities (e.g., the up direction is negative voltage for one and positive for the other). This occurs because the shaker is mounted upside down. Several vertical lines extending between -180 degrees and 180 degrees occur because at isolated points the phase is minutely above 180 degrees. In those cases, the phase is translated to about -180 degrees.

At about a frequency of 9 kHz, a sharp peak in amplitude spectrums is observed (Figure 3.4). The peak in the amplitude spectrum is accompanied by a 180-degree shift in phase spectrums. The frequency of about 9 kHz, which corresponds to a natural frequency of the system, is in fact the resonance frequency of the built-in accelerometer. In general, the response within the range of 100 Hz and 50 kHz corresponds to that of a typical single-degree-of-freedom system with a resonant frequency of about 9 kHz. A minor peak about the frequency of 10 kHz concurs with the natural frequency of the piezoelectric shaker.

The response of the same accelerometer mounted inside the PSPA sensor box is compared with the response before the accelerometer was placed inside the PSPA in Figure 3.5. The response is affected by the mounting system, the nature of the accelerometer, and the electronic circuitry of the PSPA. The low frequency, high amplitude peak corresponds primarily to the mounting assembly of the PSPA. The wide peak of the amplitude ratio and the gradual decrease in phase indicate that the system is highly damped. Fortunately, the natural frequency is about 1700 Hz, which is outside the range of interest in the PSPA analysis. A comparison of the accelerometer placement, before and after PSPA, suggests that the calibration of the accelerometers should definitely be performed after they have been placed inside the PSPA.

To demonstrate the use of these curves, the responses of the two accelerometers mounted in a typical PSPA are compared in Figure 3.6. The amplitude spectra from the two curves are similar in the range of frequencies of 100 Hz to 1000 Hz. The peak amplitude for Accelerometer 1 occurs at a lower amplitude and at a lower frequency as compared to Accelerometer 2. The phase spectra are also similar except in the ranges of about 2 kHz to 4 kHz, where the peak responses are registered.

To develop the appropriate calibration curve for phase, the response spectrum from Accelerometer 1 is divided by the response spectrum from Accelerometer 2. The results are shown in Figure 3.7. The amplitude spectrum is of little use in the calibration for propagation velocity and are shown only for the sake of completeness. The amplitude past 20 kHz is not shown because the response from the shaker unit accelerometer may not be adequate. The phase spectrum is shown up to a frequency of about 40 kHz. The reason that a higher frequency range can be assigned for a phase as compared to a magnitude is that much less energy is needed to measure a reliable phase. For the data acquisition system used, as long as the relative signal energy is not less than 35 db, the

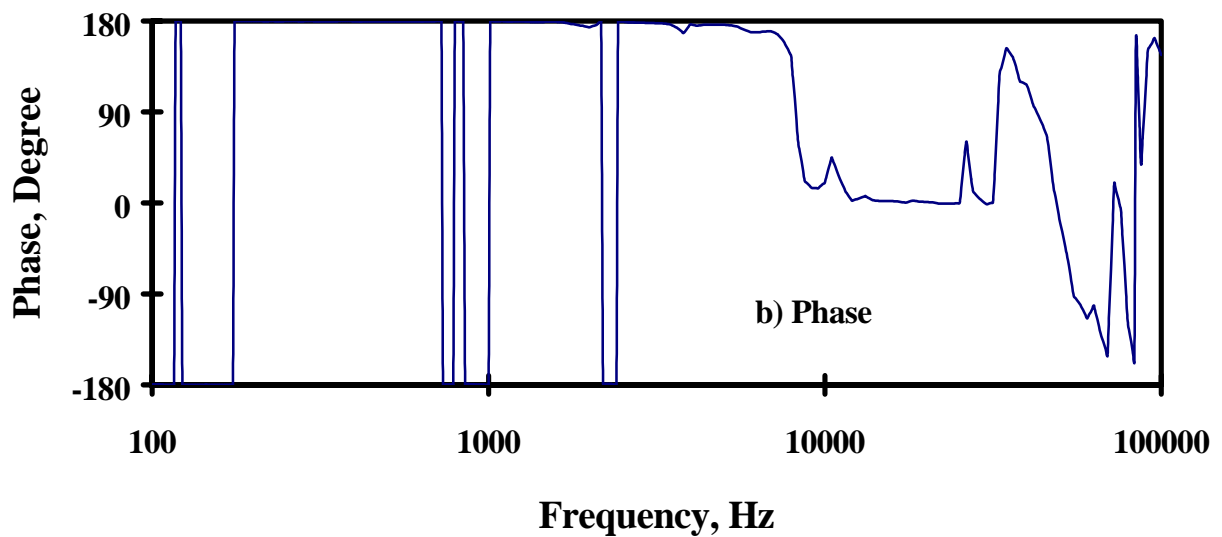
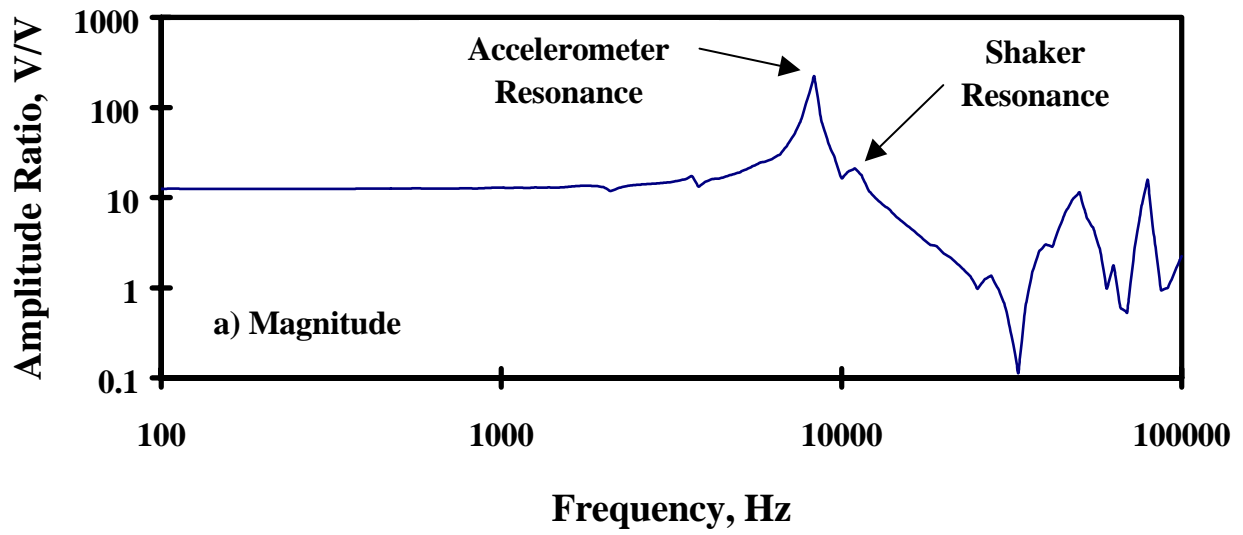


Figure 3.4 - Response of Accelerometer Outside PSPA Holder

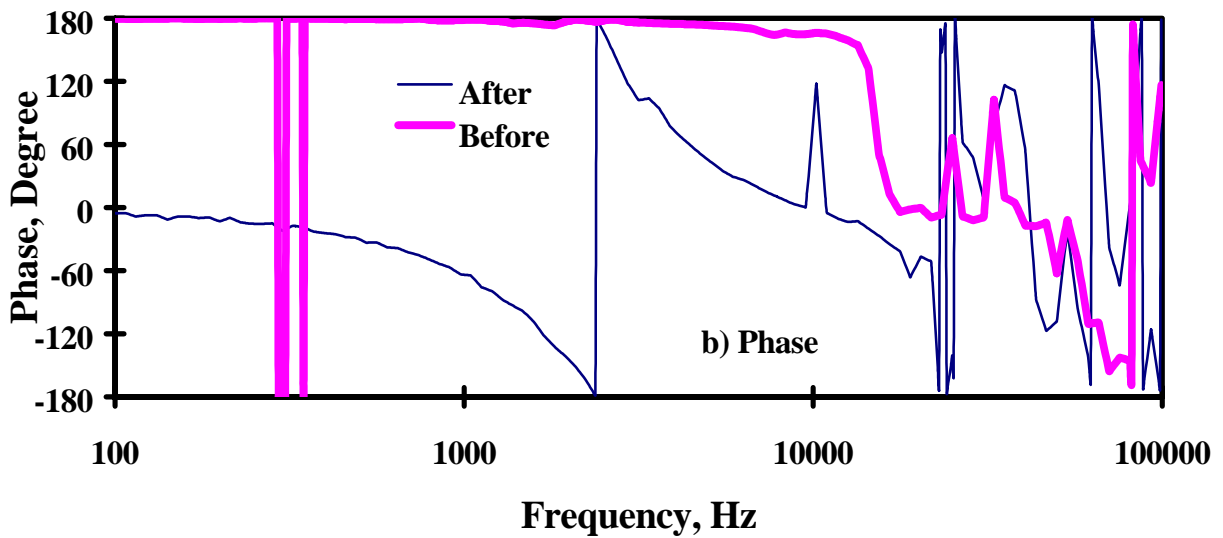
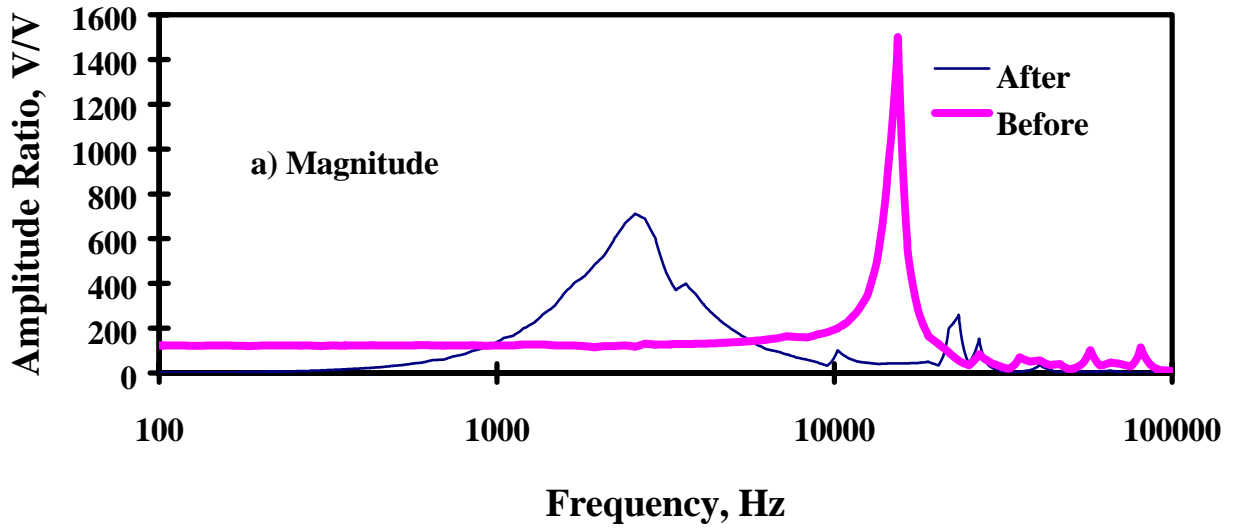
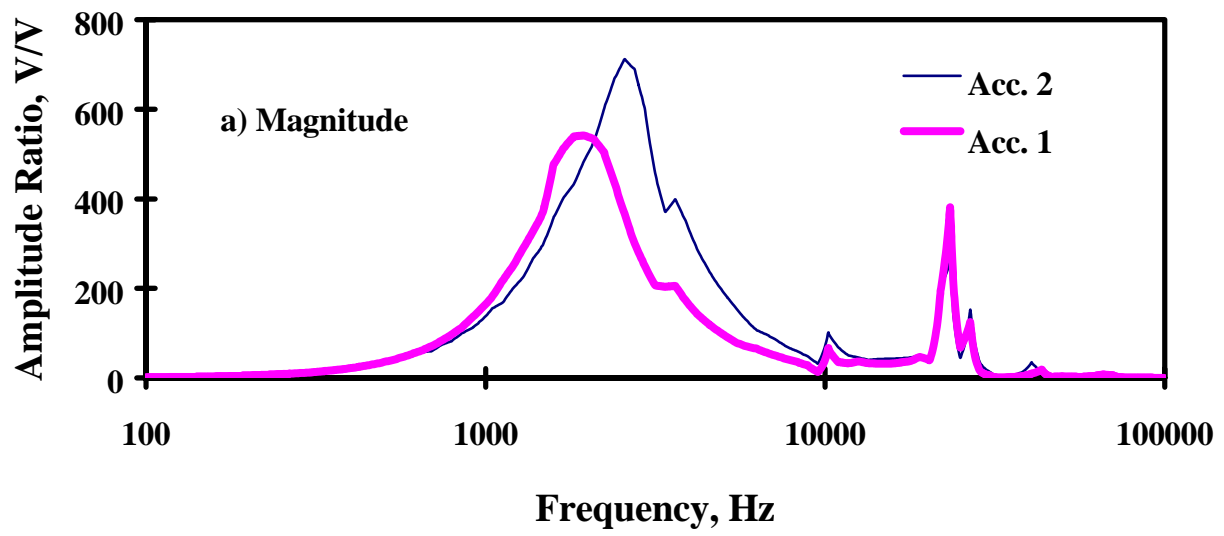


Figure 3.5 - Responses of a Typical PSPA Accelerometer Before and After Placed Inside the Sensor Holder



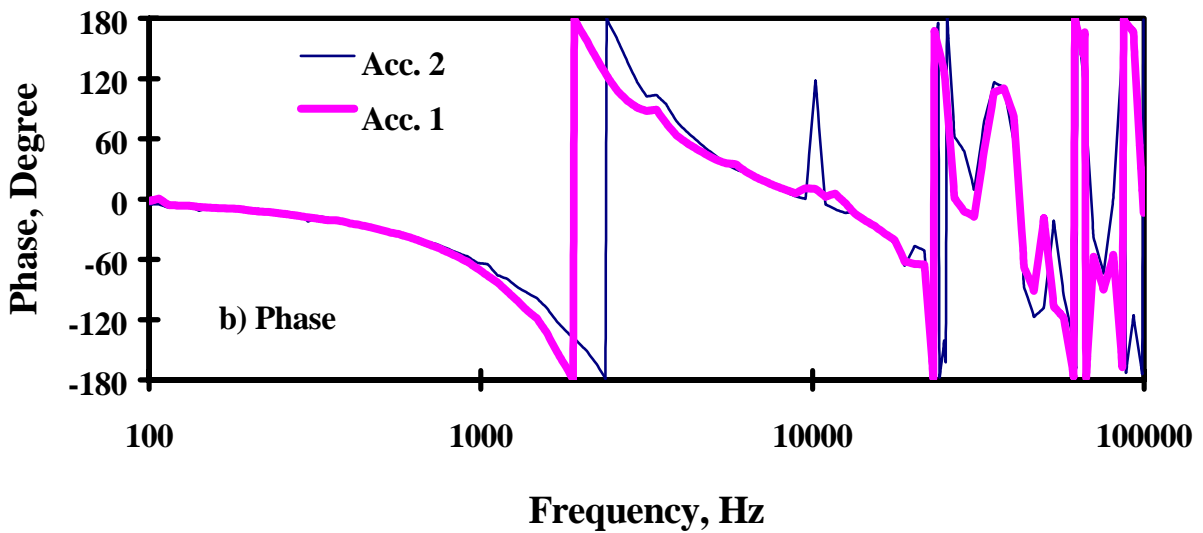
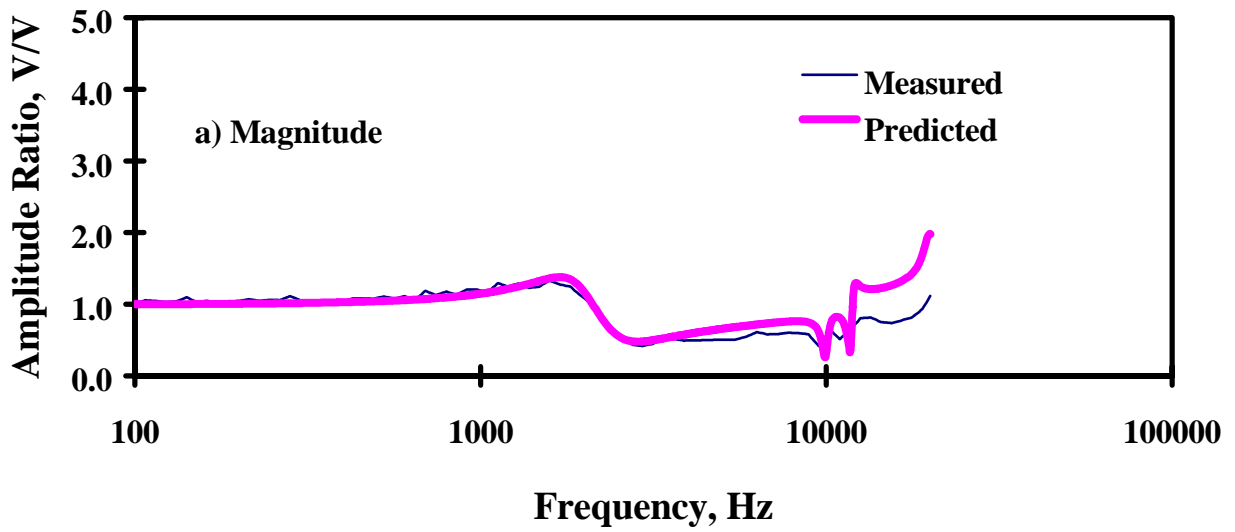


Figure 3.6 - Comparison of Response of Accelerometers 1 and 2 of PSPA

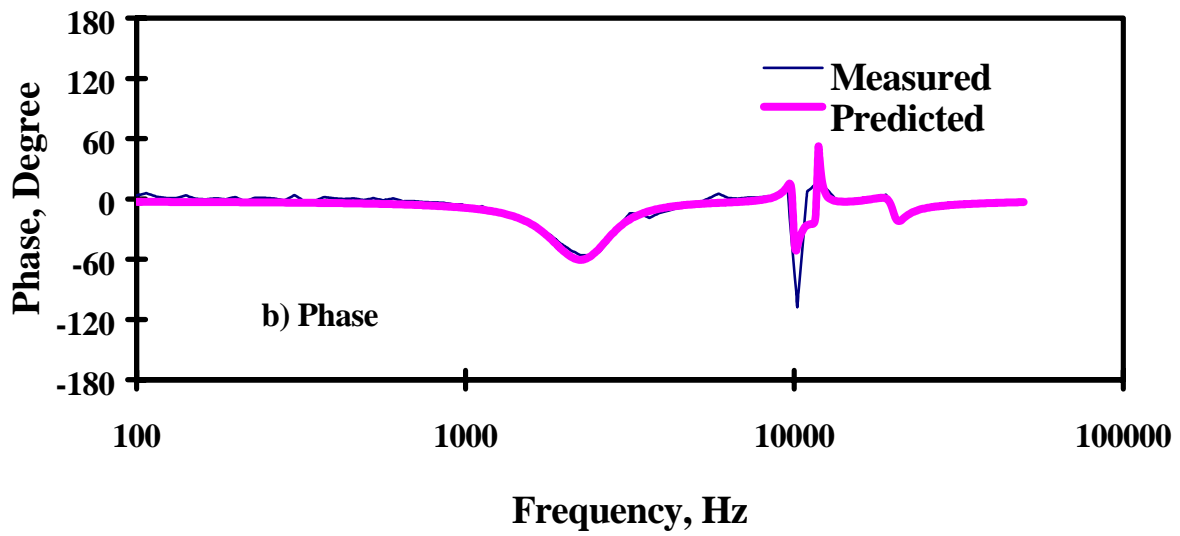


Figure 3.7 - Ratio of Frequency Response Curves of Accelerometer 1 and 2

phase can be measured reasonably well. Above a frequency of 40 kHz, the response of the shaker is too weak to generate energy that is reliably detectable by either the PSPA accelerometers or the shaker accelerometer.

Even though it may be desirable to acquire a shaker with higher response, the impact of the higher frequency energy on the calculated velocity and, consequently, on the modulus of the material, is too small to justify such an expense. The impact on accuracy is discussed later in this chapter.

In terms of implementation, the phase measured at each frequency in Figure 3.7 should be subtracted from the phase of transfer function obtained during field tests. To facilitate this task, a polynomial is fitted to the measured phase spectrum. Typical poles and zeros obtained from the curve fitting are shown in Table 3.1. The curve fitting capabilities of the dynamic signal analyzer are used. The poles and zeros can be incorporated in the PSPA data reduction program.

Table 3.1 - Poles and Zeros Obtained from Curve Fitting of the Data of Figure 3.7

Number	Zeros	Poles	Gain
1	-543.963+2500.95i	-474.209+1932.36i	712.7E-03
2	-543.963-2500.95i	-474.209-1932.36i	
3	6349.36+7559.95i	6763.3+7744.9i	
4	6349.36-7559.95i	6763.3-7744.9i	
5	102.979+9926.33i	337.041+9998.37i	
6	102.979-9926.33i	337.041-9998.37i	
7	-83.2327+11718.3i	-222.605+11871.1i	
8	-83.2327-11718.3i	-222.605-11871.1i	
9	-1263.82+20213.5i	-864.442+20025.3i	
10	-1263.82-20213.5i	-864.442-20025.3i	

As discussed in Chapter 2, the poles, zeros and gain are parameters that can be used to define a polynomial. For the PSPA, the calibration curve, $R(f)$, can be written as:

$$(3.1)$$

where f = frequency, $s = j(2\pi)f$, $j = \sqrt{-1}$, and G = gain factor. Parameter z_i is the i th zero and p_j is the j th pole.

Amplitude Calibration

The amplitude calibration of the accelerometer for the IE method can be performed using the same setup. However, the steps involved in the analysis and data reduction are slightly different. The test setup for the analysis is shown in the Figure 3.8 and 3.9. The calibration is carried out in two steps. A proximator is used first as a reference sensor. The response of the shaker's built-in accelerometer is compared with the response of the proximator. In this manner, the amplitude calibration of the shaker's built-in accelerometer is assured. In the second step, the response of the PSPA accelerometer is compared with that of the embedded accelerometer. The response obtained from the first step is integrated twice because the proximator measures deflection and the accelerometer measures acceleration. The integrated response is then multiplied by the calibration factor of the proximator. This modified response is multiplied by the response spectrum from the second step to obtain the amplitude calibration of the PSPA for the analysis of the IE results. This two-step calibration is required so that the PSPA accelerometer does not have to be disassembled for calibration.

The response spectra from the calibration of the shaker's built-in accelerometer with the proximator are shown in Figure 3.10. The response is linear up to a frequency of about 20 kHz. After that frequency, a large resonance is observed. The range of interest typically lies between frequencies of 4 kHz and 20 kHz (thicknesses of 20 in. and 4 in., respectively).

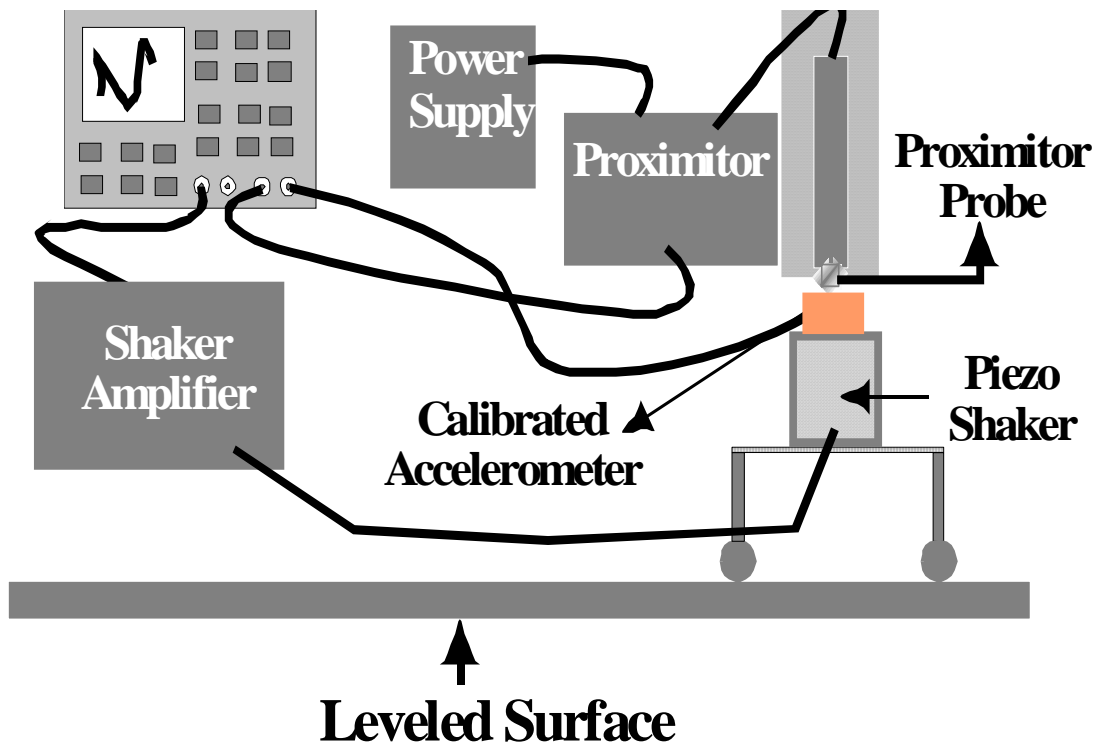


Figure 3.8 - A Schematic of Test Setup for Amplitude Calibration

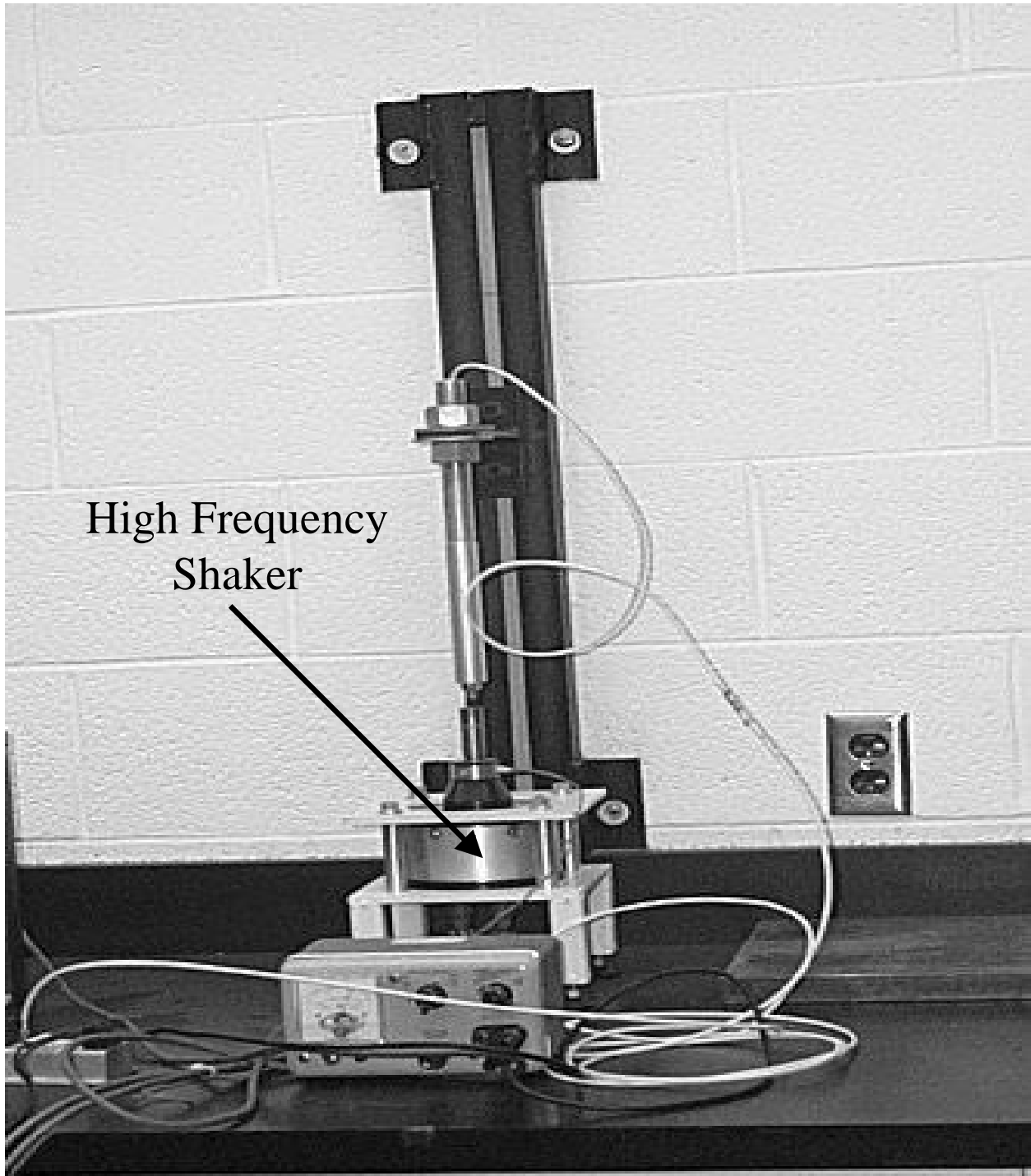
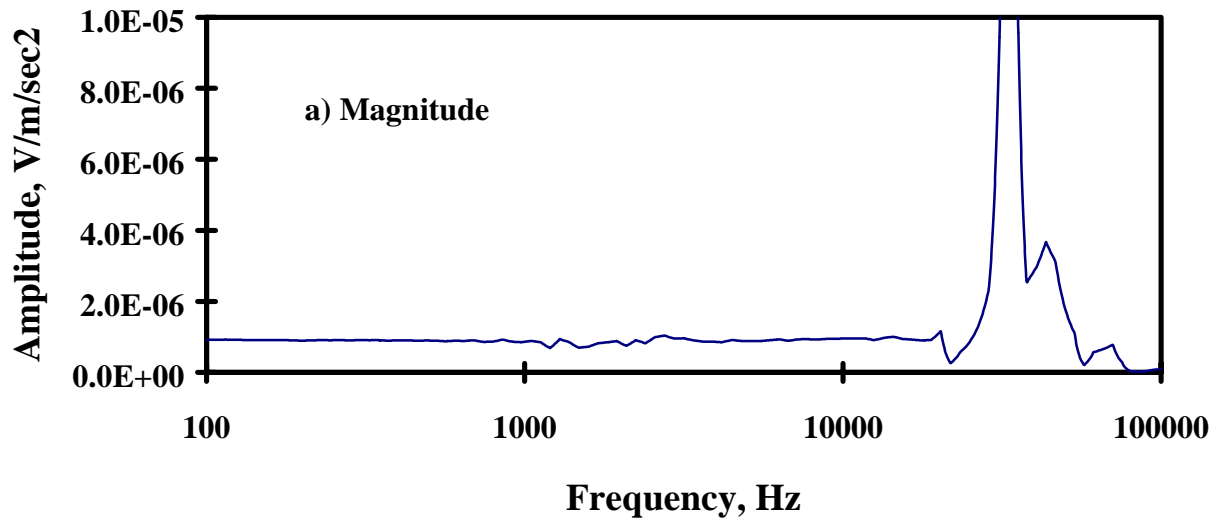


Figure 3.9 - Calibration Device Test Setup for Amplitude Calibration



The phase spectrum is constant (-180 degrees) up to a frequency of 1 kHz, above which a

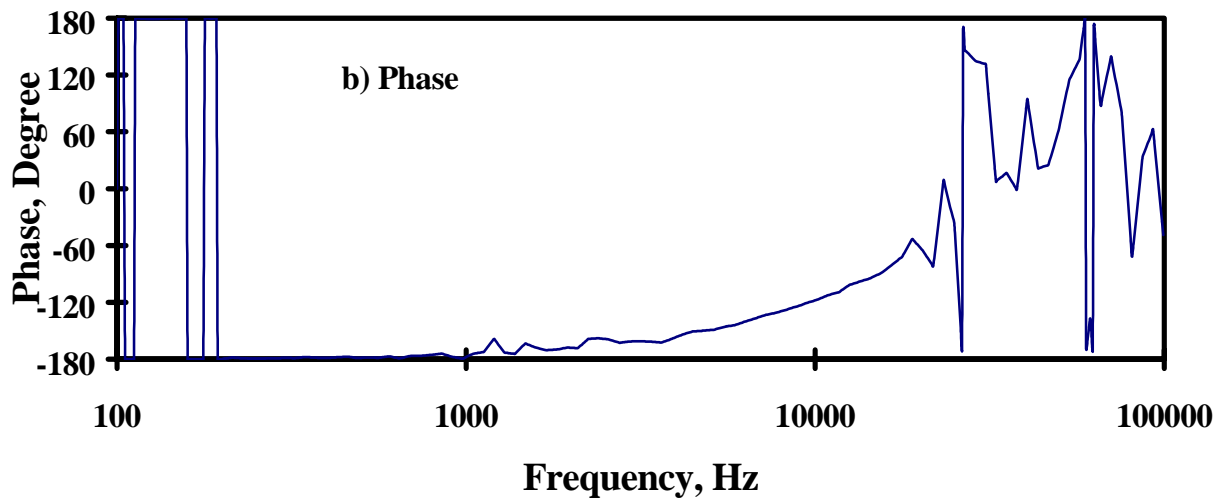


Figure 3.10 - A Typical Frequency Response of Built-in Accelerometer of Piezo-electric Shaker

gradual increase is observed. The phase spectrum resembles a highly damped system. In the IE method, both the amplitude and the phase are of importance.

The magnitude and phase spectra determined from the calibration of the PSPA accelerometer and the shaker's built-in accelerometer are shown in Figure 3.11. The method used to determine these spectra is identical to the one described in Figure 3.5 for Accelerometer 1. As a matter of fact, those results can be directly used in this process as well as for the phase calibration.

By multiplying the spectra shown in Figure 3.11 by those shown in Figure 3.10, the actual calibration curve for the IE method is determined. Such a curve is shown in Figure 3.12. The curve fitting capabilities of the dynamic signal analyzer can be used to fit the curve. The poles and zeros obtained from fitting the curve can be provided to the PSPA manufacturers for input in their data reduction program. The poles and zeros obtained from the curve fitting of the data shown in Figure 3.12 is included in Table 3.2. As reflected in Figure 3.12, the fitted and measured spectra compare reasonably well in the range of 4 kHz and 20 kHz which is of interest.

To implement a calibration curve, such as the one shown in Figure 3.12, one should divide the raw amplitude spectrum obtained from the IE test by the calibration curve. Figure 3.13 is an example of such an operation. The raw spectrum contains a low frequency peak at about 2 kHz; the pattern of the increase and the decrease in the amplitude at frequencies lower than 5 kHz is fairly close to that from the calibration process shown in Figure 3.12a. If the raw amplitude spectrum is divided by the calibration spectrum, it will result in a curve that corresponds to the curve marked as calibrated IE in Figure 3.13. This example illustrates that the results are more clearly delineated when the impact of the mounting and the electronic components are subtracted from the raw IE spectra.

A statement regarding the significance of implementing the IE calibration process cannot be made at this time due to insufficient data. Its significance depends on the thickness of the layer and the underlying materials. More data is needed before a statement can be made on this issue.

In summary, the results from this study indicate that the calibration of PSPA accelerometers can be easily performed in the laboratory. Since the equipment is portable, there is no need to develop a field calibration test procedure.

Calibration of Source

A rigorous calibration of the source is not necessary because the amplitude or time history of the input is not used in the analysis. However, it would be desirable to periodically measure the rise time of the energy imparted by the source to ensure that adequate high-frequency energy is imparted to the material. In addition, it may be desirable to measure the load intensity to ensure that the source assembly is not loose or over-stretched.

The setup used for source calibration is shown in Figure 3.14. The system consists of a plate with a 100-lb load cell embedded in it. The load cell is connected to a recording device. The PSPA is placed on top of the plate so that the source is located directly on top of the load cell. The source is fired and the response of the load cell is registered for analysis.

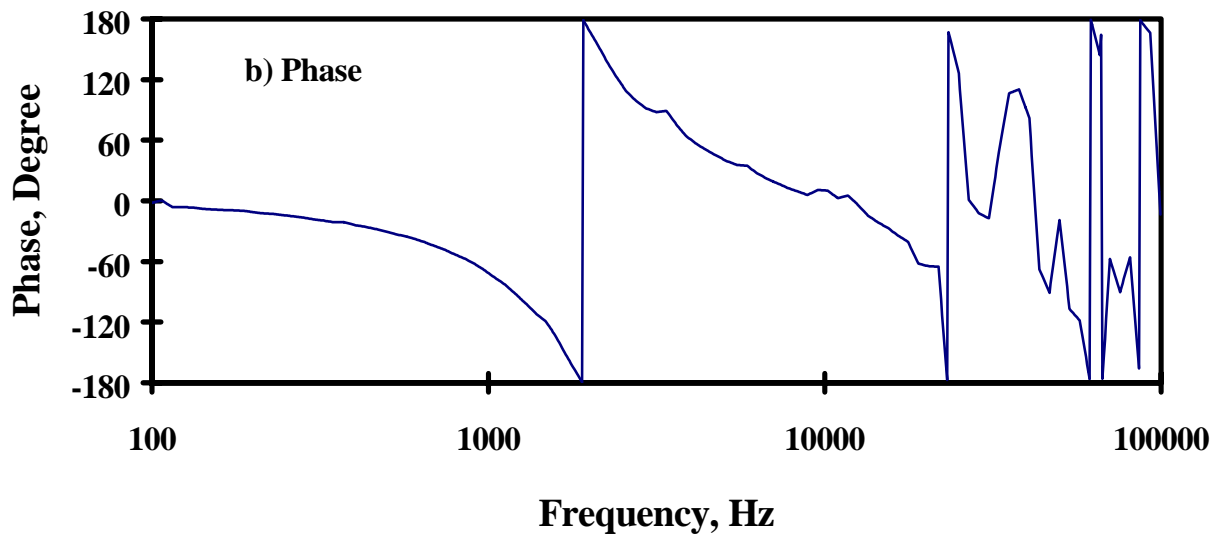
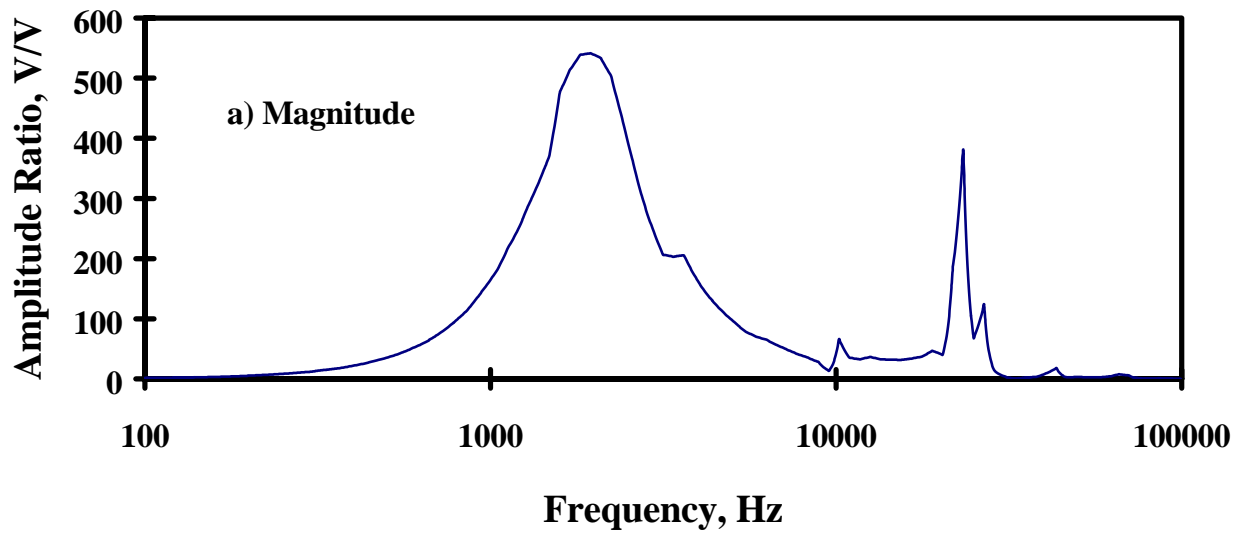


Figure 3.11 - A Typical Frequency Response of PSPA Accelerometer

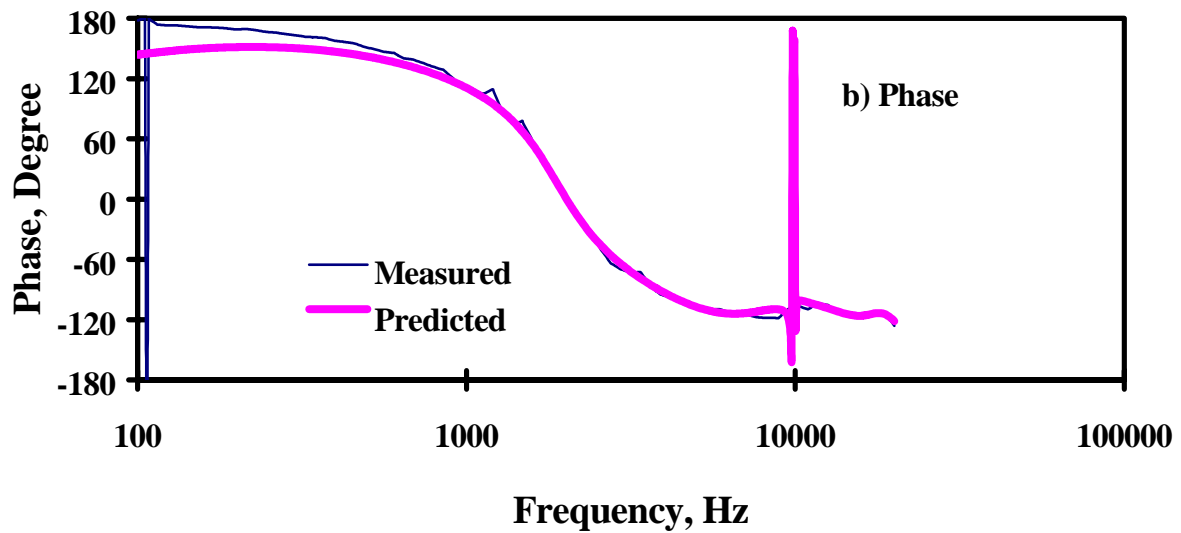
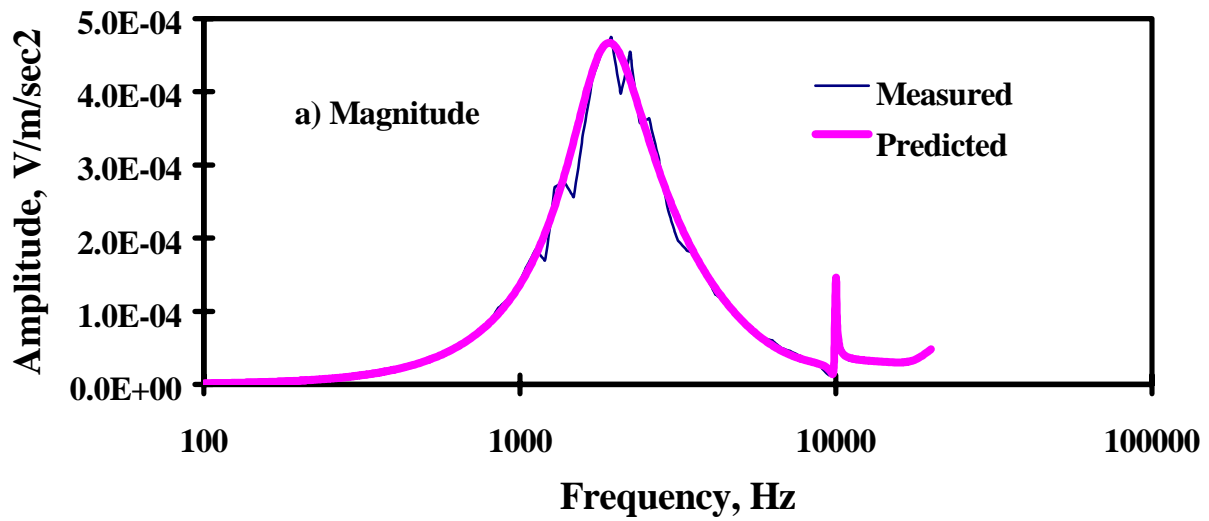


Figure 3.12 - Calibration Curves for PSPA Accelerometer

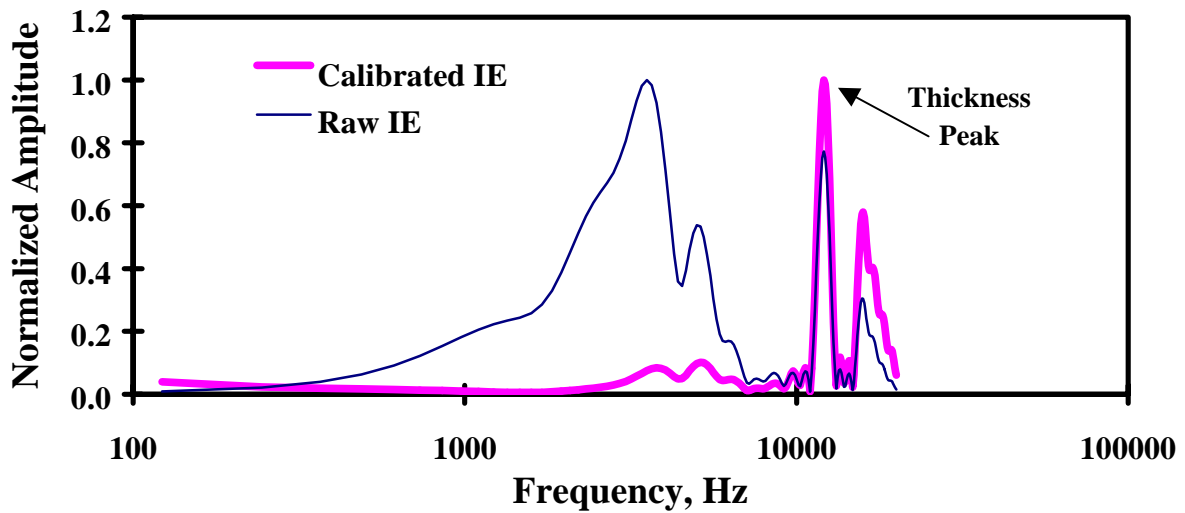
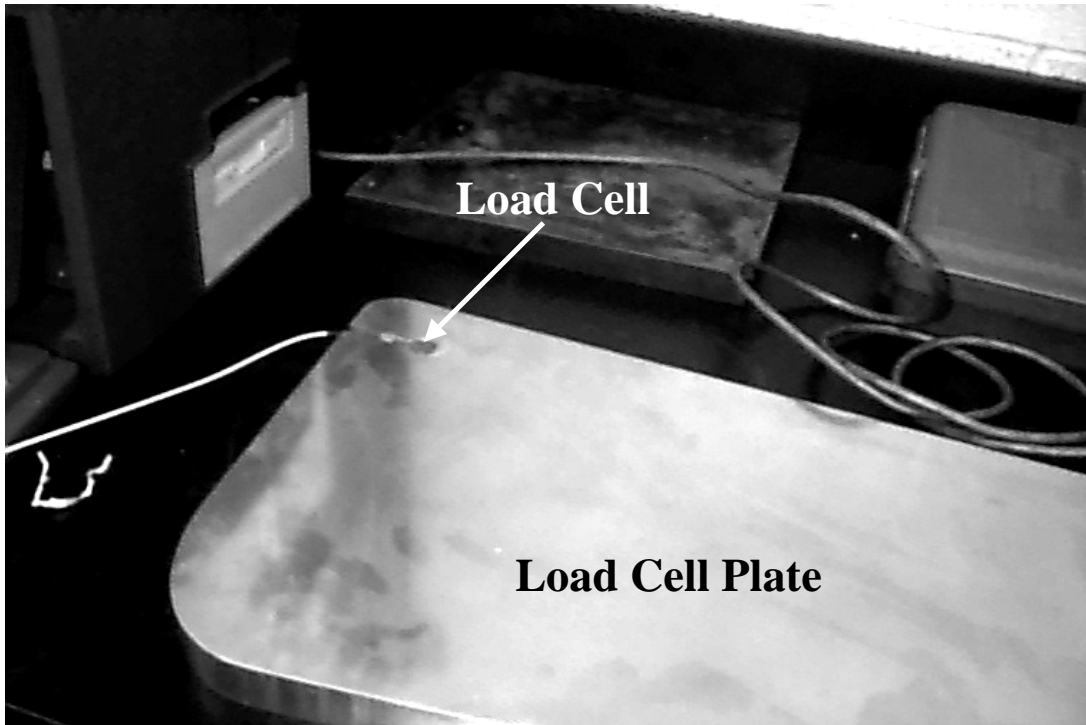


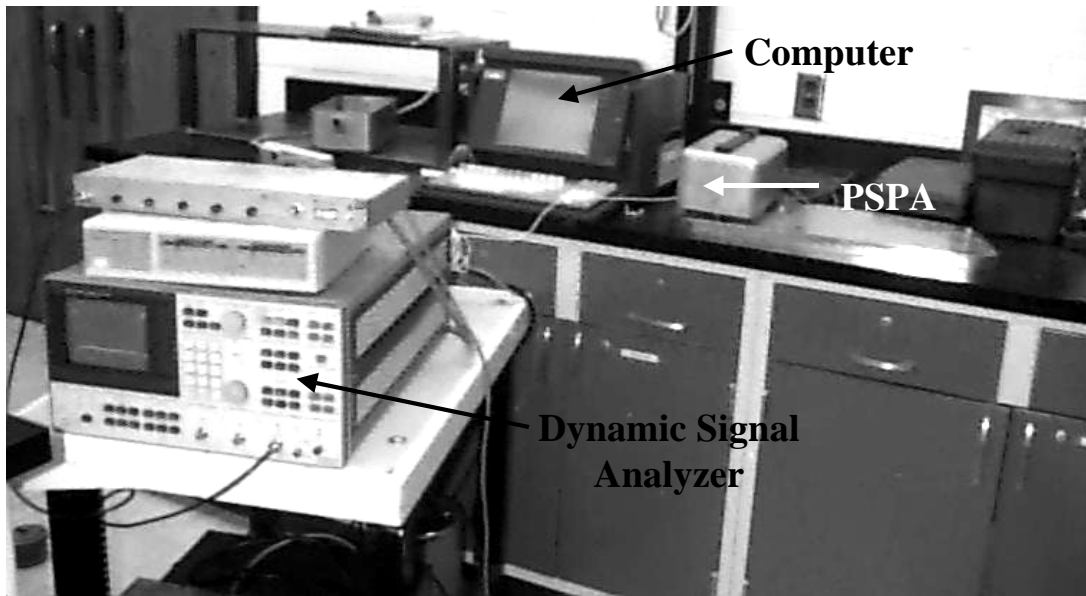
Figure 3.13 - Raw and Calibrated Response of PSPA During IE Tests

Table 3.2 - Poles and Zeros Obtained from Curve Fitting of Spectra Shown in Figure 3.12

Number	Zeros	Poles	Gain
1	-57.8981	-13483.3	7.37E-08
2	0.0	-4475.25	
3	-3264.86+7494.14i	-2052.59	
4	-3264.86-7494.14i	-563.725+1784.03i	
5	92.616+9798.3i	-563.725-1784.03i	
6	92.616-9798.3i	37.9211+9982.56i	
7	13391.9+13454.7i	37.9211-9982.56i	
8	13391.9-13454.7i	-4193.56+18913.3i	
9	-2985.89+17385.8i	-4193.56-18913.3i	
10	-2985.89-17385.8i	0	



a) Load Cell Placement



b) Test Setup

Figure 3.14 - PSPA Source Calibration Test Setup

A typical record is shown in Figure 3.15. The impulse duration should be measured as marked in the figure. For a typical PSPA, the impulse duration should be less than 125 μsec . If the impulse duration is greater than this value, the source should be serviced. In addition, the load amplitude should be measured (see Figure 3.15). If the load is less than 15 lb, the source should be serviced. A reference calibration of the load cell used in this set up is unnecessary because the exact load is not used in the analysis.

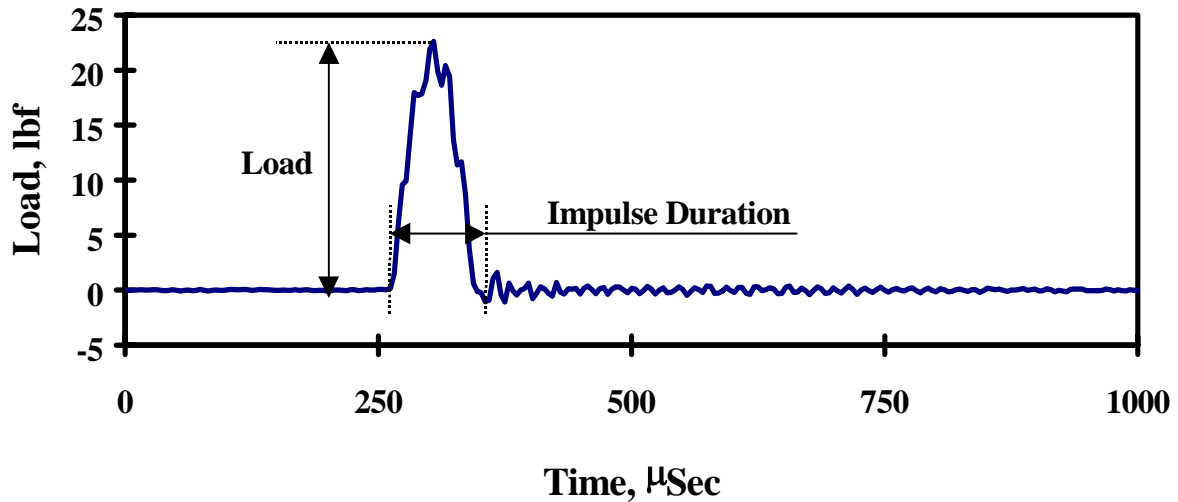


Figure 3.15 - A Typical Time-History of PSPA Source Signal

PSPA Calibration Strategy

Since the PSPA has been developed recently, no calibration procedure or strategy exists. In addition, historical data are not available to draw empirical conclusions. In this section, a preliminary calibration strategy is proposed. With time and experience, this strategy can be improved. A summary of proposed calibration procedures is shown in Figure 3.16.

The two accelerometers of PSPA should be calibrated for amplitude as well as phase shift. The amplitude calibration is used for considering the impact of the accelerometer seating and electronic components used in manufacturing the PSPA. With removal of those responses from the raw time records, identifying the thickness of the top layer becomes more reliable. Please note that in the IE method, the frequency at which the maximum amplitude occurs is of interest, not the actual amplitude. This implies that a very rigorous amplitude calibration, similar to that of FWD, is not necessary.

The phase shift calibration is primarily used to account for any artificial phase shift between the two accelerometers due to sensor mounting or electronic components. Removing such phase

shifts from the measured ones will result in more accurate modulus values from the Ultrasonic Body Wave and the Ultrasonic Surface Wave methods.

The accelerometers used in PSPA are manufactured by PCB Piezotronics, Inc. The manufacturer provides a certificate of calibration with each accelerometer that contains a NIST-traceable calibration factor. More than a decade of experience has reasonably proved to the researchers that the manufacturer’s calibration is within 2% of specified value. Therefore, a strategy is not needed for accepting or rejecting an accelerometer received from the manufacturer. Since the PSPA is a seismic tool, the actual amplitudes of the signals are not used in any of the analyses.

The calibration of PSPA can be performed at three different levels: (1) relative PSPA calibration, (2) reference calibration, and (3) accelerometer assembly diagnosis. A flow chart of a proposed calibration strategy is shown in Figure 3.17. A detailed description of each step and preliminary acceptable performance specifications are provided next. The relative calibration should be carried out regularly (say monthly or before any major project). If the result from the relative calibration is not satisfactory, the reference calibration should be carried out. If the results from the reference calibration are not satisfactory, the performance of the individual accelerometers should be assessed to determine whether the accelerometer or the electronic components are contributing to the unsatisfactory performance of the PSPA.

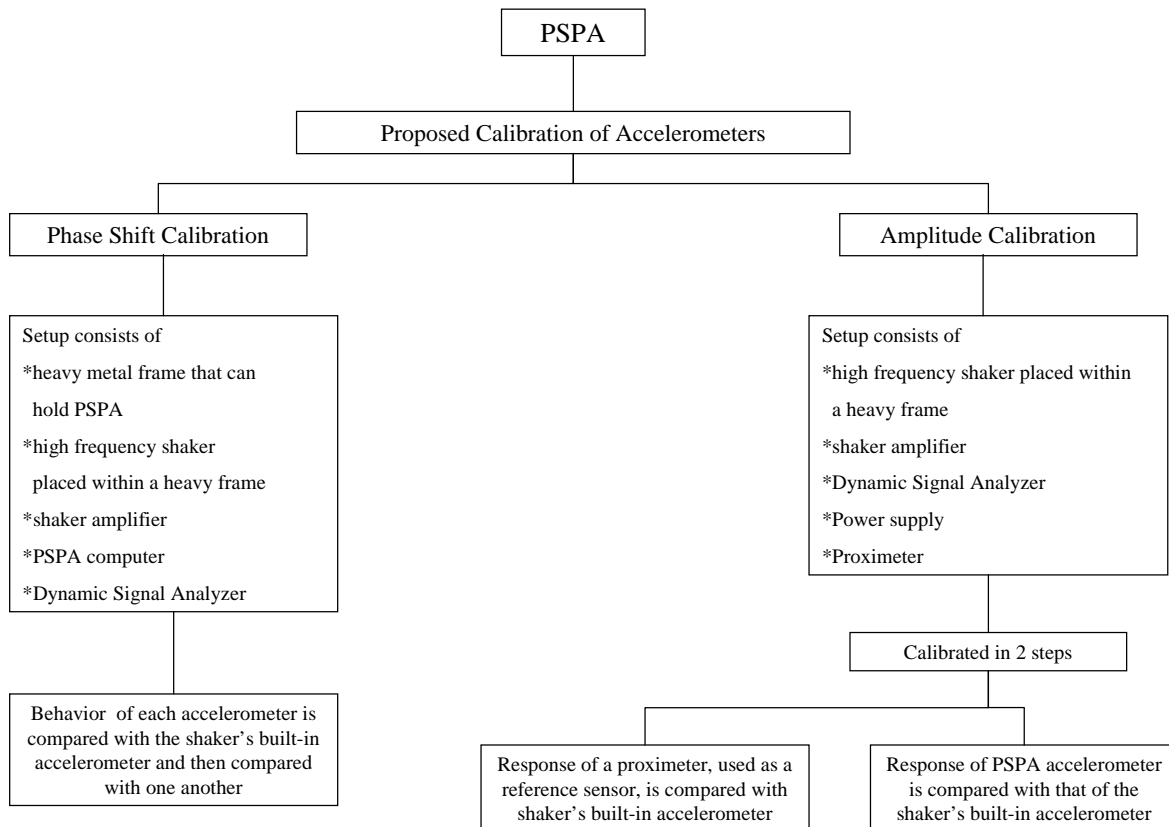


Figure 3.16 - Summary of Proposed PSPA Calibration

PSPA Calibration Strategy

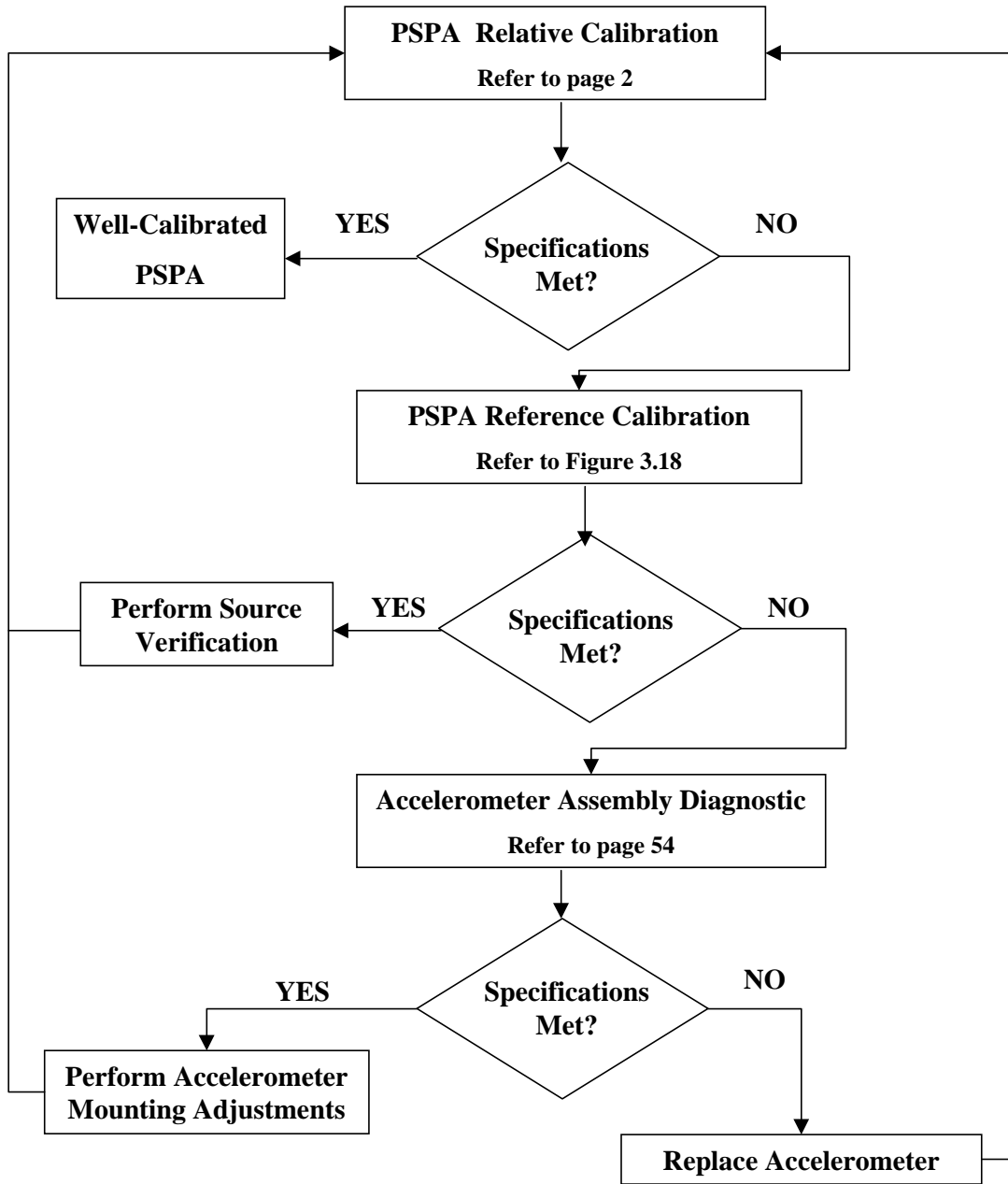


Figure 3.17 - Proposed PSPA Calibration Strategy

Relative PSPA Calibration

As a rapid verification tool, the relative calibration of the PSPA can be performed by testing a slab of known modulus and thickness. If the measured thickness and modulus are similar to the values reported for the slab, the PSPA can be considered as calibrated, and no further action is required until the next scheduled reference calibration. In addition, the SPA tests can be performed about 20 times at the same position without moving the sensor box to check the precision of the device.

The preliminary level of accuracy recommended here for the modulus and thickness is 5%. If the thickness or the velocity varies by more than 5% from the suggested value for the calibration slab, a reference calibration should be carried out. Also, if the precision of the device is more than 3%, the system should be serviced, and the tests should be repeated. The servicing of PSPA should be performed by cleaning and reseating the accelerometer and source. The manufacturer should be contacted if a problem persists. A database has to be established to set these levels in a more informed manner

Until recently, the researchers have used a concrete slab for this purpose. At this time, we are experimenting with a granite slab. The use of granite is suggested because of its precise dimensions, smooth surface, and reasonable weight.

If desired, the source characteristics can also be checked to ensure its satisfactory performance. The load cell set up described in the previous section can be used. If the imparted load is less than 15 lbf or the duration of the impulse is greater than 125 μ sec, the source should be cleaned and serviced.

Reference PSPA Calibration

The flow chart of the activities associated with the reference calibration is shown Figure 3.18. The goal is to determine the calibration curve that has to be input into the data analysis software. In addition, this calibration process can be used to determine whether the malfunction of a suspect PSPA is due to a problem with the seating of an accelerometer, due to a malfunction of an accelerometer, or due to a problem with electronic components.

This task is carried out in two parts. For the thickness measurement with the IE method, the responses of the accelerometer assembly and associated electronics are measured and removed from the raw time-histories measured with the PSPA. Following the steps described in the previous sections, a calibration curve similar to that shown in Figure 3.12 is obtained. The final products from this activity are curve fitting parameters (i.e., several poles and zeros and a gain factor similar to those reported in Table 3.2). If the amplitude or phase spectrum varies significantly from the initial one provided by the manufacturer or determined by TxDOT personnel at the time of initial delivery, the accelerometer should be put through a diagnosis calibration to determine whether the accelerometer, the accelerometer assembly or the electronic components should be adjusted or repaired. At this time not enough data are available to accurately define the acceptable ranges for changes in the calibration curve. Based on the preliminary investigation, the researchers feel that if the change in the calibration curve is more than 10%, the accelerometer should be replaced.

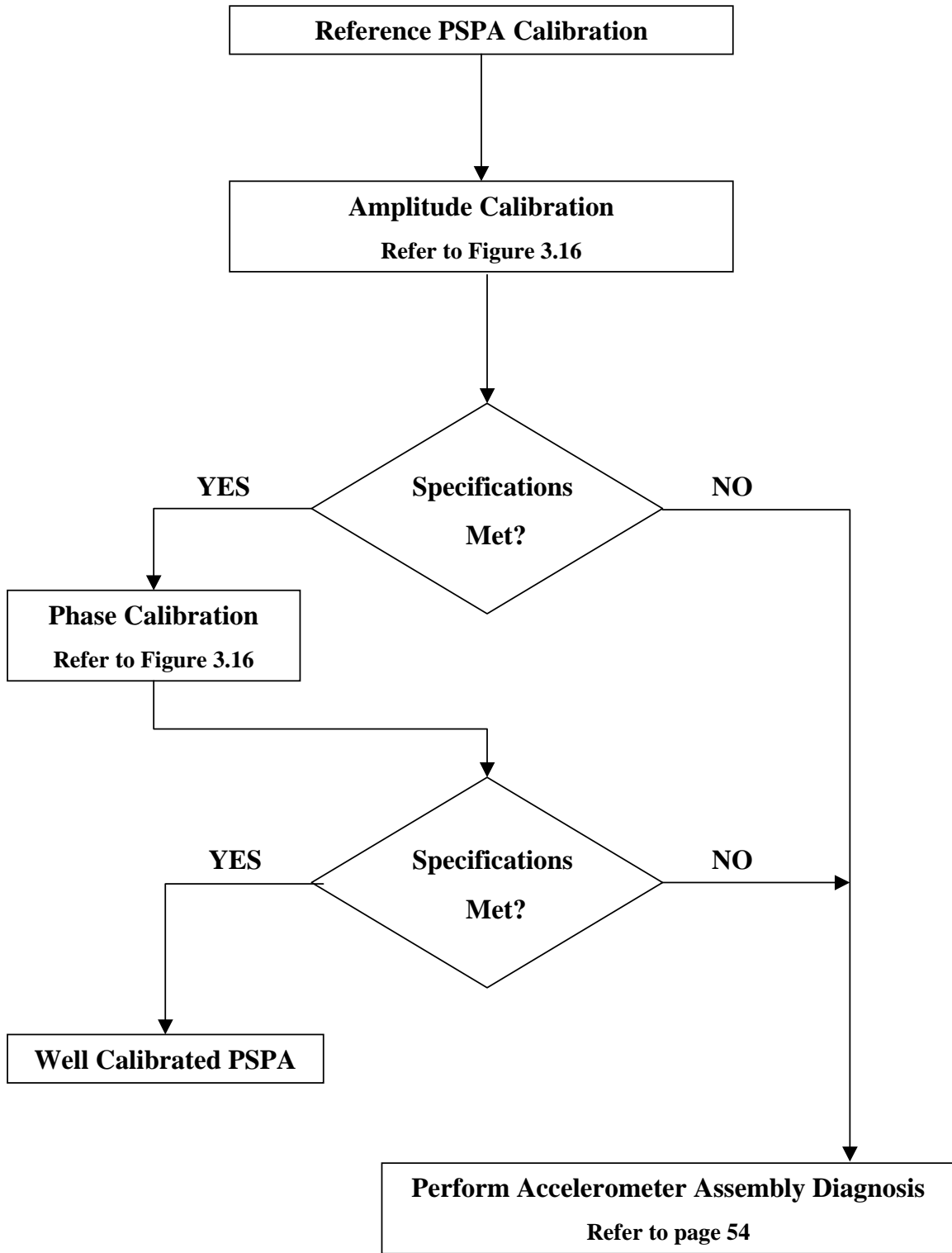


Figure 3.18 - Proposed Reference PSPA Calibration Strategy

The phase shift calibration should be also carried out to develop the calibration parameters that should be included in the analysis. Following the process described before, the outcome should be a curve similar to that shown in Figure 3.7b. Significant variation from zero phase is not desirable. However, given the state of the practice in constructing accelerometers, such differences in localized areas, especially between the natural frequencies of the two accelerometer assemblies, are anticipated. Any system related phase shift can be explicitly accounted for in the USW method. For the UBW tests, it is desirable that the system related phase shift be close to zero.

Significant changes between consecutive phase shift calibration spectra should be investigated as described above for the amplitude calibration for thickness. Once again, a database should be developed so that reasonable performance specifications can be developed.

Accelerometer Assembly Diagnosis

During the reference calibration, one cannot identify the exact source of the problem with a PSPA accelerometer system. The diagnostic steps, described below, can be used to determine the source of the potential problem.

In this step, the accelerometer is removed from the PSPA and is subjected to the calibration process shown in Figure 3.3. If the accelerometer does not exhibit an amplitude and phase spectra similar to that showed in Figure 3.4, the accelerometer should be replaced. Otherwise, the vendor of the PSPA should be contacted. At this time, the researchers are in the process of developing a calibration process for the electronic components of the PSPA. A preliminary process has been developed. However, the process is not robust enough to ensure that the circuit board will not be damaged during the calibration.

If the accelerometer is the source of the problem, it should be replaced with a new one. A reference calibration should be performed to update the phase shift calibration curve of the PSPA system. If the accelerometer close to the source is replaced, an amplitude calibration for IE test should also be carried out.

It should be emphasized that the proposed calibration strategy is preliminary. Further evaluation and fine-tuning are needed before it is finalized.

Chapter 4

Seismic Pavement Analyzer

The Seismic Pavement Analyzer (SPA) is similar to the PSPA in terms of its principles of operation; however, it is more comprehensive. A standard calibration procedure for the SPA also did not exist and had to be developed under this project.

The major components of the SPA, as shown in Figure 4.1, include eight receivers (five accelerometers and three geophones), the receiver mounting members, two pneumatic impact sources, and a raise-lower mechanism. These are mounted on a light trailer for towing behind a vehicle.

In addition to the tests performed with the PSPA, the SASW and the Impulse Response (IR) tests can be performed with the SPA. The IR method is used to determine the modulus of subgrade reaction for rigid pavements and an overall modulus for flexible pavements. The Spectral-Analysis-of-Surface-Waves (SASW) method can determine the modulus profile of a pavement section. A detailed description of the SPA can be found in Nazarian et al. (1993).

For accurate and precise determination of pavement properties, it is essential to calibrate the five accelerometers, three geophones, and two load cells of the SPA. The calibration procedures developed in the last two chapters can be used for the calibration of SPA sensors with few modifications. The two farthest geophones and four adjacent accelerometers need to be calibrated for the phase shift, similar to that of the PSPA. The accelerometer involved in the IE test and the geophone involved in the IR test should be calibrated for the amplitude. The high and low frequency load cells need to be calibrated similar to that of the FWD. Specifically, accelerometer A1 (see Figure 4.1) needs to be calibrated for the amplitude, and accelerometers A1 through A5 for the phase shift. Similarly, geophone G1 needs to be calibrated for the amplitude and geophone G2 and G3 for the phase shift. The calibration procedure for each sensor is described in the following sections. In addition, a calibration strategy in a manner similar to that used for the PSPA is proposed for the future calibration of the SPA.

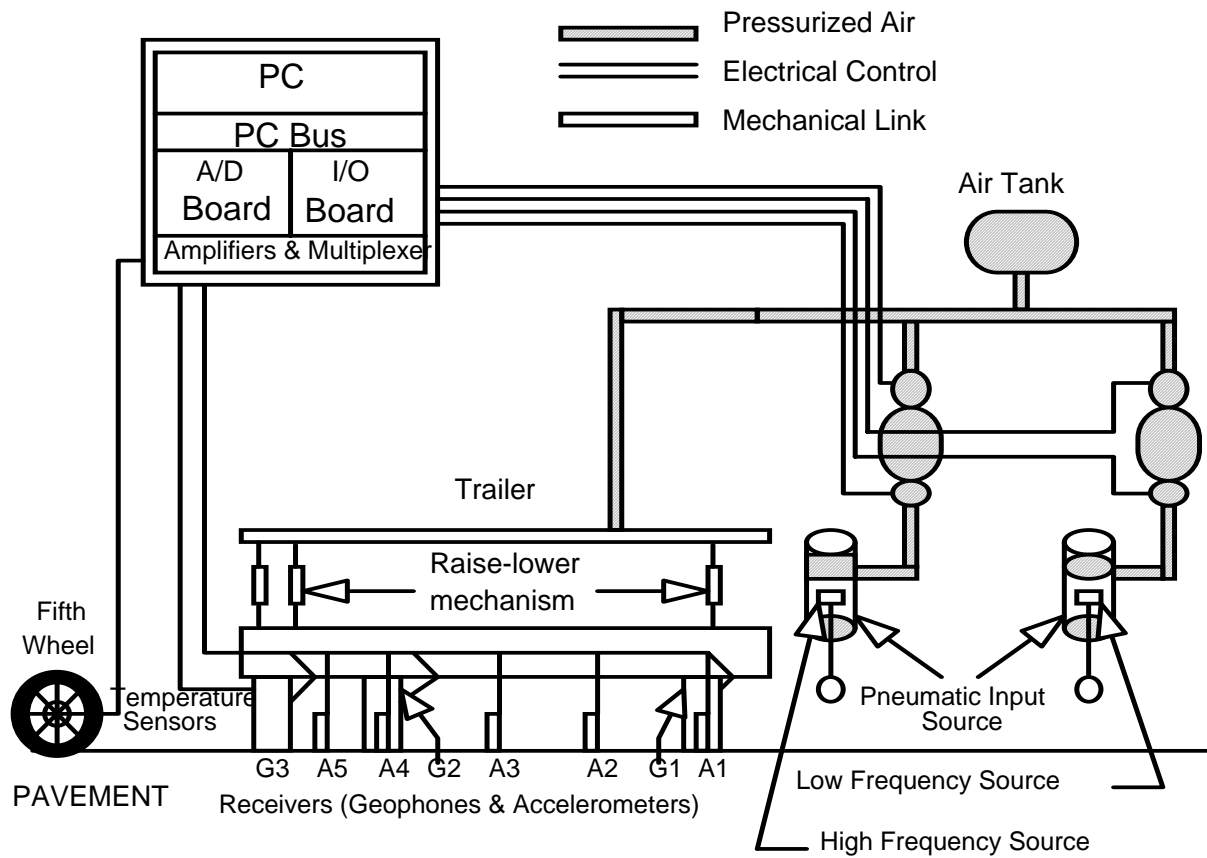


Figure 4.1 - A Schematic of Seismic Pavement Analyzer

Proposed Calibration of Accelerometers

Phase Shift Calibration

The setup required for calibrating the SPA accelerometers is shown in Figure 4.2 and Figure 4.3. The setup is similar to that used for the calibration of the FWD sensors with the only exception that the low- frequency shaker is replaced by a high-frequency shaker. The accelerometer to be calibrated is lowered on top of the piezo-shaker using the raise-lower mechanism of the SPA. The outputs of the built-in accelerometer of the shaker and the SPA accelerometer are connected to a dynamic signal analyzer. A break-out box has been developed to conveniently perform this task. The shaker is excited in a swept-sine mode using a built-in feature of the dynamic signal analyzer.

Dynamic Signal Analyzer with Random Function Generator

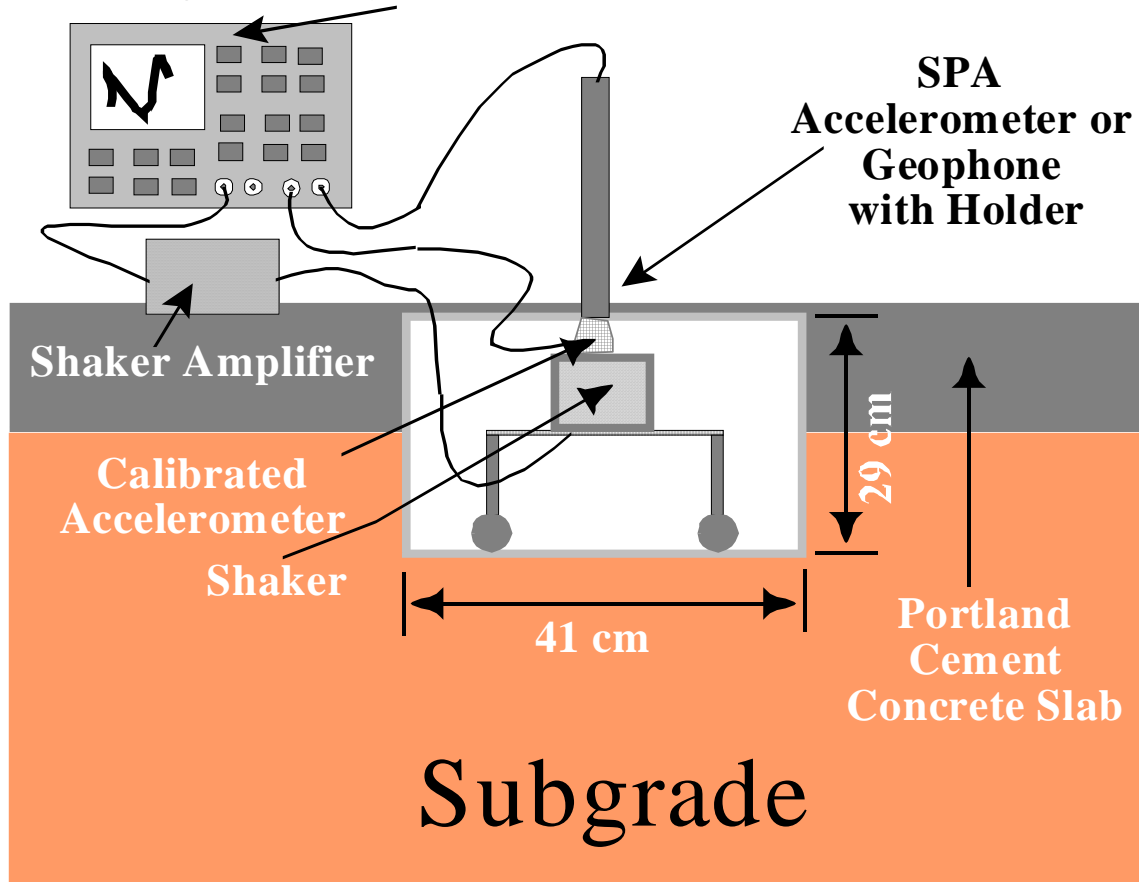
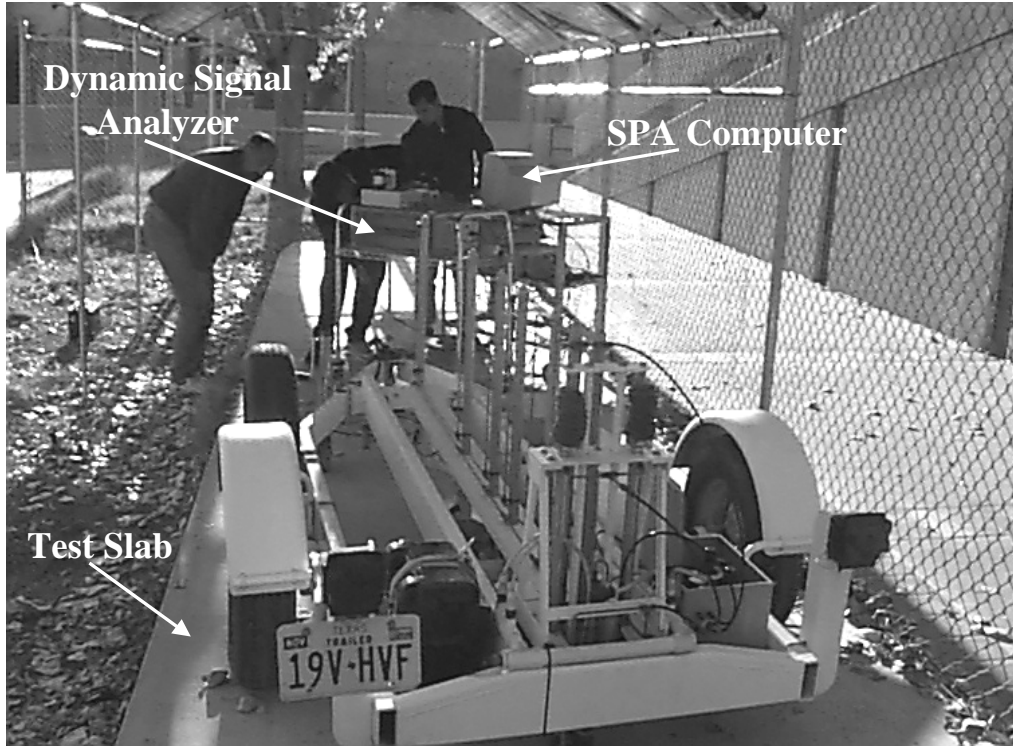
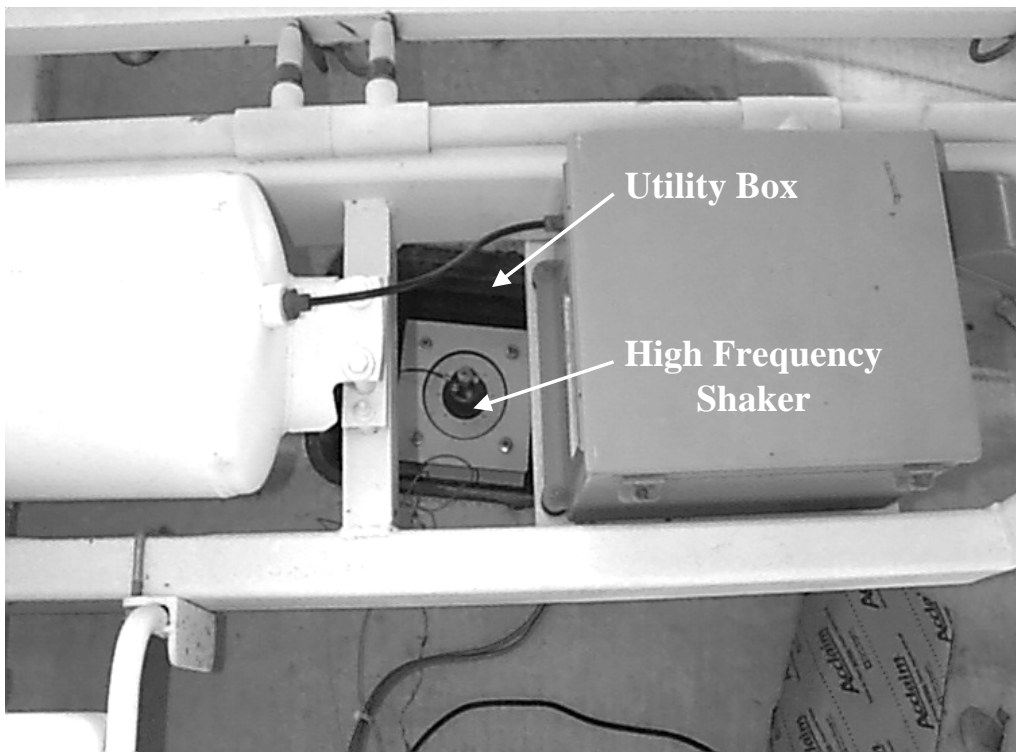


Figure 4.2 - A Schematic of Field Calibration of SPA Accelerometer or Geophone



a) SPA



b) High Frequency Shaker (Inside Utility Box)

Figure 4.3 - SPA Accelerometer and Geophone Calibration Test Setup

The phase calibration of the SPA accelerometers is similar to that of the PSPA. By comparing the calibration of the two SPA accelerometers relative to the built-in accelerometer, one can determine the phase shift calibration. The calibration curve is the ratio of the transfer functions of Accelerometers 2 and 3 obtained in that manner. The calibration results in the range of 100 Hz to 30 kHz are of interest.

To demonstrate the use of these curves, the responses of two accelerometers (A2 and A3) mounted in a typical SPA are compared in Figure 4.4. The amplitude spectra from the two curves are similar in the range of frequencies of 100 Hz to 1000 Hz. The peak amplitude of A2 is slightly higher than that of A3. The frequency associated with the peak amplitude is the same for both accelerometers. The phase spectra of A2 and A3 are almost identical up to a frequency of 5 kHz. At frequencies greater than 5 kHz, the phase values show similar trends with some variation.

The amplitude spectrum is shown in Figure 4.5a. This graph is included for completeness since it is not used. The phase spectrum associated with the difference between the two spectra of accelerometers 2 and 3 (shown in Figure 4.4) is depicted in Figure 4.5b. The phase shift between the two accelerometers is almost zero up to a frequency of 2,500 Hz. Past this frequency, because of differences in the resonant frequencies of the accelerometer systems, a relative phase shift of up to 120 degrees is observed. If such phase shifts are not considered in the analysis, localized errors in velocity of less than 12% for a typical AC layer and less than 6% for a typical PCC layer should be anticipated. Because of the averaging process involved in determining the final dispersion curve, the global impact is less pronounced. The variation in the phase is larger than that observed for the PSPA (see Figure 3.7).

The phase measured at each frequency in Figure 4.5 should be subtracted from the phase of the transfer function obtained during field tests. To facilitate this task, a polynomial is fitted to the measured phase spectrum. Typical poles and zeros, obtained from the curve fitting routines built into the dynamic signal analyzer, are shown in Table 4.1. In a similar manner, phase spectra for accelerometer pairs 1 and 2, 3 and 4, and 4 and 5 can be obtained. The poles and zeros can be incorporated in the SPA data reduction program.

Amplitude Calibration

The amplitude calibration of accelerometer 1 of the SPA can be performed using the same setup used for phase calibrations. The calibration process is carried out in two steps that are very similar to those described for the PSPA accelerometer. In the first step, a proximator is used as a reference sensor to verify the amplitude calibration of the shaker's built-in accelerometer (see Figure 3.3). In the second step, the response of the SPA accelerometer is compared with that of the shaker's built-in accelerometer. The amplitude ratio spectrum of accelerometer 1 relative to the shaker's accelerometer is shown in Figure 4.6a. A resonant frequency of about 3 kHz is observed. Several small amplitude peaks corresponding with the natural frequency of the accelerometers and shaker can also be seen in the range of frequencies of 10 kHz to 20 kHz. The phase spectrum in Figure 4.6b is also used to ensure full compatibility.

The amplitude calibration spectrum of accelerometer A1 is obtained by multiplying the spectra shown in Figures 3.10 and 4.5. The results are shown in Figure 4.7, and the poles and zeros obtained from curve fitting of the data are shown in the Table 4.2.

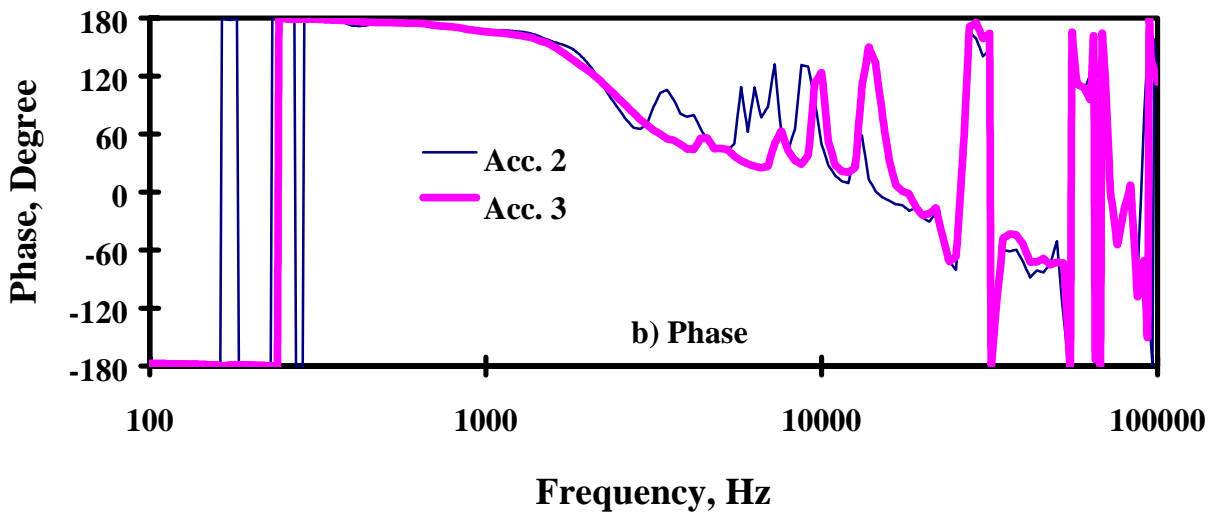
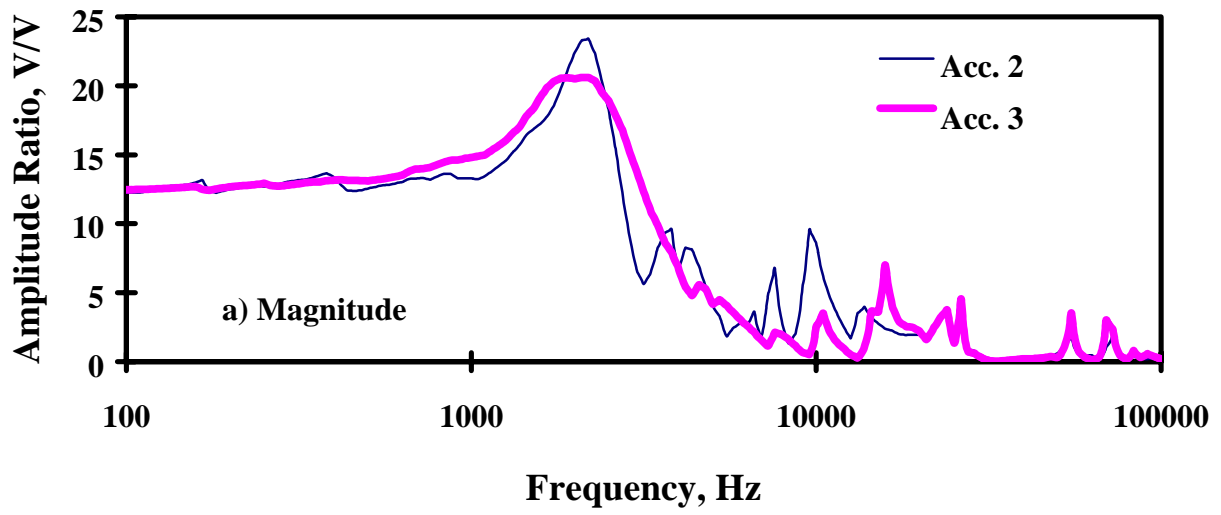


Figure 4.4 - Comparison of Response of Accelerometers 2 and 3 of SPA

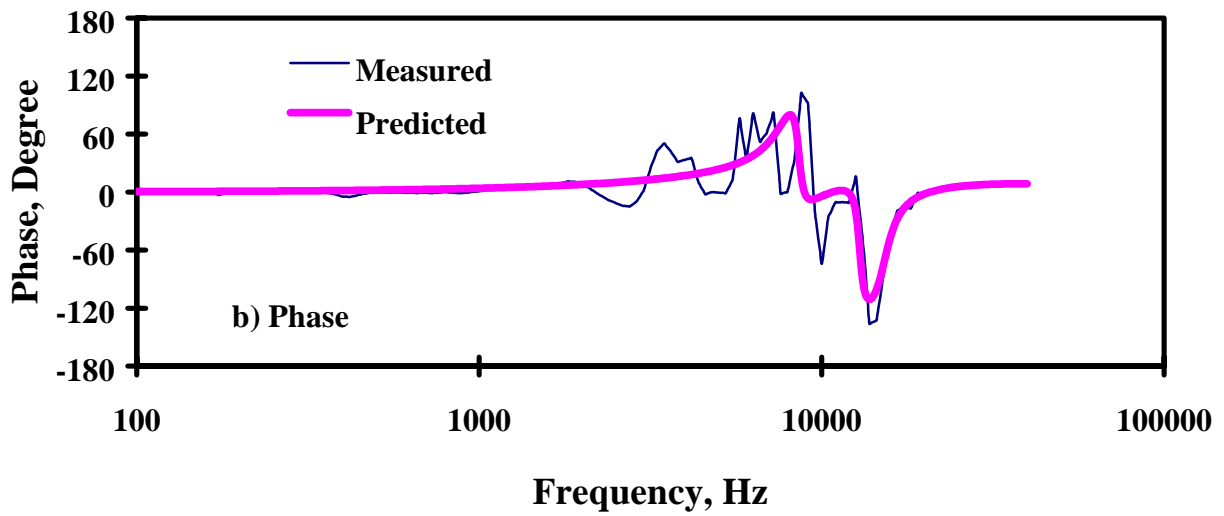
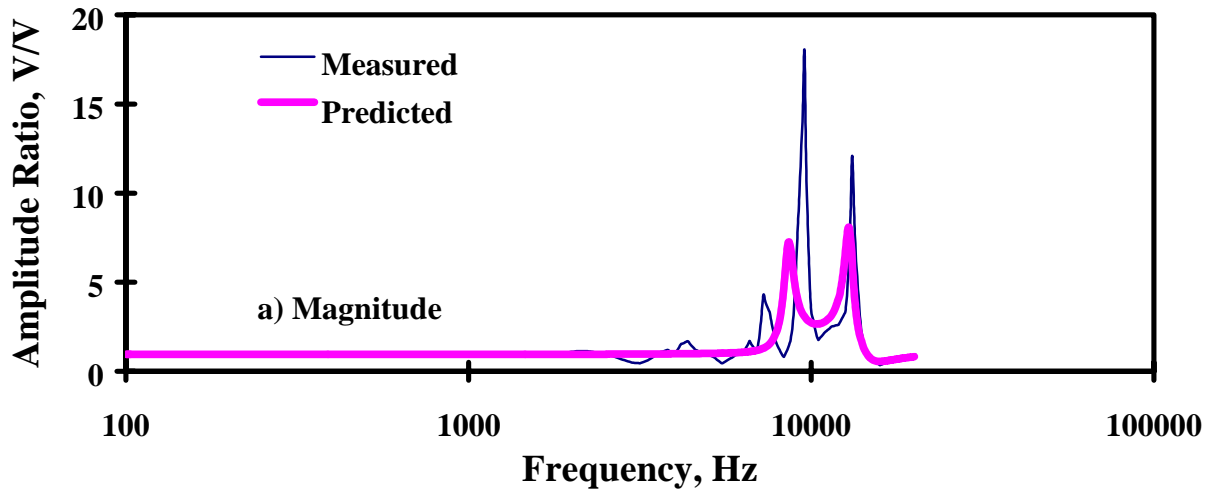


Figure 4.5 - Phase Calibration Spectrum for Accelerometers 2 and 3 Pair

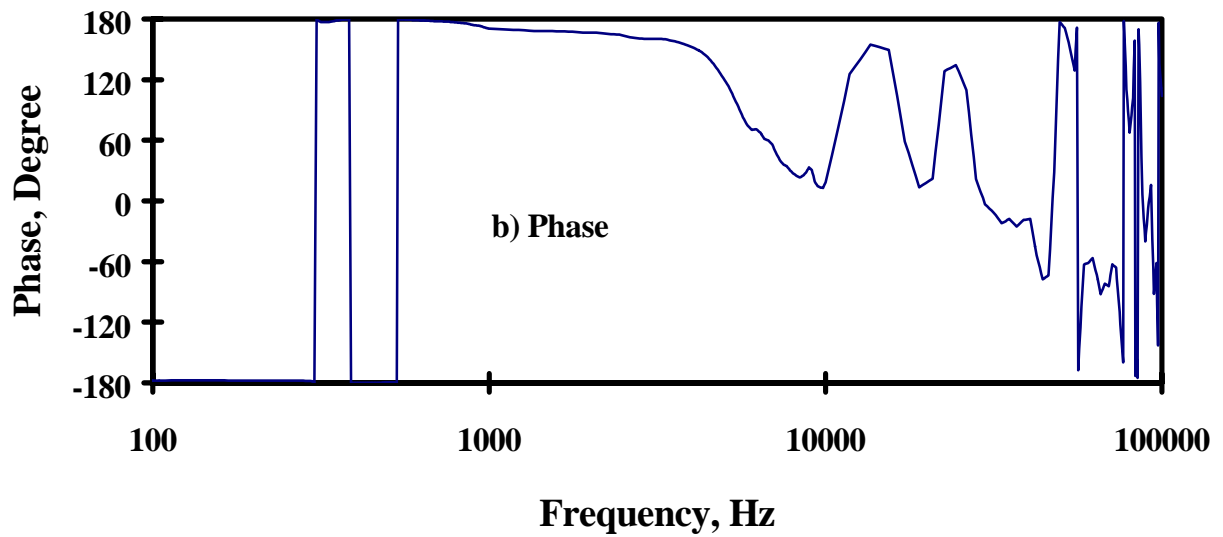
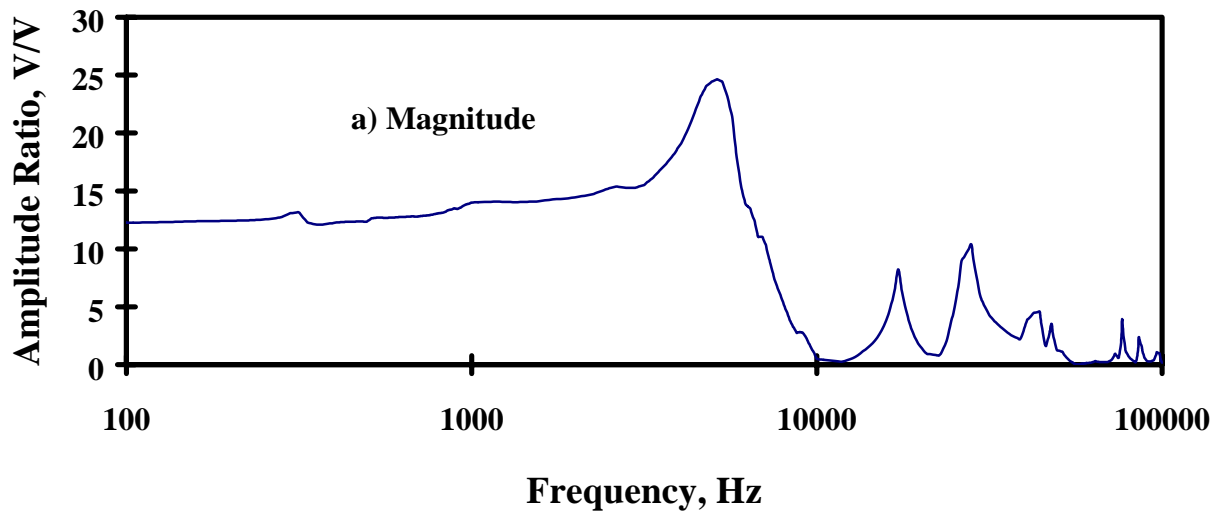


Figure 4.6 - Amplitude Ratio Spectrum of Accelerometer 1 of SPA

Table 4.1 - Poles and Zeros Obtained from Fitting a Curve to Data Shown in Figure 4.5

Number	Poles	Zeros	Gain
1	-27843.2	-15012	1.43
2	-256.776+8576.7i	-1183.18+7981.07i	
3	-256.776-8576.7i	-1183.18-7981.07i	
4	-365.857+12921.9i	-1270.28+15157.1i	
5	-365.857-12921.9i	-1270.28-15157.1i	

Table 4.2 - Poles and Zeros Obtained from Fitting a Curve to Data Shown in Figure 4.7

Number		Poles	Gain
1	3189.91	1685.22	3.23E-05
2	9359.49	27077.7	
3	-3780.26+2669.41i	-648.619+2929.41i	
4	-3780.26-2669.41i	-648.619-2929.41i	
5	-149.63+10582.9i	-279.185+11961.9i	
6	-149.63-10582.9i	-279.185-11961.9i	
7	100.972+13656.8i	-181.474+15829.9i	
8	100.972-13656.8i	-181.474-15829.9i	
9	453.977+16558.4i	-7895.45+25999.9i	
10	453.977-16558.4i	-7895.45-25999.9i	

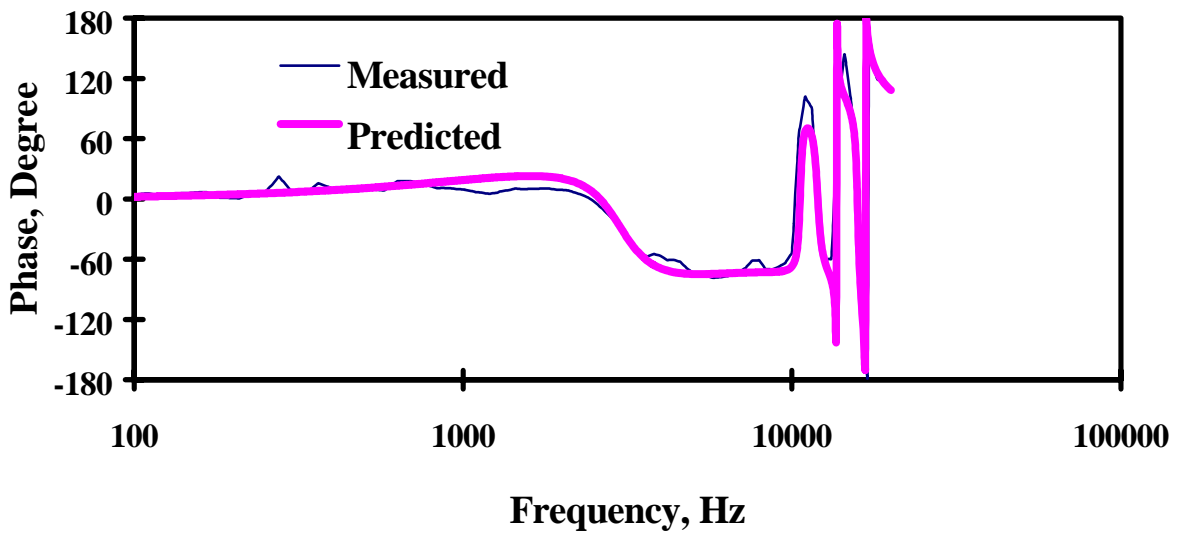
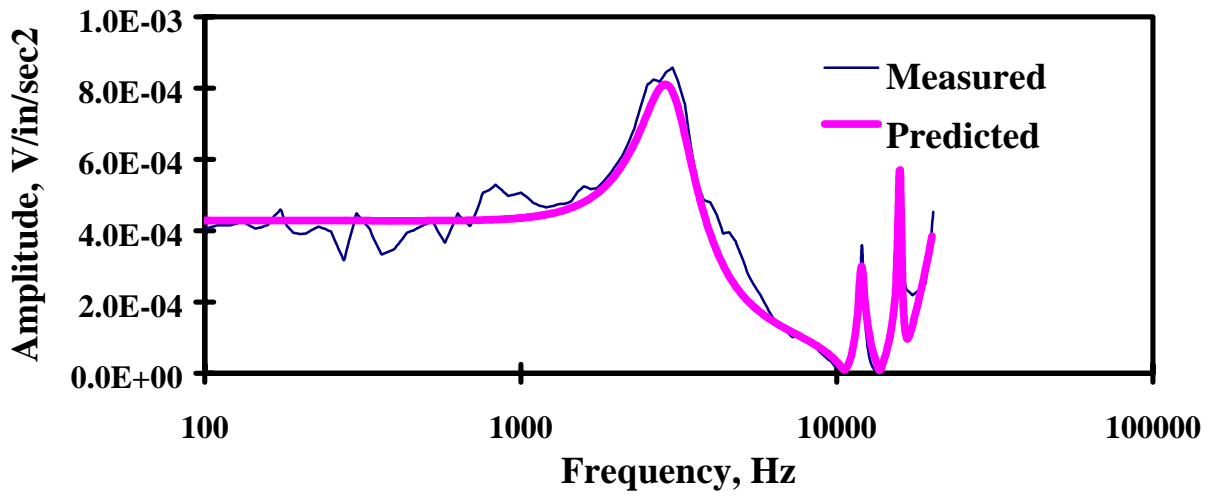


Figure 4.7 - Amplitude Calibration of SPA Accelerometer 1

Proposed Calibration of Geophones

Phase Shift Calibration

The phase shift calibration should be carried out between geophones 2 and 3 (see Figure 4.1). These two geophones are used in the SASW method. The calibration procedure is identical to that for the SPA accelerometers with one exception. The calibration process is carried out between frequencies of 10 Hz and 1000 Hz.

The relative amplitude and phase shift spectra between the two SPA geophones and the shaker's built-in accelerometer are compared in Figure 4.8. The amplitude ratios, as shown in Figure 4.8a, vary by a factor of about 2. This indicates that geophone 3 is about 2 times more sensitive than geophone 2 because of the built in amplifiers associated with each sensor. The phase spectra, on the other hand, are similar (see Figure 4.8b).

The phase calibration spectrum, which, as usual, is obtained by subtracting the two phase spectra in Figure 4.8b, is included in Figure 4.9b. The phase shift values throughout the spectrum deviate very little from zero. The poles and zeros obtained by curve fitting are shown in Table 4.3. The fitted and measured amplitude spectra (Figure 4.9a) and the phase spectra (Figure 4.9b) compare favorably.

Amplitude Calibration

To produce accurate IR test results, geophone 1 should be calibrated for amplitude. The procedure followed and equipment used are almost identical to those described for calibrating the FWD geophones. The only difference is that the calibration up to a frequency of 200 Hz is necessary.

As a quick review, the first step is to verify the calibration of the geophone with a proximator (see Figure 2.5). In the second step, geophone 1 of the SPA is lowered on top of the shaker and is calibrated under a swept sine condition.

The variation in the amplitude ratio spectrum of the SPA geophone with respect to the shaker geophone is shown in Figure 4.10a. The SPA geophone is approximately 5 to 10 times more sensitive than the calibration geophone in the range of frequencies of 1 Hz to 500 Hz. The phase shift spectrum between the SPA and calibration geophones is shown in Figure 4.10b. The phase varies by less than ± 20 degrees in the range of frequencies of 1 Hz to 500 Hz.

By multiplying the spectra shown in Figure 2.5 by those of Figure 4.10, the calibration spectra for geophone 1 of the SPA is obtained. Such curves are shown in Figure 4.11. These spectra can be conveniently incorporated into the analysis of the IR data through a curve-fitting process. The poles and zeros obtained from the dynamic signal analyzer can be utilized to identify the geophone characteristics. The differences between the measured and fitted curves are at the most a few degrees. The fitted curves are compared with the measured data in Figure 4.11, and the results are comparable. The phase spectra, shown in Figure 4.11b, are quite close in the range of frequencies 1 Hz to 500 Hz. This information can be entered in the SPA data reduction program for further analysis.

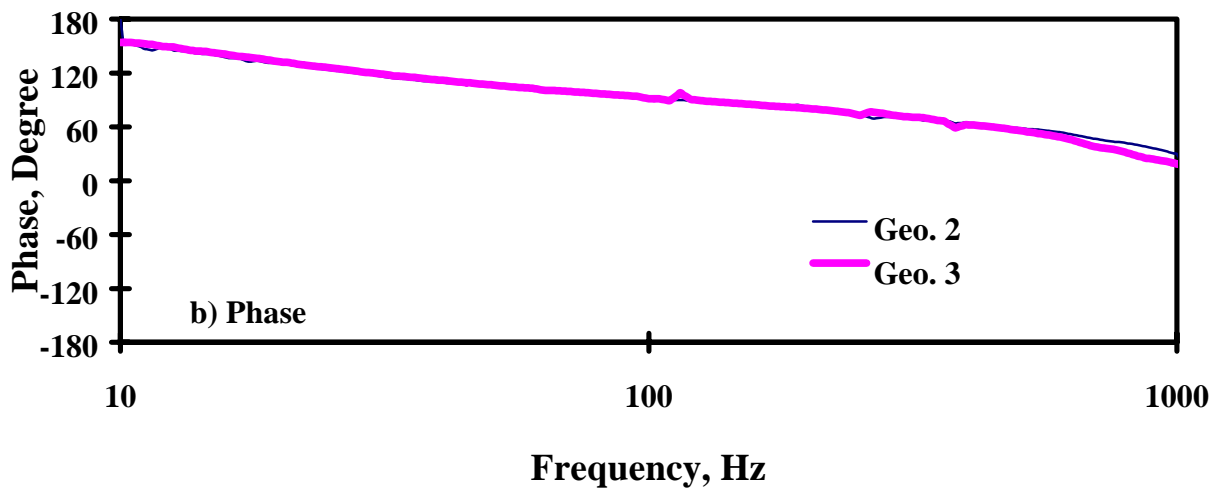
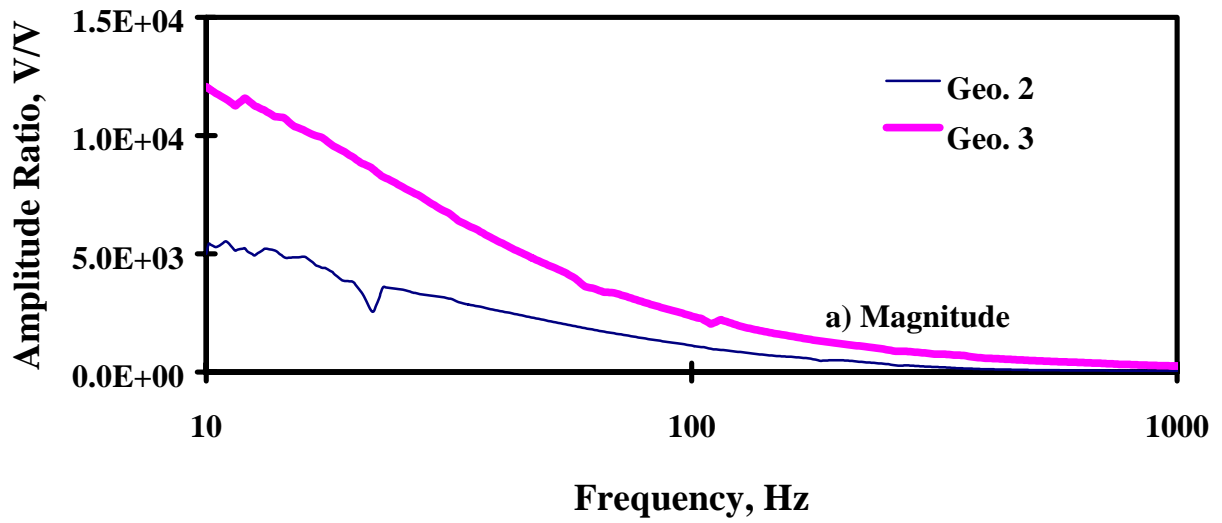


Figure 4.8 - Comparison of Response of Geophones 2 and 3 of SPA

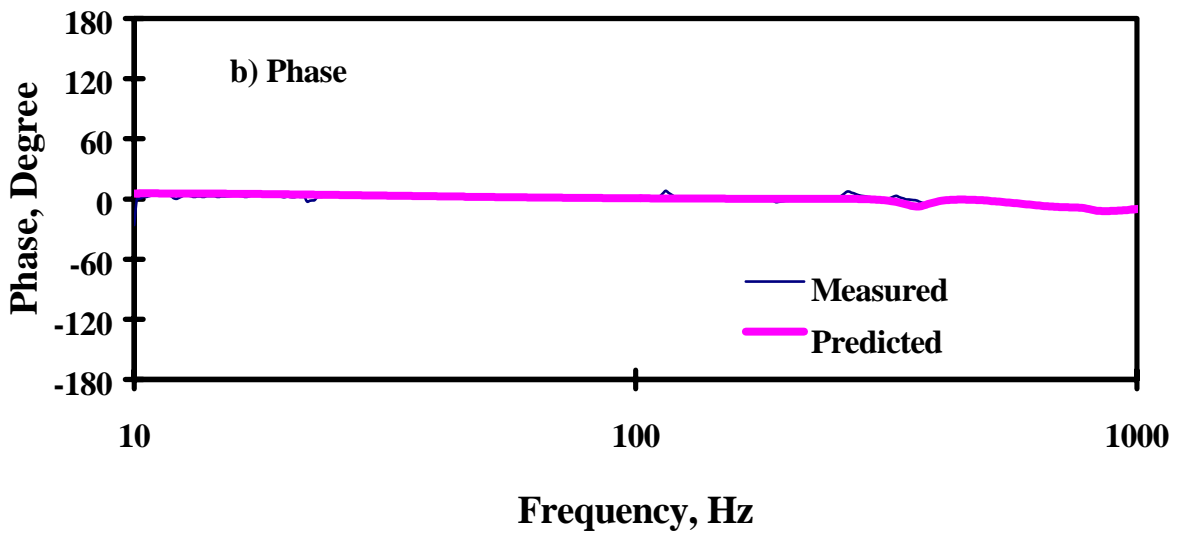
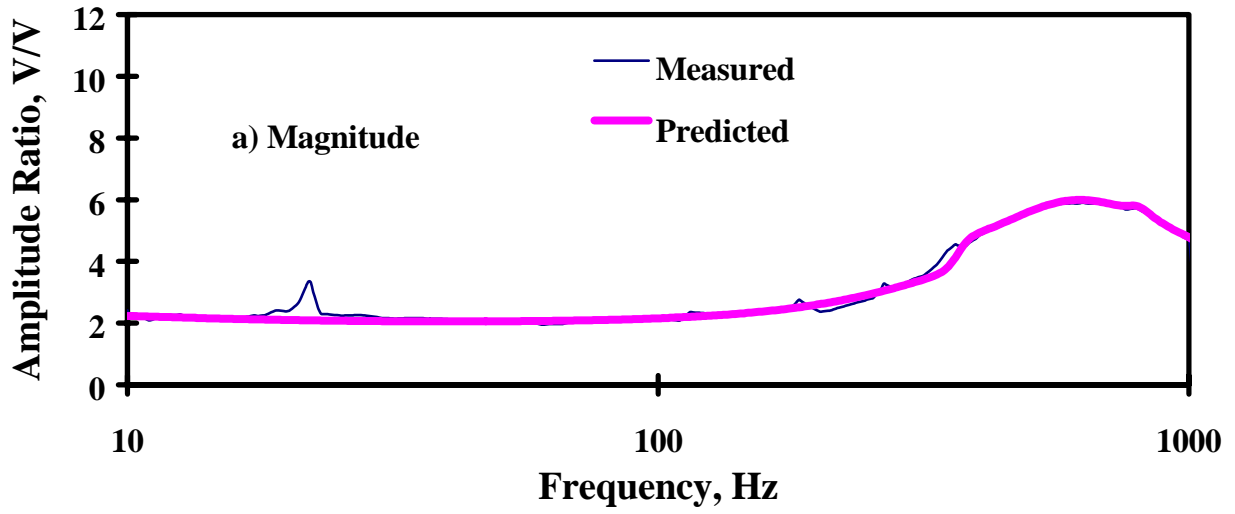


Figure 4.9 - Ratio of Frequency Response Curves of Geophone 2 and 3

Table 4.3 - Poles and Zeros Obtained from Fitting Curve to Data Shown in Figure 4.9

Number	Poles	Zeros	Gain
1	-8270	-499	11.15
2	9.86	12	
3	422+335i	418+97.1i	
4	422-335i	418-97.1i	
5	30.80+368i	31.2+363i	
6	30.80-368i	31.2-363i	
7	-329.97+530i	-1260+533i	
8	-329.97-530i	-1260-533i	
9	-52+797i	-54.5+795i	
10	-52-797i	-54.5-795i	

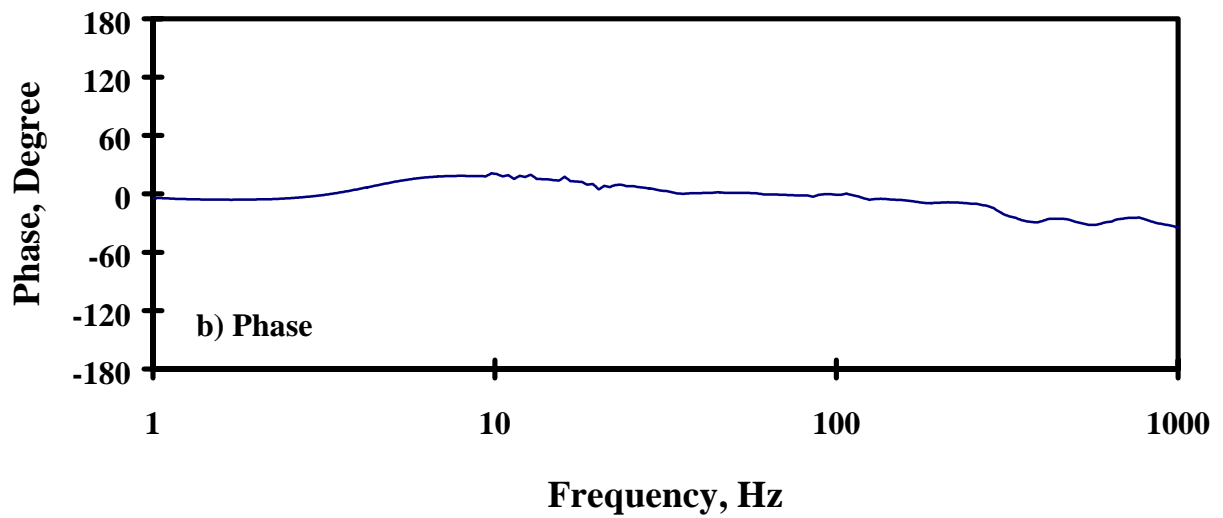
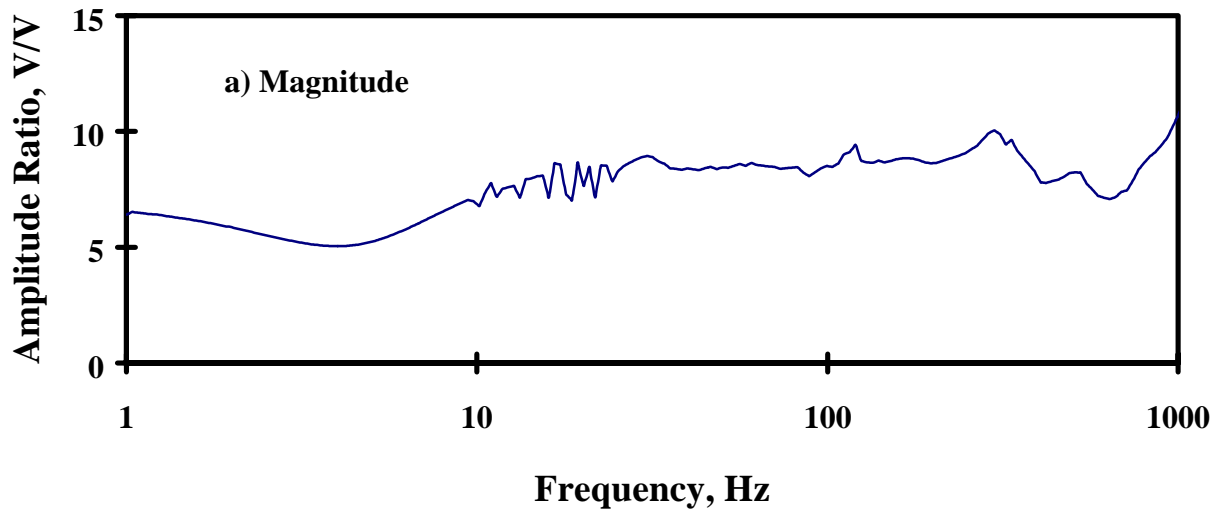


Figure 4.10 - Field Calibration of SPA Geophone 1

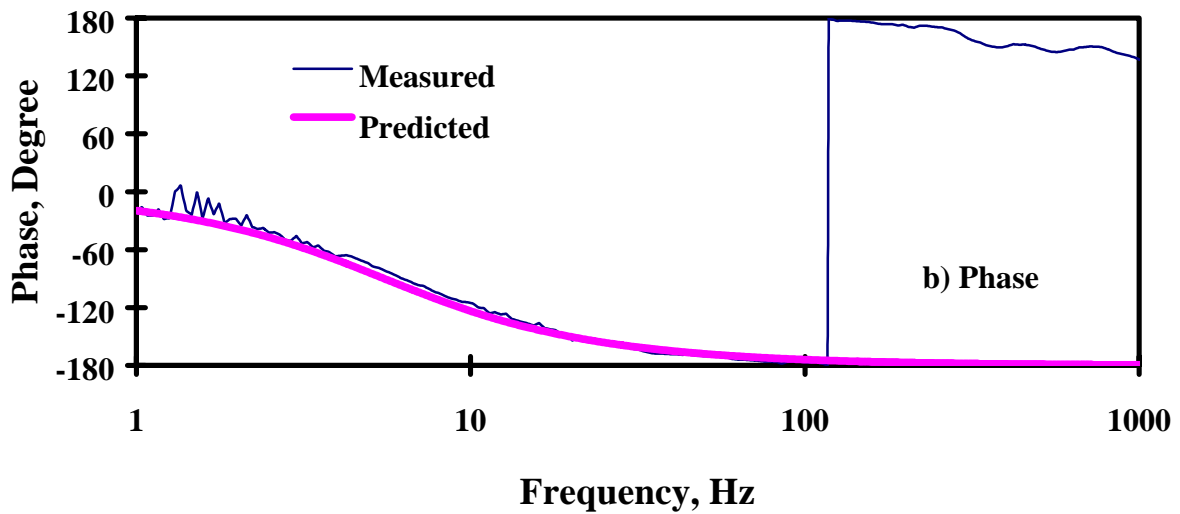
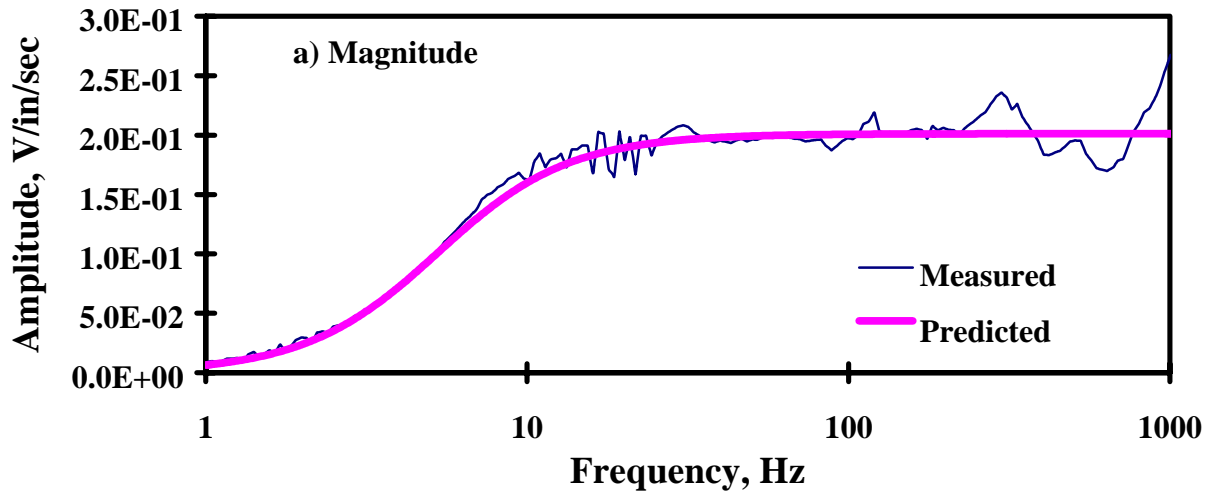


Figure 4.11 - Calibration Amplitude Spectra for Geophone 1 of SPA

Proposed Calibration of Load Cells

The calibration procedures for the high- and low-frequency load cells are very similar to those for the FWD load cell. The only difference is that only one of the three load cells used in the calibration of the FWD is used. If necessary, the calibration of the reference load cell can be verified under an MTS system, as discussed in Chapter 2.

A test setup for this task is shown in Figure 4.12. A steel plate is placed under the SPA load cell assembly. Both load cells can be calibrated with the same setup. The calibration load cell is placed directly under the high-frequency or the low-frequency load cell. The SPA load cell is then manually activated to directly impact the calibration load cell. Tests are normally carried out at four load levels, with 10 repetitions at each load level. The two load cells are connected to a recording device, in a manner similar to that used for the FWD system.

The load level applied by each of the SPA load cells is controlled by a pressure regulator. In routine testing, the pressures are not changed. However, for the calibration purposes, the air pressure is changed so that the calibration curve over a range of load intensities can be obtained. The SPA has three pressure regulators. To change the load intensity, the pressure regulator shown in Figure 4.13 should be used.

Typical load time-histories from the calibration load cell and the SPA's low-frequency load cell are shown in Figure 4.14. The duration of the impulse is about 1 msec. The load cell of the SPA is about 2.5 times more sensitive than the calibration one. In addition, a high-frequency low amplitude energy is superimposed on the SPA's load cell record. This energy is believed to be related to the reflection of the energy within the piston rod of the load cell assembly. The frequency content of this signal is too high to be of any consequence since the load intensity is used only in the IR method.

The variation in output of the SPA low-frequency load cell as a function of the load imparted to the reference load cell is shown in Figure 4.15. The two variables are well correlated since the R^2 -value is about 0.99 with a standard error of estimate of 8.36. The calibration value for the low-frequency load cell system consisting of the impacts of the electronic components and the mounting system is about 0.5 mv/lbf.

Since in the IR method the data analysis is conducted in the frequency-domain, it is prudent to measure the variation in the amplitude or phase shift as a function of frequency for the low-frequency load cell system. The variations in the amplitude or phase shift can be due either to the mounting of the load cell or the characteristics of the electronic components. To determine this information, a transfer function between the SPA load cell and the calibration load cell should be developed. The two load cells are attached to a spectrum analyzer. The input signals are Fourier-transformed and divided by one another. This experiment is carried out only at load levels typically used during the SPA operations. The result from one experiment is shown in Figure 4.16. The amplitude spectrum is fairly constant with frequency. The amplitude on the average is about 2.2, indicating the SPA load cell is more sensitive than the calibration load cell. Perhaps it is necessary to purchase a more sensitive load cell to be used for calibration. The new load cell was not purchased in this study for economical reasons. The phase varied about 10 degrees up to a frequency of 200 Hz (see Figure 4.16b). This variation is sufficiently small that it should not be of much concern in the current methodology used to interpret IR data. For more sophisticated analyses, these changes can be considered in a similar manner as that used for accelerometers or geophones.

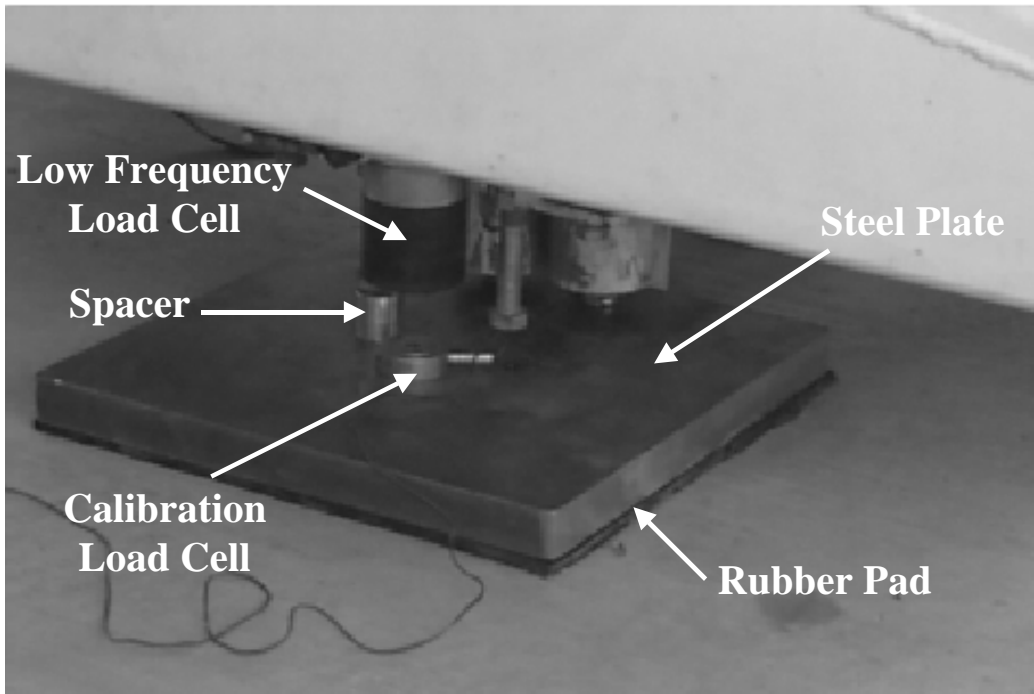


Figure 4.12 - SPA Load Cell Calibration Test Setup

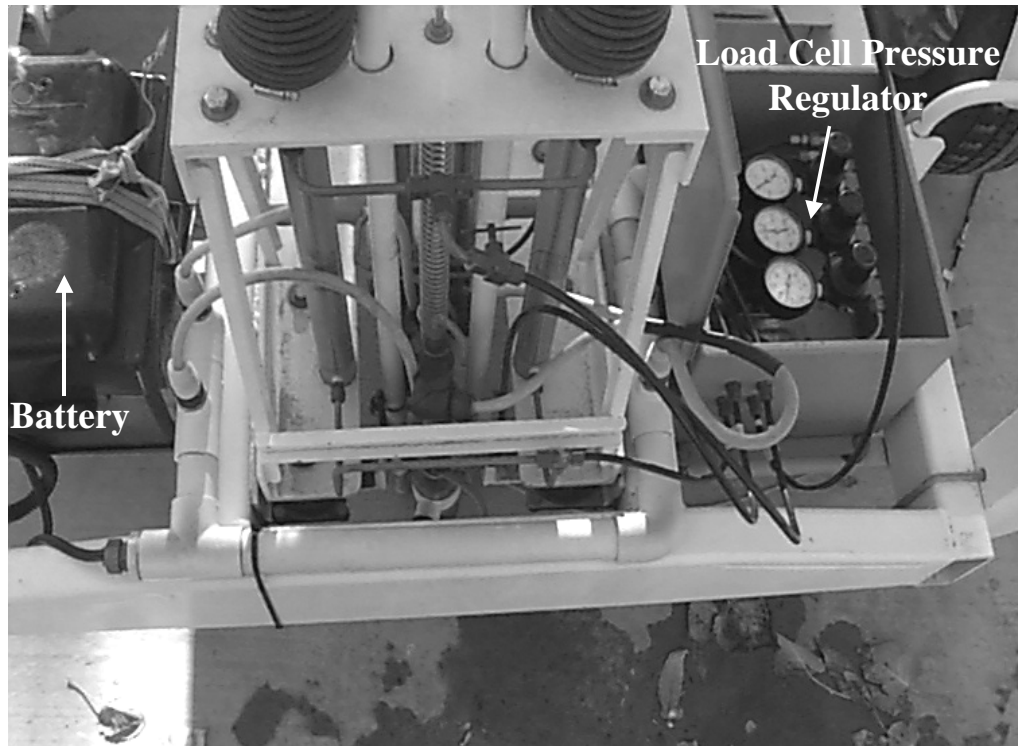


Figure 4.13 - SPA Pressure Level Setup

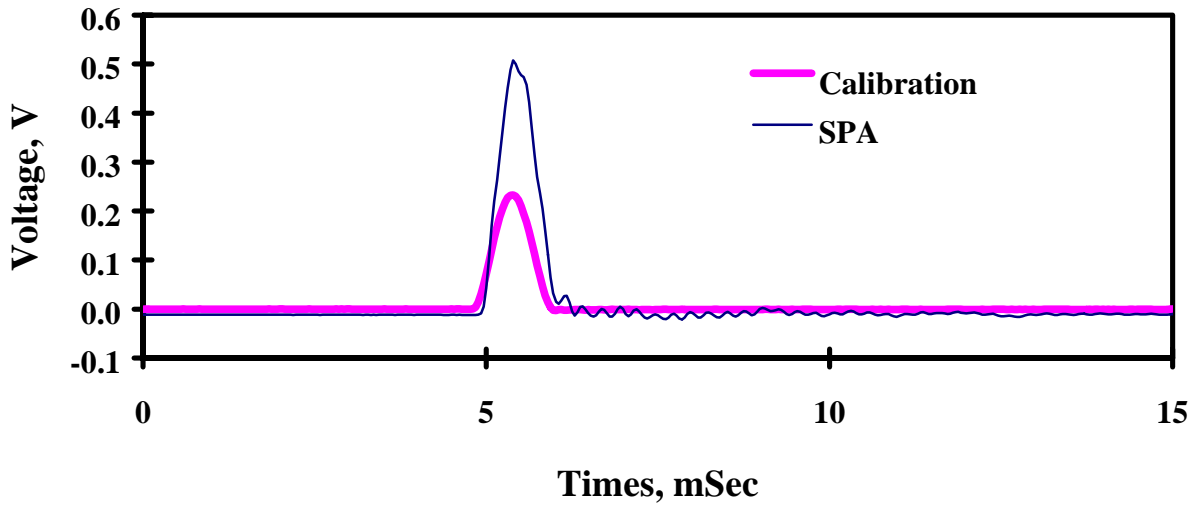


Figure 4.14 - A Typical Load Time-History from the Calibration and Low-Frequency SPA Load Cells

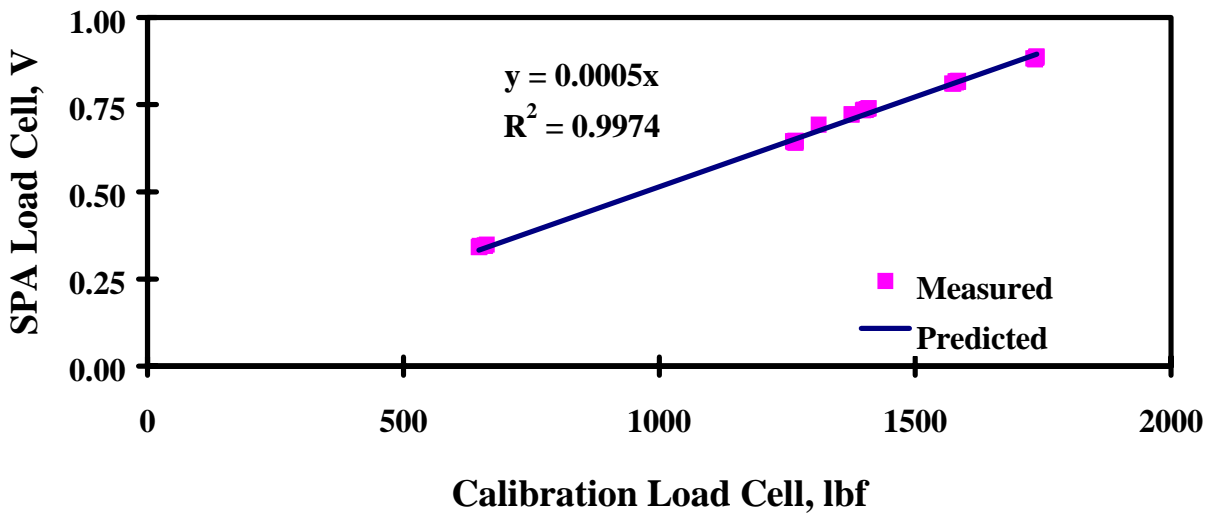


Figure 4.15 - A Typical Calibration Curve of SPA Low-Frequency Load Cell

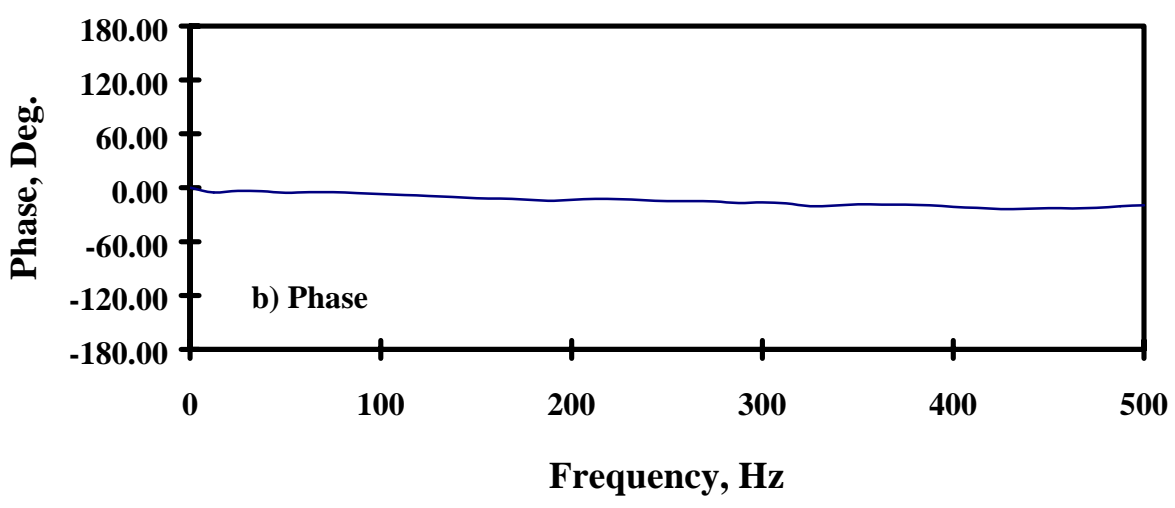
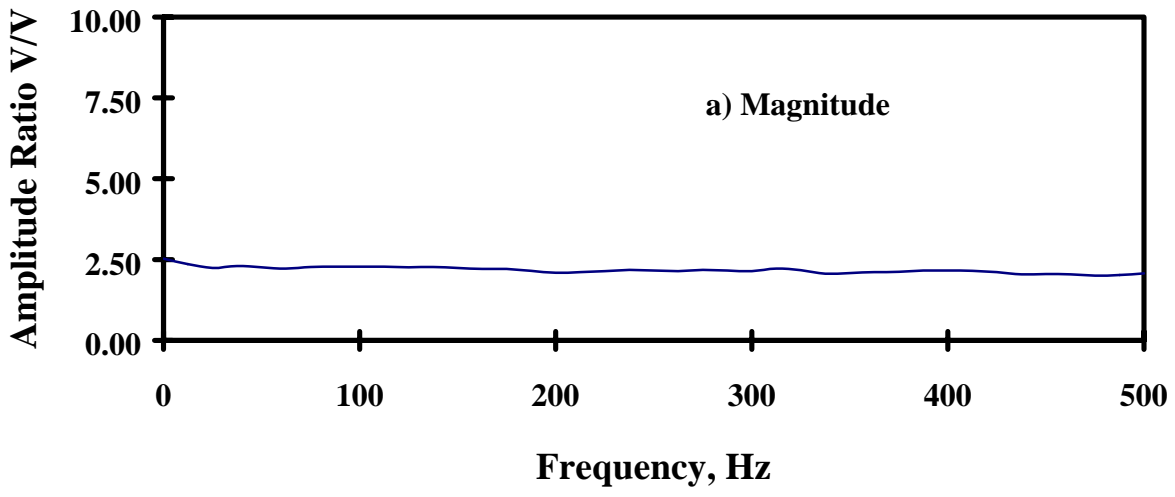


Figure 4.16 - A Typical Frequency Response of Low-Frequency Load Cell

The same process as described above is repeated for the high-frequency load cell. A typical load time history of high-frequency load cell is shown in Figure 4.17. The impulse duration is approximately 160 μ sec, and the maximum applied load is around 800 lbf. The SPA load cell is 25 times more sensitive than the calibration load cell. The calibration curve from this activity is shown in Figure 4.18. The R^2 -value is about 0.99 and the standard error of estimate is 0.105. The calibration value for the high-frequency load cell is about 3 mv/lbf.

SPA Calibration Strategy

The SPA calibration strategy for the most part is similar to the PSPA and FWD strategies. In this section a preliminary procedure is proposed. However, since historical data are not available to draw definite conclusions, the proposed strategy should be modified with time. A summary of the proposed calibration process is shown in Figure 4.19.

Relative Calibration

A relative calibration process for SPA would be difficult because of the cost involved in developing the facility. A massive PCC block (approximately 20 ft long, 12 ft wide, and 8 ft deep) could be poured and used for relative calibration of SPA similar to that of PSPA. In addition, better quality control effort is needed to make sure that the material properties of PCC block are consistent. However, this is an expensive option and may be evaluated in future research projects.

Reference Calibration

The flow chart of the activities associated with the reference calibration is shown in Figure 4.20. The goal is to determine the calibration curve that has to be input into the data analysis software. In addition, this calibration process can be used to determine whether the malfunction of a suspect SPA is due to the problems with the assembly of an accelerometer or geophone, due to malfunction of an accelerometer or geophone, or due to problems with electronic components.

This task is carried out in three phases. In phase one, accelerometers are calibrated for amplitude as well as phase shift. From the steps described in the previous sections, calibration curves similar to the one shown in Figures 4.5 and 4.7 are obtained. The final products, from this activity, are curve fitting parameters (i.e., several poles and zeros and a gain factor similar to those reported in Tables 4.1 and 4.2). If the amplitude or phase spectrum varies significantly from the initial one provided by the manufacturer or determined by TxDOT personnel at the time of initial delivery, the accelerometer should be put through a diagnosis calibration to determine whether the accelerometer, the accelerometer assembly or the electronic components should be adjusted or repaired. At this time not enough data are available to accurately define the acceptable ranges for changes in the calibration curve. In the second phase, the geophones are calibrated for amplitude as well as phase shift. The process is similar to that for accelerometers.

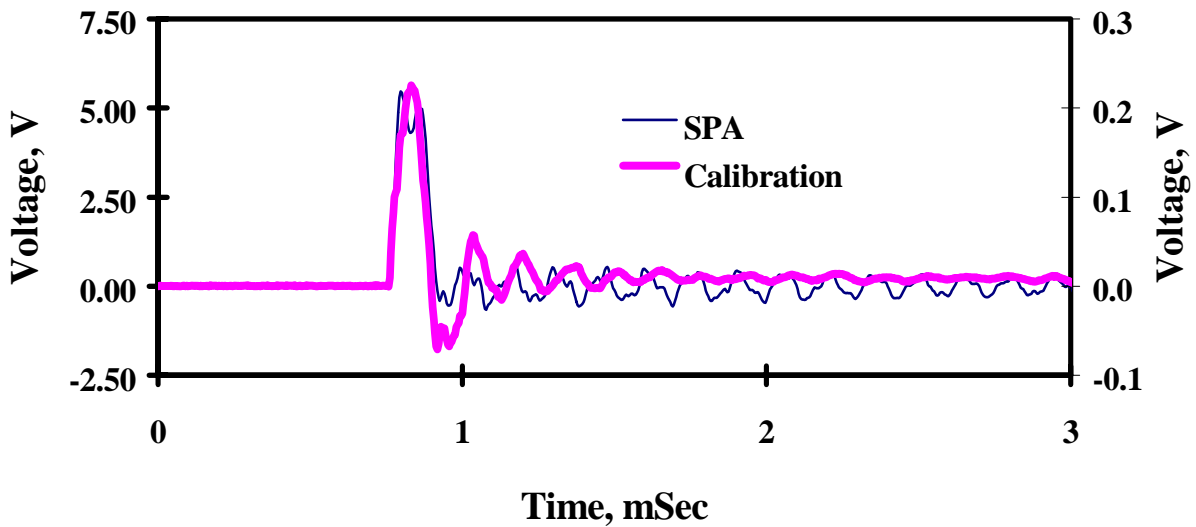


Figure 4.17 - A Typical Load Time-History from the Calibration and High-Frequency SPA Load Cells

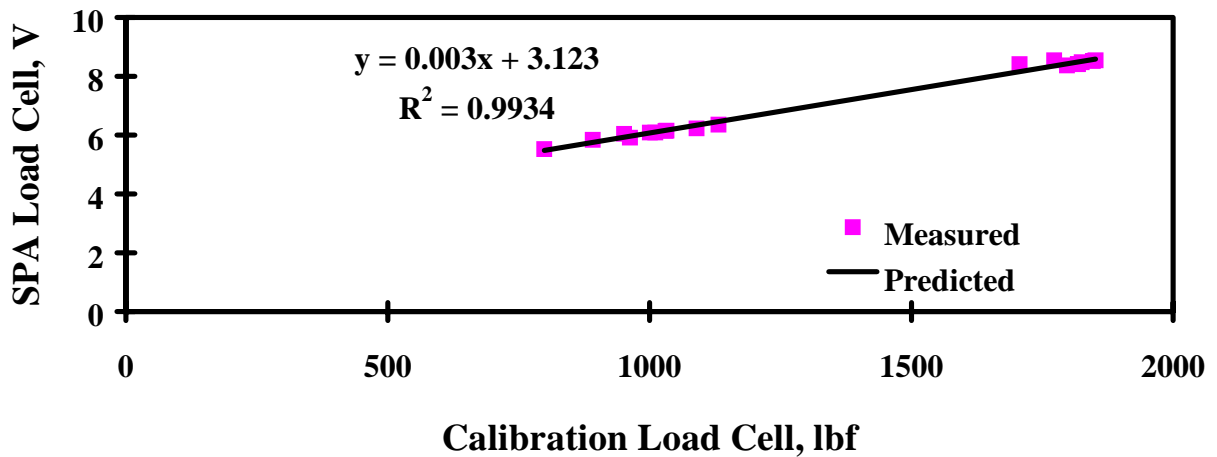


Figure 4.18 - A Typical Calibration Curve of SPA High-Frequency Load Cell

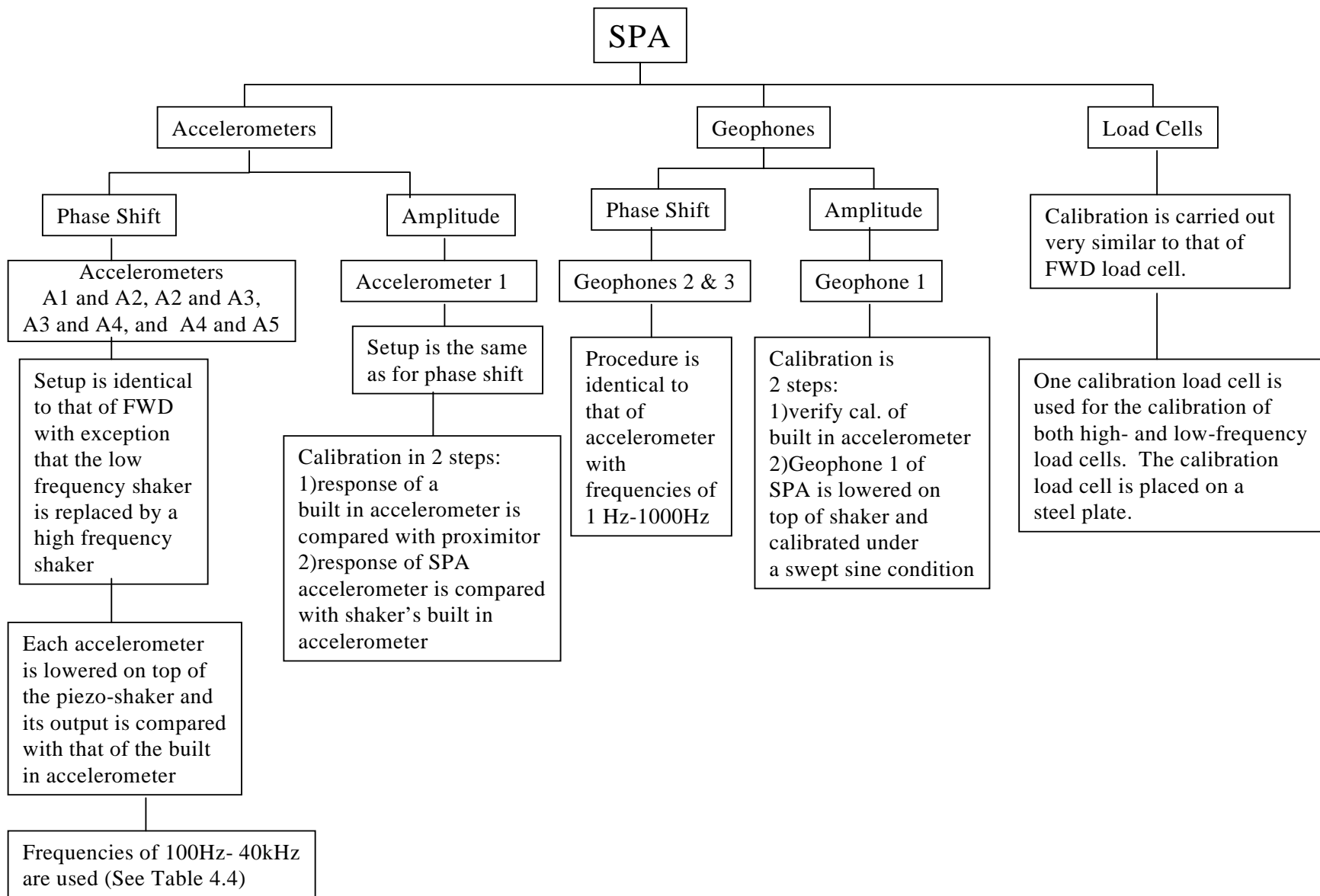


Figure 4.19 - Summary of Proposed SPA Calibration

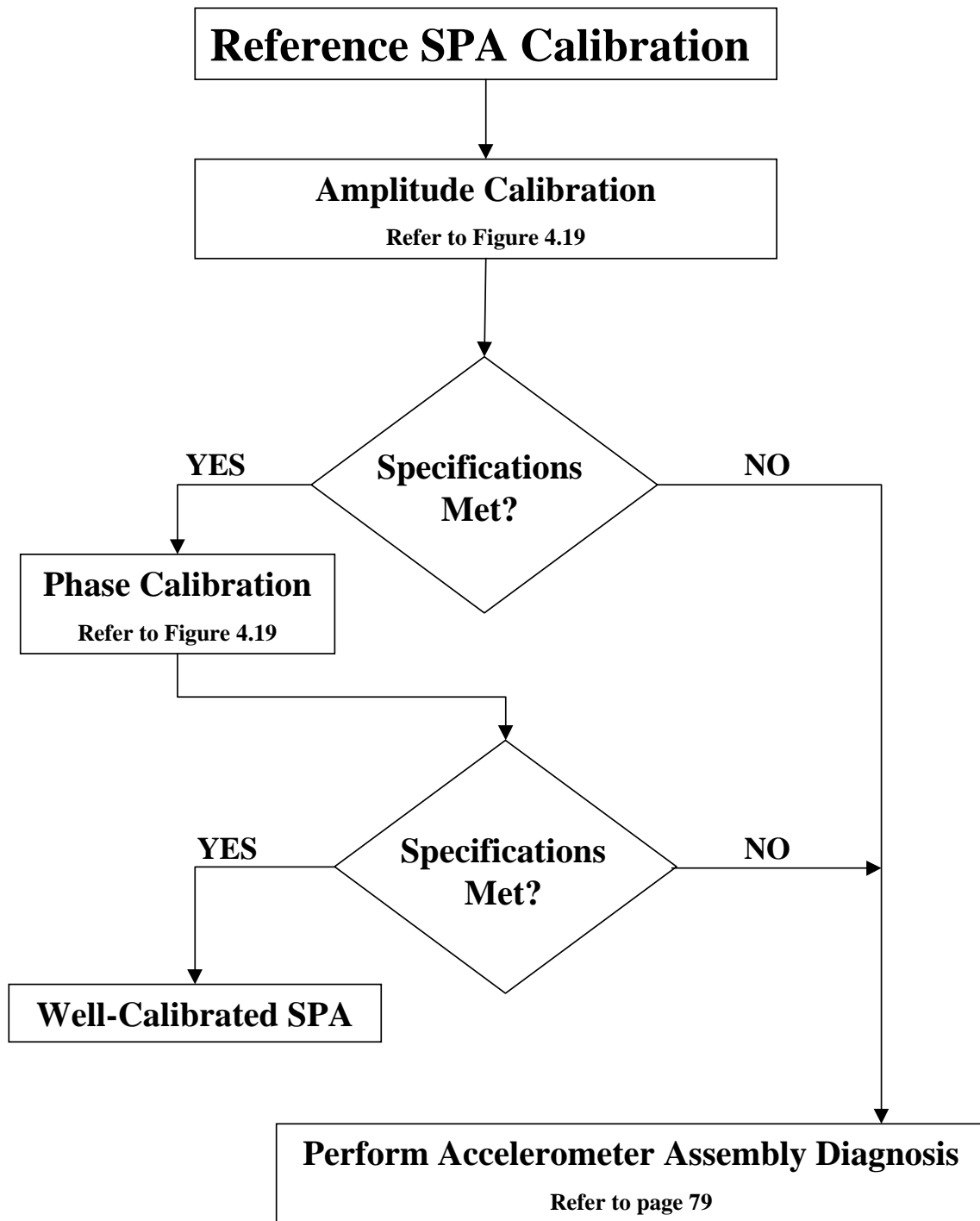


Figure 4.20 - Proposed Reference SPA Calibration Strategy

In the third phase, the load cell calibration should be performed using the setup shown in Figure 4.12 and steps suggested in that section. The load levels measured with the SPA and the calibration system should be compared. If the differences are less than 3%, the calibration factor should be adjusted. For larger differences, the SPA load cell system should be inspected and replaced, and the load cell should be re-calibrated. Alternatively, the load cell itself should be replaced.

Accelerometer or Geophone Assembly Diagnosis

During the reference calibration, one cannot identify the exact source of the problem with a SPA accelerometer or geophone system. The diagnostic steps, described below, can be used to determine the source of the potential problem.

In this step, the accelerometer or geophone is removed from the SPA and is subjected to the calibration process. If the accelerometer or geophone does not exhibit an amplitude and phase spectra similar to the one shown in Chapter 2 or 3, then the accelerometer or geophone should be replaced. Otherwise, the vendor of the SPA should be contacted. A preliminary process for developing a calibration procedure for the electronic components of the SPA has been developed. However, the process is not robust enough to ensure that the circuit board will not become damaged during the calibration. The reference calibration should be performed, after the faulty accelerometer or geophone is replaced, to update the phase shift or amplitude calibration curve of the SPA system.

It should be emphasized that the proposed calibration strategy is preliminary. Further evaluation and fine-tuning are needed before it is finalized.

Accelerometers

The accelerometers used in SPA are manufactured by PCB Piezotronics, Inc. The manufacturer provides a certificate of calibration with each accelerometer that contains a NIST-traceable calibration factor. More than a decade of experience has reasonably proved to the researchers that the manufacturer's calibration is within 2% of specified value. Therefore, a strategy to accept or reject an accelerometer received from the manufacturer is not needed. Since the SPA is a seismic tool, the actual amplitudes of the accelerometers are not used in any of the analyses.

The accelerometers are used for the IE method, USW and UBW method and SASW method. For the reference calibration associated with the USW, UBW and SASW, the phase shifts are of concern. The five accelerometers of SPA should be calibrated for phase shifts. As a reminder, the phase shift calibration is primarily used to account for any artificial phase shift between the two accelerometers due to sensor mounting or electronic components. The poles and zeros for each set of adjacent accelerometers (i.e., accelerometer pairs A1-A2, A2-A3, A3-A4 and A4-A5) should be established. The focus of the curve fitting should be progressively towards lower frequency ranges as the accelerometers farthest from the source are calibrated. The optimum frequency ranges are summarized in Table 4.4. The preliminary acceptance criterion is similar to those for the PSPA.

Table 4.4 - Optimal Frequency Ranges to be Considered in Reference Calibration of SPA Accelerometers for Phase Shift

Sensor Pair	Minimum Frequency	Maximum Frequency
A1-A2	2 kHz	40 kHz
A2-A3	1 kHz	35 kHz
A3-A4	500 Hz	20 kHz
A4-A5	100 Hz	10 kHz

The amplitude calibration should also be carried out for accelerometers 1 and 2 as a part of a reference calibration pertinent to the IE method. With the amplitude calibration, the impact of the accelerometer seating and electronic components used in manufacturing the SPA from the IE response is removed. Once again, in the IE method, the frequency at which the maximum amplitude occurs is of interest (not the actual amplitude). A very rigorous amplitude calibration, similar to that for FWD, is not necessary. The preliminary acceptance criteria are the same as for the PSPA (see Chapter 3).

Geophones

Geophones 2 and 3 are used for the SASW tests. Therefore, they require a phase shift calibration. On the other hand, geophone 1, used for the IR tests, requires an amplitude calibration.

The geophones used in the SPA are quite similar to those used in the FWD. As such, the acceptance criteria for the units are identical to those suggested for the FWD geophones in Chapter 2.

The phase shift calibration should be carried out as discussed in this chapter. The calibration spectrum should be similar to that shown in Figure 4.8. If the calibration characteristics deviate much from the one shown, the geophone should be removed and calibrated in the laboratory following the set up shown in Figure 2.3. If the response of the geophone by itself is similar to that shown in Figure 2.4, the problem is potentially in the electronic components or the geophone holder. The manufacturer should be contacted for the proper remedy. If the geophone is defective, it should be replaced and the appropriate calibration should be carried out.

Once again, the researchers are developing an electronic test to evaluate the condition of the electronic components. However, it has not been finalized.

Load Cell Calibration

The load cells used in SPA are manufactured by PCB Piezotronics, Inc. The manufacturer provides a certificate of calibration with each load cell that contains a NIST-traceable calibration factor. More than a decade of experience has reasonably proved to the researchers that the manufacturer's calibration is within 2% of specified value. Therefore, the researchers recommend that the calibration be carried out after the sensor is installed in the device.

The low-frequency and high-frequency load cells should be calibrated at the time of the delivery of the SPA. These calibration factors can be used as an initial reference for evaluating their in-service performance. The low-frequency load cell should be capable of applying an impulse of less than 1.5 msec with a load of not less than 1,000 lb. (4.5 kN). Similarly, the high-frequency load cell should apply an impulse of less than 200 μ sec in duration of at least 500 lb. (2.2 kN). If, during routine testing, the performance of one or both of the load cells is not satisfactory, the load cell assembly and the pneumatic system should be inspected. First, an internal electronic check, provided in the SPA software, should be carried out to ensure that the cabling is not defective. By conducting a calibration of the load cell, one can evaluate the condition of the source assembly. The calibration steps suggested in the previous section should be used. If the response of either of the load cells differs, approximately, by more than 5% from the response measured initially, the load cell assembly should be disassembled, cleaned, and reassembled. If the impulse width is longer than those specified above, the pistons should be oiled or serviced. If the difference between two consecutive values is less than 5%, the new factor should be input into the SPA data reduction program.

Chapter 5

Closure

This report contains recommendations and procedures for calibrating three nondestructive testing devices. The three devices are the Falling Weight Deflectometer (FWD), the Seismic Pavement Analyzer (SPA), and the Portable Seismic Pavement Analyzer (PSPA).

The existing calibration strategies for the FWD were reviewed and modified so that the device can be calibrated more conveniently and more comprehensively. The calibration is carried out along a slab. The unique features of the proposed methodology are as follows:

- The FWD does not have to be disassembled for the calibration.
- The impact of the sensor holder on the response of the sensor can be quantified.
- The variation in calibration parameters as a function of frequency can be developed so that the full-waveform analyses can be performed accurately.

The calibration procedures for the SPA and the PSPA are, for the most part, significantly different. The highlights of the calibration process are as follows:

- Means of measuring any artificial phase shift between the response of the sensors used to calculate wave propagation velocity are developed. An unaccounted phase shift will distort the propagation velocities measured with these devices.
- To optimize the detection of thickness, the impact of the sensor assembly is delineated and accounted for. Procedures for quantifying the impact of the sensor assembly are proposed.
- The duration and strength of the loads applied to the pavement should also be considered to ensure proper behavior of the system. Protocols for defining the satisfactory behavior of the SPA and PSPA sources are defined.

One of the important achievements in this project was developing preliminary strategies for systematically determining the possible source of malfunction of either one of the NDT devices. With time, these preliminary guidelines can be improved, and the criteria associated with them can be adjusted.

In the researcher's opinion, the project has lead to implementable products and protocols that can be used by TxDOT. More experience is needed to improve the hardware and software associated with each calibration setup. A database should be initiated and maintained for this purpose.

References

- Baker, M. R., Crain, K., and Nazarian, S. (1995), "Determination of Pavement Thickness with a New Ultrasonic Device," Research Report 1966-1, Center for Highway Material Research, The University of Texas at El Paso, El Paso, TX, 53p.
- Nazarian, S., Yuan, D., and Weissinger, E. (1997), "Comprehensive Quality Control of Portland Cement Concrete with Seismic Methods," Transportation Research Record 1575, Transportation Research Board, Washington, D.C.
- Nazarian, S., Yuan, D., and Baker, M. (1995), "Rapid Determination of Pavement Moduli with Spectral-Analysis-of-Surface-Waves Method," Research Report 1243-1, The University of Texas at El Paso, 76 p.
- Nazarian, S., Baker, M. R., and Crain, K. (1993), "Fabrication and Testing of a Seismic Pavement Analyzer," Report H-375, Strategic Highway Research Program, Washington, DC, Dec., 156 pp.
- Nazarian, S., Tandon, V., and Briggs, R. C. (1991), "Development of an Absolute Calibration System for Nondestructive Testing Devices," Transportation Research Record 1293, Transportation Research Board, Washington, D.C.
- Nazarian S. and Stokoe, K. H., II (1986), "A Theoretical Sensitivity Study of the Falling Weight Deflectometer Device on Determining Moduli of Farm-to-Market Roads," Technical Memorandum IAC936-4, Center for Transportation Research, The University of Texas at Austin.
- Sansalone, M., and Carino, N. J. (1989), "Detecting Delamination in Concrete Slabs with and without Overlay the Impact-Echo Method," ACI Materials Journal, Vol. 86, No. 2, Mar.-Apr., pp. 175-184.
- Tandon, V. (1990), "Development of an Absolute Calibration System for Nondestructive Testing Devices," Master of Science Thesis, Department of Civil Engineering, The University of Texas at El Paso, El Paso.

Appendix A

Specifications of Equipment Used

Table A.1 Specifications of Matching Network (Manufactured by Wilcoxon Research, Inc.)

Description	Units	Values
Model		N7C
Input Voltage, maximum	Vrms	42
F4 Channel		
Current, Maximum (Circuit Breaker)	amps rms	1.5/2.5
Fixed Output	Vrms	42
Frequency Range	Hz	10 - 5000
F7 Channel		
Voltage Output (Switch Position A)	Vrms	300
Frequency Range	Hz	1 - 25
Voltage Output (Switch Position B)	Vrms	500
Frequency Range	Hz	1 - 13
Voltage Output (Switch Position C)	Vrms	800
Frequency Range	Hz	1 - 5

Table A.2 Specifications of F4 Electromagnetic Shaker system (Manufactured by Wilcoxon Research, Inc.)

Description	Units	Values
Model		F4/Z820WA
Usable Frequency Range	Hz	10 - 7500
Maximum Continuous Current	amp rms	1.5
Maximum Continuous Current w/ Air Cooling	amps	2.5
Nominal Electrical Impedance	Ohms	25
DC Electrical Resistance	Ohms	13
Resonance Frequency, blocked	Hz	30
Forced Air Cooling Pressure, Maximum	psi	25

Table A.3 Specifications of Electromagnetic Shaker System Accelerometer (Manufactured by Wilcoxon Research, Inc.)

Description	Units	Values
Accelerometer Model		F4
Voltage Sensitivity	mV/g	100
Frequency Response (± 0.5 dB)	Hz	10 - 2000
Frequency Response (± 1.0 dB)	Hz	6 - 3000
Frequency Response (± 3.0 dB)	Hz	3 - 6000
Power Requirements, Voltage Source	VDC	18 - 30
Current Regulating Diode	mA	2 - 10
Bias Output Voltage, Nom.	VDC	12
Output Impedance	Ohms	<100
Electrical Noise Broadband 2.5 Hz - 25 kHz, nom	mg	700
Electrical Noise Spectral 10 Hz	$\mu\text{g}/\sqrt{\text{Hz}}$	100
Electrical Noise Spectral 100 Hz	$\mu\text{g}/\sqrt{\text{Hz}}$	10
Electrical Noise Spectral 1000 Hz	$\mu\text{g}/\sqrt{\text{Hz}}$	1

Table A.4 Specifications of Electromagnetic Shaker System Force Gage (Manufactured by Wilcoxon Research, Inc.)

Description	Units	Values
Impedance Head Model (Force Gage)		Z820WA
Voltage Sensitivity	mV/lb	100
Frequency Response (±0.5 dB)	Hz	10 - 2000
Frequency Response (±1.0 dB)	Hz	6 - 3000
Frequency Response (±3.0 dB)	Hz	3 - 6000
Power Requirements, Voltage Source	VDC	18 - 30
Current Regulating Diode	mA	2 - 10
Bias Output Voltage, Nom.	VDC	12
Output Impedance	Ohms	<100
Electrical Noise Broadband 2.5 Hz - 25 kHz, nom	mlb	500
Electrical Noise Spectral 10 Hz	μlb/√Hz	60
Electrical Noise Spectral 100 Hz	μlb/√Hz	10
Electrical Noise Spectral 1000 Hz	μlb/√Hz	1
Mass Below Force Gage (including stud)	gram	140
Effective Stiffness	lb/in	>500,000,000

Table A.5 Specifications of Piezoshaker System (Manufactured by Wilcoxon Research, Inc.)

Description	Units	Values
Model Number		F7
Usable Frequency Range	Hz	500-20,000
Maximum Input Voltage	V rms	800
Capacitance	μF	0.010
Weight with Sensing Transducer	grams	1134
Contact Area (Diameter)	mm	15.2
Input Connector		Bendix SPOZA-8-3P
Cable Supplied	m	3

Table A.6 Specifications of Piezoshaker System Transducers (Manufactured by Wilcoxon Research, Inc.)

Description		Units	Values
Model			Z7
Accelerometer	Charge Sensitivity	pC/g	6
	Voltage Sensitivity	mV/g	12
	Capacitance	pF	500
	Frequency Range	Hz	1 to 14,000
Force Gage	Charge Sensitivity	pC/N	49
	Voltage Sensitivity	mV/N	25
	Capacitance	pF	2000
	Frequency Range	Hz	1 to 40,000
	Mass Below Force Gage	grams	20

Table A.7 Specifications of Arbitrary Waveform Generator (Manufactured by Wavetek San Diego, Inc.)

Description	Units	Values
Model Number		75
Waveform Resolution	points	8192 x 4095
Amplitude Range (50 ohms)	Vp	±0.005 - 5
Amplitude Range (open circuit)	Vp	±0.01 - 10
Offset Range (50 ohms)	V	+5 to -5
Maximum Offset Range (open circuit)	v	±10
Resolution	digits	3
Sample Rate Range	Hz	0.02 - 2 E+6
Frequency Resolution	digits	4
Input Impedance	KW	100
Vibration	Hz	5 - 55
Power	rms	90 - 128, 180 - 256
Shock	g	30

Table A.8 Specifications of Vibration Exciter (Manufactured by MB Electronics. A Division of Textron Electronics, Inc.)

Description	Units	Values
Model Number		EA 1250
Frequency Range	cps	5 - 10000
Frequency Range Usable to	cps	20000
Force Vector	lbs	15
Vector Capability	in./sec	70
Displacement	in.	0.5
Max. Acceleration with Internal Accelerometer	g	49
Moving Weight with Internal Accelerometer	lbs	0.255
First Resonance	cps	8900
Power ($\pm 5\%$)	V	9
Power ($\pm 5\%$)	A	4.2
Power	W	28
Driver Coil Resistance	ohms	0.65

Table A.9 Specifications of High Resolution PSPA Accelerometer (Manufactured by PCB Piezotronics, Inc.)

Description	Units	Values
Model		352A
Voltage Sensitivity	mV / g	1000
Frequency Range ($\pm 5\%$)	Hz	5 to 8000
Frequency Range ($\pm 10\%$)	Hz	3 to 10000
Resonant Frequency	kHz	≥ 25
Amplitude Range	$\pm g$ pk	4
Resolution (broadband)	g pk	0.0001
Mechanical Shock Limits	$\pm g$ pk	1000
Amplitude Linearity	%	± 1
Transverse Sensitivity	%	≤ 5
Base Strain Sensitivity	g/m^3	≤ 0.001
Excitation Voltage	VDC	20 to 30
Constant Current Excitation	mA	2 to 20
Output Impedance	ohms	≤ 300
Output Bias Voltage	VDC	8 to 14

Table A.10 Specifications of Power Amplifier (Manufactured by Wilcoxon Research, Inc.)

Description	Units	Values
Model Number		PA7C
Amplifier Channels		2
High Pass Filter for F4 Channel	Hz	15
High Pass Filter for F7 Channel	Hz	440
Power per Channel	W	115
Combined Channels Power (into 8 ohms)	W	230
Total Harmonic Distortion (20 Hz to 20 kHz)	%	<0.020
Intermodulation Distortion (Into 8 ohms, 1-115 W)	%	<0.005
Frequency Response (Into 8 ohms, at 1 W, -3dB)	Hz	1 - 50000
Input Impedance	KOhms	2.5
Input Limit	Vrms	2.2
Power Consumption (both Channels)	VA	840
AC Power Line	V	120
AC Power Line	Hz	60

Table A.11 Specifications of High Resolution SPA Accelerometer (Manufactured by PCB Piezotronics, Inc.)

Description	Units	Values
Model		352A78
Voltage Sensitivity	mV / g	100
Frequency Range ($\pm 5\%$)	Hz	5 to 15000
Frequency Range ($\pm 10\%$)	Hz	3 to 18000
Resonant Frequency	kHz	≥ 45
Amplitude Range	$\pm g$ pk	50
Resolution (broadband)	g pk	0.001
Mechanical Shock Limits	$\pm g$ pk	5000
Amplitude Linearity	%	± 1
Transverse Sensitivity	%	≤ 5
Base Strain Sensitivity	g/m^3	≤ 0.001
Excitation Voltage	VDC	20 to 30
Constant Current Excitation	mA	2 to 20
Output Impedance	ohms	≤ 300
Output Bias Voltage	VDC	8 to 14

Table A.12 Specifications of Geophone (Manufactured by Mark Products, Inc.)

Description	Units	Values
Model		L15B
Natural Frequency	Hz	4.5
Shunt Resistance	kOhms	6.65
Coil Resistance	Ohms	380
Transduction Constant for Open Circuit	Volts/in/Sec	0.916
Geophone Transduction Constant	Volts/in/Sec	0.867
Frequency Tolerance	Hz	±0.5